# MATHEMATICAL MODELLING OF SOLIDIFICATION PROCESSES

### **A THESIS**

Submitted in partial fulfilment of the requirements for the award of the degree

of

**DOCTOR OF PHILOSOPHY** 

in

**MATHEMATICS** 



by
SUSHIL KUMAR



DEPARTMENT OF MATHEMATICS
INDIAN INSTITUTE OF TECHNOLOGY ROORKEE
ROORKEE-247 667 (INDIA)
MARCH, 2007

© INDIAN INSTITUTE OF TECHNOLOGY, ROORKEE, 2007 ALL RIGHTS RESERVED



## INDIAN INSTITUTE OF TECHNOLOGY ROORKEE ROORKEE

#### CANDIDATE'S DECLARATION

I hereby certify that the work which is being presented in the thesis entitled MATHEMATICAL MODELLING OF SOLIDIFICATION PROCESSES in partial fulfilment of the requirements for the award of the Degree of Doctor of Philosophy and submitted in the Department of Mathematics of the Indian Institute of Technology Roorkee, Roorkee is an authentic record of my own work carried out during a period from March, 2002 to March, 2007 under the supervision of Professor V. K. Katiyar, Department of Mathematics, Indian Institute of Technology Roorkee, Roorkee.

The matter presented in this thesis has not been submitted by me for the award of any other degree of this or any other institute.

(SUSHIL KUMAR)

This is to certify that the above statement made by the candidate is correct to the best of my knowledge.

(Dr. V. K. Katiyar)

Professor

Department of Mathematics Indian Institute of Technology Roorkee

Roorkee- 247 667 (INDIA)

Date: March 22, 2007

Signature of Supervisor

Signature of External Examiner

## **ACKNOWLEDGEMENT**

First and foremost I would like to thank my supervisor and mentor Dr. V. K. Katiyar, Professor, Department of Mathematics, Indian Institute of Technology Roorkee, Roorkee, for lending his extensive experience and incredible broad vision to this thesis work.

I am also thankful to Dr. S. P. Sharma, Professor & Head, Department of Mathematics, Indian Institute of Technology Roorkee, Roorkee for providing valuable advice, computational and other infrastructural facilities during my thesis work.

I acknowledge the critical input and constructive suggestions of Student Research Committee (SRC) and other faculty members who helped me to improve my research work.

The financial support from Council of Scientific and Industrial Research (CSIR), New Delhi, India, is also gratefully acknowledged without which this work would not have been possible.

I have no words to define my sincere thanks to my family members and relatives for their blessings, patience and moral support.

I will miss the friendship of everyone at IIT Roorkee specially Dr. Mukesh Kumar, Manoj Thakur, Sumit Kumar, Shiv Kumar Gupta, Deepak Kumar Tiwari, Dr. Braham Pal Singh, Dr. Naveen Bijalwan, Krishan Pratap Singh, Kuldeep Negi, Rishi Asthana, Ashish Srivastava who have been a constant source of entertainment and encouragement that kept me going through many ups and downs of my masters and doctorate student experience.

I owe a great deal of thanks to my lab colleagues Gaurav Varshney, Jai Kumar, Ashok Kumar, Vipin Verma, Somna Mishra, Ruch Agrawal, Priya Pathak and Sarita for their kind support. Thanks are also due to Shailendra, Khajan Chand Pandey, Kamal Singh and Prabhat Singh.

Last but not the least I would like to thank the divine force of blessings of Almighty God who never let me trapped in difficulties.

#### **ABSTRACT**

Heat transfer phenomena involving phase change also known as moving boundary problem are associated with many practical application like metal casting, environmental engineering, thermal energy storage system, aerodynamic ablation, thawing of foodstuff, cryopreservation and cryosurgery etc. Cryosurgery is use of extremely low temperature with an instrument called as cryoprobe to damage all cancer cells while sparing adjacent healthy tissues.

During phase change, interface between the frozen and unfrozen phase is moving with time and the boundary conditions at this interface require specific treatment. Except initial and boundary conditions, two more conditions are needed on the moving boundary, one to determine the boundary itself and another to complete the solution of the heat equation in each region.

These problems are non-linear due to the existence of a moving boundary between the two phases associated with the release of latent heat. Neither position nor the velocity of the interface can be predicted in advance. Mathematical analysis becomes yet more complicated, when the physical properties of the system are temperature dependent.

Phase change problems have a limited number of analytical solutions. These solutions are limited for one dimensional, infinite or semi-infinite region with simple boundary conditions. Numerical methods appear to offer a more practical approach for solving phase change problems. Various methods have been proposed for the numerical solution of phase change problems based on front tracking, front fixing and fixed domain approach. Numerical

methods based on enthalpy effective heat capacity formulation are most popular methods to solve phase change problems,

The present thesis entitled Mathematical modelling of solidification processes deals with some phase change problems in biology and alloy. Numerical solutions are obtained using finite difference method. The whole work is presented in the form of six chapters, as follows

Chapter 1 is introductory in nature and gives a brief account for solidification process, its mathematical formulation and numerical solution in biology and alloy. At the end of the chapter, summary of the whole work embodied in the thesis is given.

In **chapter 2**, the effect of cryoprobe diameter, cryoprobe temperature and heat generation due to metabolism and blood perfusion, on phase change heat transfer process during cryosurgery in lung tumor has been analyzed numerically. Results show that (i) increase in cryoprobe diameter, (ii) decrease in cryoprobe freezing temperature, lead to increase in minimum temperature, freezing rate, freezing area in tissue and decrease in tumor freezing time. Further decrease in minimum temperature, cooling rate, freezing area and an increase in time to freeze tumor has been observed with the presence of heat source term compared to the case where heat source term was not included.

In chapter 3, Pennes bioheat Equation is used to find transient temperature profile, freezing and thawing interface during combined cryosurgery and hyperthermia treatment of lung. Three blood re-flow patterns when (i) blood vessel take very short time to resume its function on thawing (Case 1), (ii) blood vessel are completely destroyed (Case 2) and (iii) blood vessel need a time delay to resume on thawing (Case 3), the frozen tissue, were also taken into account [Zhang, 2002]. The temperature raising in tissue has been found highest

for case 1 and least for case 2. Temperature profiles and phase change interfaces are obtained for all cases. Information obtained are beneficial to know whether the tumor has been damaged or not, and to minimize the damage to neighboring healthy lung tissue by over-freezing and overheating, and hence to optimize the treatment planning.

In **chapter 4**, transient temperature profile and position of phase change interfaces are obtained numerically, which is important to apply cryosurgery precisely. Informations from this study are significant for the operation of a successful cryosurgical treatment and can also be applied to cryopreserved living organ.

In chapter 5, a mathematical model has been developed to study the phase change phenomena during freezing and thawing process in biological tissues considered as porous media. Numerical simulation is used to study the effect of porosity, on the motion of freezing and thawing front and transient temperature distribution in tissue. It is observed that porosity has significant effect on transient temp profile and phase change interfaces, further decrease in freezing and heating rate has been found with increased value of porosity.

In **chapter 6**, transient heat transfer analysis has been done to study the effect of volumetric heat generation on one-dimensional solidification in finite media with convective cooling. The whole process is divided in four different stages [Katiyar, 1989]. It is found that motion of freezing interface slows down with increase in heat generation rate, while it accelerates with respect to increased rate of convective cooling.

### List of Figures

- Figure 2.1 Schematic representation of physical problem.
- Figure 2.2 Temperature profile for cryoprobe of 3, 5 and 8 mm diameter.
- Figure 2.3 Phase change interfaces for cryoprobe of (A) 3 mm, (B) 5 mm and (C) 8 mm diameter.
- Figure 2.4 Temperature profile for cryoprobe freezing temperature (A) -120 °C, (B) -150 °C and (C) -196 °C.
- Figure 2.5 Phase change interfaces for cryoprobe freezing temperature (A) -120 °C, (B) 150 °C and (C) -196 °C.
- Figure 2.6 Temperature profile for the case with and without heat source term (q).
- Figure 2.7 Phase change interfaces for the cases (A) without q and (B) with q.
- Figure 3.1 Schematic representation of physical problem.
- Figure 3.2 Phase change interface during freezing at y = 2.0 cm.
- Figure 3.3 (a) Transient temperature profile in tissues during freezing at  $t = 200 \,\mathrm{sec}$ .
- Figure 3.3 (b) Transient temperature profile in tissues during freezing at t = 400 sec.
- Figure 3.3 (c) Transient temperature profile in tissues during freezing at t = 600 sec.
- Fig 3.3 (d) Transient temperature profile in tissues during freezing at t = 800 sec.
- Figure 3.4 (a) Lower phase change interface during freezing.
- Figure 3.4 (b) Upper phase change interface during freezing.
- Figure 3.5 Position of thawing interfaces at y = 2.0 cm.
- Figure 3.6 (a) Upper phase change interface during thawing.
- Figure 3.6 (b) Lower phase change interface during thawing.

- Figure 3.7 (a) Transient temperature profile during thawing at t = 900 sec.
- Figure 3.7 (b) Transient temperature profile during thawing at at t = 1136 sec.
- Figure 3.7 (c) Transient temperature profile during thawing at at t = 1350 sec.
- Figure 3.8 (a) Transient temperature profile for case1 during heating at t = 1600 sec.
- Figure 3.8 (b) Transient temperature profile for case1 during heating at t = 1800 sec.
- Figure 3.8 (c) Transient temperature profile for case1 during heating at t = 1950 sec.
- Figure 3.8 (d) Transient temperature profile for case1 during heating at t = 2100 sec.
- Figure 3.9 (a) Transient temperature profile for case2 during heating at t = 1600 sec.
- Figure 3.9 (b) Transient temperature profile for case2 during heating at t = 1800 sec.
- Figure 3.9 (c) Transient temperature profile for case2 during heating at t = 1950 sec.
- Figure 3.9 (d) Transient temperature profile for case2 during heating at t = 2100 sec.
- Figure 3.10 (a) Transient temperature profile for case3 during heating at t = 1600 sec.
- Figure 3.10 (b) Transient temperature profile for case3 during heating at t = 1800 sec.
- Figure 3.10 (c) Transient temperature profile for case3 during heating at t = 1950 sec.
- Figure 3.10 (d) Transient temperature profile for case 3 during heating at t = 2100 sec.
- Figure 4.1 Schematic geometry of three-layer skin model.
- Figure 4.2 Transient temperatures for  $t \le 1500$  sec.
- Figure 4.3 Position of phase change interfaces during freezing.
- Figure 4.4 Position of phase change interfaces during thawing.
- Figure 4.5 Transient temperature for  $1500 \le t \le 2100$  sec.
- Figure 5.1 Schematic diagram for a tissue: (a) tissue and (b) averaging volume.
- Figure 5.2 Position of lower interface during freezing for different value of porosity.
- Figure 5.3 Position of upper interface during freezing for different value of porosity.

- Figure 5.4 Transient temperature at point A(x = 1.5 cm).
- Figure 5.5 Transient temperature at point B(x = 3.5 cm).
- Figure 5.6 Position of lower interface during thawing for different value of porosity.
- Figure 5.7 Position of upper interface during thawing for different value of porosity.
- Figure 6.1: Schematic of physical problem.
- Figure 6.2 Temperature profile in region at different time t for  $h = 1500 \text{W/m}^2$  °C and  $q = 500 \text{kW/m}^3$ .
- Figure 6.3 Position of liquidus interface with time for different value of q.
- Figure 6.4 Position of solidus interface with time for different value of q.
- Figure 6.5 Temperature profile in region at different time t for case 1 ( $q = 700 \text{kW/m}^3$ ,  $h = 1000 \text{W/m}^2 \, ^{\circ}\text{C}$ ).
- Figure 6.6 Temperature profile in region at different time t for case 2 ( $q = 1100 \text{kW/m}^3$ ,  $h = 1000 \text{W/m}^2 \, ^{\circ}\text{C}$ ).
- Figure 6.7 Temperature profile in region at different time t for case 3  $h = 2000 \text{W/m}^2 \, ^{\circ}\text{C}$ ,  $q = 2500 \text{kW/m}^3$ ).
- Figure 6.8 Temperature profile in region at different time t for case 4 (  $h = 3500 \text{W/m}^2 \, ^{\circ}\text{C}$  ,  $q = 2500 \text{kW/m}^3$  ).
- Figure 6.9 Temperature profile in region at different time t for case 5 (  $h = 4500 \text{W/m}^2$  °C,  $q = 2500 \text{kW/m}^3$ ).

#### List of Tables

- Table 2.1: Thermal properties of tissues.
- Table 2.2: Position of freezing interfaces after 900 sec freezing for cryoprobes with 3 mm, 5 mm and 8 mm diameter.
- Table 2.3: Time to reach freezing interface at tumor-lung boundary for cryoprobes with 3 mm, 5 mm and 8 mm diameter.
- Table 2.4: Position of freezing interfaces after 2000 sec freezing for cryoprobes with  $T_s = -120 \,^{\circ}\text{C}$ ,  $-150 \,^{\circ}\text{C}$  and  $-196 \,^{\circ}\text{C}$ .
- Table 2.5: Time to reach freezing interface at tumor-lung boundary for cryoprobes with  $T_s = -120 \,^{\circ}\text{C}$ ,  $-150 \,^{\circ}\text{C}$  and  $-196 \,^{\circ}\text{C}$ .
- Table 3.1: Temperature at point P for three blood re-flow patterns during heating.
- Table 4.1: Properties of Three-Layer Skin model.
- Table 5.1: Thermal properties of tissue.
- Table 5.2: Penetration distance and time of freezing interfaces for different value of porosity.
- Table 5.3: Meeting position and time of thawing interfaces for different value of porosity.
- Table 6.1: Thermophysical properties of Sn-5wt%Pb alloy.
- Table 6.2: Position of liquidus interface in steady state for different value of q.
- Table 6.3: Position of solidus interface in steady state for different value of q.

## List of Publication

- (i). Numerical Simulation of cooling of Tumor Embedded in Lung during Cryosurgery. in Proceeding: International Conference on Biomedical Engineering (ICBME-05) Singapore.
- (ii). Bio-heat Distribution in Spherical Tissue Layers: An Application to Thermal Spherical Tumor. in Proceeding: International Conference on Biomedical Engineering (ICBME-05) Singapore.
- (iii). Numerical Simulation of Thawing Process of Biological Tissues as Porous Media During Cryosurgery, presented in 5<sup>th</sup> world congress on Biomechanics, Munich (Germany) from July, 29 to Aug 4, 2006. abstract in: Journal of Biomechanics Vol-39 Supp 1(2006) pp S384
- (iv). Numerical Study of Thawing Problem in Skin and Subcutaneous Tissues, in 15<sup>th</sup> international conference on Mechanics in Medicine and Biology, Singapore.
- (v). Numerical sudy on phase change heat transfer process during combined hyperthermia and cryosurgical treatment of lung cancer, (communicated).
- (vi). A parametric study on phase change heat transfer process during cryosurgery of lung tumor, (communicated)

## **CONTENTS**

Chapters	Page No.
1. General Introduction	1-25
1.1 Introduction	1
1.2. Solidification	2
1.2.1. Mathematical Formulation	3
1.3. Heat Transfer in Biological Tissues	4
1.3.1. Pennes Model	4
1.3.2. The Chen and Holmes (CH) Model	5
1.3.3. The Weinbaum, Jiji and Lemons (WJL) Model	7
1.3.4. The Weinbaum and Jiji (WJ) Model	9
1.4. Cryosurgery	11
1.4.1. Mechanism of Tissue Injury during Cryosurgery	11
1.4.2. Extracellular and Intracellular Ice Crystallization	12
1.4.3. Mathematical Formulation of Cryosurgery	13
1.4.4. Some Terminologies	15
1.5. Solution Methodology	15
1.5.1. Introduction	15
1.5.2. Analytical Methods	16
1.5.3. Numerical Solution	17
1.5.4. Enthalpy Method	18
1.5.5. Finite Difference Method	20
1.6. Plan of Thesis	21
2. Parametric Study on Phase Change Heat Transfer Process during (	Cryosurgery of Lung
Tumor	27-49
2.1. Introduction	27
2.2. Problem Description	29
2.3. Mathematical Model	29
2.3.1. Governing Equation	29

2.3.2. Assumptions	30
2.3.3. Initial and Boundary Conditions	30
2.4. Numerical Solution	31
2.5. Results and Discussion	33
2.5.1. Effect of Cryoprobe Radius	33
2.5.2. Effect of Cryoprobe Temperature	34
2.5.3. Effect of Metabolism and Blood Perfusion	36
2.6. Conclusion	37
3. Numerical Study on Phase Change Heat Transfer during Combined Hyperthe	ermia and
Cryosurgical Treatment of Lung Cancer	51-85
3.1. Introduction	51
3.2. Problem Description	52
3.3. Mathematical Model	53
3.3.1. Governing Equation	53
3.3.2. Assumptions	53
3.3.3. Initial and Boundary Conditions	54
3.4. Numerical Solution	55
3.5. Results and Discussion	56
3.6. Conclusion	58
4. Numerical Study on Freezing and Thawing of Skin: A Three Layer Model	87-101
4.1. Introduction	87
4.2. Problem Description	88
4.3. Mathematical Model	89
4.3.1. Assumptions	89
4.3.2. Governing Equation	90
4.3.3. Initial and Boundary Conditions	90
4.4. Numerical Solution	91
4.5. Results and Discussion	92
4.6. Conclusion	93
5. Mathematical Modelling of Freezing and Thawing Process in Tissues as a Por	ous
Media	103-123
5.1. Introduction	103

5.2. Mathematical Model	105
5.3. Numerical Solution	107
5.4. Results and Discussion	108
5.5. Conclusion	110
6. Transient Heat Transfer in Finite Media with Energy Gen	eration and Conv
Cooling	125-15
6.1. Introduction	125
6.2. Problem Description	126
6.3. Mathematical Model	127
6.3.1. Governing Equation	127
6.3.2. Assumptions	128
6.3.3. Initial and Boundary Conditions	128
6.4. Numerical Solution	129
6.5. Results and Discussion	129
6.6. Conclusion	135
Bibliography	153-17

.

.

## Chapter 1

#### GENERAL INTRODUCTION

#### 1.1 INTRODUCTION

Mathematical modelling is the application of mathematics to explain and predict real world behavior. It essentially consists of translating real world problems into mathematical problems, solving the mathematical problems and interpreting theses solution in the language of real world.

Heat is defined as energy transferred by virtue of a temperature difference. It is a vector quantity, flowing in the direction of decreasing temperature. There are three ways that heat may be transferred between substances at different temperatures-conduction, convection, and radiation.

Conduction: Transfer of energy from more energetic to the less energetic particles of the substance due to the interaction between the particles is known as heat conduction. The law of heat conduction, also known as Fourier's law is given as

$$F = -k\nabla T. (1.1)$$

The heat flux, F is the heat transfer rate per unit area perpendicular to the direction of heat flow, and k is thermal conductivity; it is characteristic of the material.

Convection: It involves one or more fluid those interact with each other or with a solid boundary in such a way that energy is transferred into or out of the fluid system [123]. The flow of heat is due to bulk, macroscopic movement of matter from a hot region to a cool region, as opposed to the microscopic transfer of heat between atoms involved with conduction. The convective heat flux between a solid surface and the fluid surrounding is

proportional to the difference between the temperature of solid and surrounding fluid and is often written as

$$F = h(T_s - T_{\infty}), \tag{1.2}$$

where, F is heat flux,  $T_s$  and  $T_\infty$  are surface and surrounding fluid temperature. h is termed as convection heat transfer coefficient. It depends on conditions on boundary layer, which are influenced by surface geometry, the nature of fluid motion, and an assortment of fluid thermodynamics and transport properties. It is also called as Newton's law of cooling.

Radiation: The third mode of heat transmission is due to the electromagnetic wave propagation, which can occur in a total vacuum as well as in a medium. According to Stefan-Boltzmann law the radiant heat flux from a body is proportional to the fourth power of its absolute temperature

$$F = \sigma T^4, \tag{1.3}$$

where T is the absolute temperature, the constant  $\sigma$  called as Stefan-Boltzmann constant is independent of surface, medium and temperature; its value is  $5.6697 \times 10^{-8} \text{ W/m}^2\text{-K}^4$ .

#### 1. 2 SOLIDIFICATION

Solidification is the phase change problem i.e. from liquid phase to solid phase. Since phase transformation can take place only by lowering of free energy of system, one has to study the phenomena of heat extraction from the liquid region. Problems of heat conduction involving solidification are complicated because the interface between the solid and liquid phase moves as the latent heat is absorbed or liberated at the interface [32]. These problems are also known as "Moving Boundary Problems" (MBP). MBPs are associated with time dependent boundary problems, where the position of

moving boundary has to be determined as a function of time and space [Zerroukat, 1993]. The first published discussion of such problems seems to be that by Stefan in a study of the thickness of polar ice, and for this reason the problem of freezing is frequently referred to as the "Stefan problems" [129]. Solidification process can be grouped into two major categories: Solidification of pure substances and Solidification of an alloy. Solidification of pure substances is usually characterized by a sharp solid/liquid interface. On the other hand a mixed-phase region characterizes solidification of an alloy. The mixed phase region commonly termed as the mushy region, is a combination of liquid solute and solid crystals [1].

#### 1.2.1 Mathematical Formulation

During phase change, interface between the frozen and unfrozen phase is moving with time and the boundary conditions at this interface require specific treatment. Except initial and boundary conditions, two more conditions are needed on the moving boundary, one to determine the boundary itself and another to complete the solution of the heat equation in each region. For 1-D phase change problems with cooling at x = 0, the conditions at moving interface, x = S(t) is given as [77]

$$k_{s} \frac{\partial T_{s}}{\partial x} - k_{l} \frac{\partial T_{l}}{\partial x} = \rho L \frac{dS(t)}{dt} \qquad at \, x = S(t)$$
 (1.4a)

$$T_l = T_s = T_{ph}$$
 at  $x = S(t)$ , (1.4b)

while the heat conduction equations in solid and liquid region are given by

$$\rho_{l}c_{l}\frac{\partial T_{l}}{\partial t} = \frac{\partial}{\partial x}\left(k_{l}\frac{\partial T_{l}}{\partial x}\right) \qquad \qquad S(t) \leq x \leq d \qquad \text{(in liquid region)}, \qquad (1.5)$$

$$\rho_s c_s \frac{\partial T_s}{\partial t} = \frac{\partial}{\partial x} \left( k_s \frac{\partial T_s}{\partial x} \right) \qquad 0 \le x \le S(t) , \qquad \text{(in solid region)}, \qquad (1.6)$$

where T is temperature; L, latent heat;  $\rho$ , density; c, specific heat; k, thermal conductivity; d, length of the whole region and subscripts l, s and ph stand for liquid, solid and phase change respectively.

Solidification process occurs mainly in metal casting [152], environmental engineering [78], thermal energy storage system [57], aerodynamic ablation, freezing and thawing of foodstuff [33], cryopreservation [105] and cryosurgery etc. [36, 155].

#### 1.3 HEAT TRANSFER IN BIOLOGICAL TISSUES

Heat transfer in biological tissues involve complicated processes such as heat conduction in tissues, heat transfer due to perfusion of arterial-venous blood through the pores of the tissue, metabolic heat generation and external interactions such as electromagnetic radiation emitted from cell phones. Energy transport in biological tissues is usually referred to as bio-heat equation.

Thermal models for blood perfused tissues have been used in a wide range of application in temperature regularization [91, 95, 96, 117-119, 135], tumor detection [58, 60, 88, 90, 92, 97, 130, 131], cryosurgery [7, 9, 13, 38, 45, 111], hyperthermia [5, 44, 59] etc. Various models have been proposed in the literature to model the heat transport phenomena in blood perfused tissues

## 1.3.1 Pennes Model [99]:

This is the earliest model for energy transport in tissues and is given as

$$\rho c \frac{\partial T}{\partial t} = \nabla k \cdot \nabla T + (\rho c)_b w_b (T_b - T) + Q_m$$
(1.7)

where  $\rho$  is density of tissue; k, thermal conductivity;  $c_b$ , specific heat of blood;  $w_b$ , blood perfusion rate; T, temperature; t, time;  $T_b$ , arterial blood temperature and  $Q_m$  is the metabolic heat generation in the tissue.

Pennes considered all the properties appearing for the conduction and thermal storage terms to be for the tissue, while he referred to the blood properties in the blood perfusion  $\operatorname{term}\left((\rho c)_b w_b(T_b-T)\right)$ . He assumed that the arterial blood temperature  $T_b$  is uniform throughout the tissue, while he considered the vein temperature to be equal to the tissue temperature, which is denoted by T at the same point. Pennes model is most popular and is quite useful because of its simplicity. He postulated therefore that the total energy exchange by the flowing blood could be modeled as a non-dimensional heat source, whose magnitude is proportional to the volumetric blood flow and the difference between local tissue and major supply arterial temperatures.

#### 1.3.2 The Chen and Holmes (CH) Model [23]

In the CH model blood vessels are grouped into two categories: large vessels, each of which is treated separately, and small vessels that, in view of their small size and large number, are treated as part of the continuum that also includes the tissue. Some of these small vessels are nevertheless thermally significant, as their temperature differ from that of the adjacent tissue. The heat transfer between the small blood vessels and tissue was then studied in detail and separated into three modes.

First Mode: This mode reflects the equilibration of blood temperature, initially at that of a large vessel, with tissue temperature. Although the control volume includes only small vessels, it is assumed to be sufficiently large to enclose all small vessel bifurcations. Therefore, the blood exits the control volume essentially at the average temperature of the confined tissue. Hence the thermal contribution due to the temperature difference between the entering blood and the tissue within the control volume is similar to the perfusion term in Pennes Equation and describes as

$$q_p = w(\rho c)_b (T_b - T), \qquad (1.8a)$$

where w refers only to the blood flow within vessels in control volume and  $T_b$  represents only the temperature of the blood within the largest vessels.

Second Mode: This mode of the vascular contribution to tissue heat transfer relates to the already thermally equilibrated vessels. This mode deals with the part of heat transfer that take place when the flowing blood convects heat against a tissue temperature gradient. Because of thermal equilibrium, the blood temperature essentially equals that of the tissue, T, and the contribution takes the form

$$q_c = (\rho c)_b \, \overline{u} \, \nabla T \,, \tag{1.8b}$$

where  $\overline{u}$  represents the net volume flux vector of the blood permeating a unit area of the control surface.

Third Mode: This mode describes the thermal contribution due to the small temperature fluctuations of nearly equilibrated blood along the tissue temperature gradient. This mode of heat transfer is proportional to the tissue temperature gradient and depends on the local microvascular structure. This gives rise to the tensor  $\bar{k}_p$ , denoted as "perfusion conductivity",

and the contribution of this mode to the heat transfer can be thus described by the conduction equation

$$q_{pc} = -\nabla \cdot k_p \nabla T \,. \tag{1.8c}$$

The "perfusion conductivity" depends on the local blood flow velocity  $(\bar{\nu})$  within the vessel, the relative angle  $(\gamma)$  between the direction of the blood vessel and the local tissue temperature gradient and on the number of the vessels (n) included in the control volume.

The CH model of the bio heat transfer is obtained by replacing the single perfusion term in Pennes model (1.7) with the vascular contribution equation (1.8) and is given by

$$\rho c \frac{\partial T}{\partial t} = \nabla \cdot k \nabla T + (\rho c)_b w(T_b - T) - (\rho c)_b \overline{u} \cdot \nabla T + \nabla \cdot k_p \nabla T + Q_m.$$
(1.9)

The application of this model is more difficult compared to the Pennes model, because of some knowledge on the local vascular geometry is needed.

#### 1.3.3 The Weinbaum, Jiji and Lemons (WJL) Model [62]

To develop the model an in-depth evaluation of the thermally equilibration length of various geometrical configuration of the vasculature that may exist in the peripheral tissue layer was conducted. Thermal equilibrium length of the individual vessel is defined as the length of blood vessel for which the temperature difference between blood and tissue is reduced to 1/e of its initial value.

Based on anatomically observations in peripheral tissue and on high spatial resolution measurements, Weinbaum et al. [62] concluded that the main contribution of local blood perfusion to heat transfer in the tissue is associated with an incomplete counter-current heat exchange mechanism between pairs of arteries and veins and not with heat exchange at the

level of capillaries. Neglecting axial conduction, the energy conservation for a thermally significant artery and vein yields

$$\pi(\rho c)_b \cdot \frac{d(nr_b^2 \bar{V}.T_a)}{ds} = -n \cdot q_a - 2\pi(\rho c)_b nr_b g \cdot T_a, \qquad (1.10a)$$

$$\pi(\rho c)_b \cdot \frac{d(nr_b^2 \bar{V}.T_v)}{ds} = -n \cdot q_v - 2\pi(\rho c)_b nr_b g \cdot T_v. \tag{1.10b}$$

The terms on the left-hand side of equation (1.10) represent the heat convected along the path of arteries and veins, respectively within the control volume. This mode of heat transfer is determined by vessel number density (n), vessel radius  $(r_b)$  and blood velocity  $(\overline{V})$  within the vessel. On the right-hand side, the first term represents the heat conducted through the vessel wall, and the second term represents energy carried out off, or into the blood vessel via the connecting capillaries, defined as the bleed-off blood. Equation (1.10) can be simplified by recourse to the mass conservation law:

$$\frac{d(nr_b^2.\overline{V})}{ds} = -2nr_bg. \tag{1.11}$$

Substituting equation (1.11) in equation (1.10) with recourse to the energy conservation principle for the tissue control volume, the following set of three coupled equations are obtained [62]

$$(\rho c)_b \pi r_b^2 \overline{V} \cdot \frac{dT_a}{ds} = -q_a, \qquad (1.12a)$$

$$(\rho c)_b \pi r_b^2 \overline{V} \cdot \frac{dT_v}{ds} = -q_v, \qquad (1.12b)$$

$$\rho c \frac{\partial T}{\partial t} = \nabla k \cdot \nabla T + ng \left(\rho c\right)_b \cdot \left(T_a - T_v\right) - n\pi r_b^2 \left(\rho c\right)_b \overline{V} \cdot \frac{d\left(T_a - T_v\right)}{ds} + Q_m. \tag{1.12c}$$

The left-hand side of equation (1.12c) represents the heat accumulated within the tissue control volume. On the right-hand side, the terms represent respectively, the heat

conducted in the direction of vessel path, the energy exchange via capillary bleed-off and the net heat exchange between tissue and artery vein pair.

In WJL model, the second term on the right-hand side of equation (1.12c) resembles the perfusion term in Pennes model. Weinbaum et al. [62] claimed however that in the peripheral tissue, where the counter current vessels are small, the contribution of this term to heat transfer is minor, while becomes more significant in the deep muscles tissues. A precise experimental validation of this theoretical model is still lacking at least in part due to its complexity, but also because a meaningful application requires a detailed description of the associated vascular architecture. In addition, such an intricate model usually requires a numerical approach, which presently prevents online calculations, which are essential for many practical applications. Further WJL model probably requires the most detail about the vascular structure. These factors make the WJM model difficult to apply to most tissues or a variety of thermal conditions.

#### 1.3.4 The Wainbaum and Jiji (WJ)Model [146]

Weinbaum and Jiji [146] derived a simplified model, readily solvable and applicable for on-line calculation to overcome the difficulties of applying their three equation model to practical situation. The main underlying assumption in the simplifying model was that the mean tissue temperature can be approximated by an average temperature of the adjacent counter-current pair of closely spaced and nearly equilibrated vessels, i.e.

$$T \simeq \frac{T_a + T_v}{2} \,. \tag{1.13a}$$

Moreover, they assumed that most of the heat conducted out through the wall of an arteriole arrives at, and is conducted in through, the wall of its paired vein, such that

$$q_a = q_v = \sigma k (T_a - T_v), \tag{1.13b}$$

substituting equation (1.13) in WJM model [62], the WJM model reduces to a single differential equation for the tissue temperature T [146].

$$\rho c \frac{\partial T}{\partial t} = \frac{\partial}{\partial x} \left( k_{eff} \frac{\partial T}{\partial x} \right) + Q_m. \tag{1.14}$$

In this equation, the heat transfer due to the blood flow gives rise to an effective conductivity tensor  $k_{eff}$ , that represents both the capillary bleed-off and the heat exchange between tissue and adjacent vessel. For one dimensional case, where blood vessel and temperature gradient are in the same direction, it gives

$$k_{eff} = k \left[ 1 + \frac{n[\pi r_b^2(\rho c)_b V \cos \gamma]^2}{\alpha . k^2} \right].$$

The results of computer simulations reported by Baish et al. [5, 6], Wissler et al. [147, 148] and Charney et al. [21, 22] suggested that the WJ model can only be applied either to muscle tissue (with low blood perfusion) that contains blood vessels with diameter,  $d < 0.2 \,\mathrm{mm}$  or to tissue in general where  $\varepsilon < 0.3$ .

In summary, in locations where most of the vessels are paired such as muscle, the WJ and Pennes models can be used in the small vessel regions and large vessel region, respectively. The region of transition in vascular dimensions, as well as convective effects in vicinity of large vessels, have to be considered separately, as none of the presently known single equation model is suitable for this region. If a major portion of the vessels are not paired, the CH model may be used for regions with small vessels. A review of the chronological development of mathematical models of bioheat transfer has been given by Channey et al. [20]. Due to its simplicity, the Pennes model [99] is still the most commonly

used model for thermal energy transport in biological tissues.

#### 1.4 CRYOSURGERY

Cryosurgery, also referred as cryotherephy or cryoabalation, is use of extremely low temperature to damage all cancer cells while sparing adjacent healthy tissue. This surgical technique is based on the cryotoxic effect of low temperature. It is safe, efficient, inexpensive, easy to perform, does not have major side effects. It is used for many types of tumors e. g. liver, prostate, bone tumors, vaginal tumors, skin cancer and hemorrhoids etc. During cryosurgery freezing is induced using a cryprobe, made of specific metal. The tip of which is used to generate low temperature area in the diseased tissue region. Heat is removed by cryoprobe and freezing interface propagates from the probe surface into the tissue damaging the tissue along the way. After the desired region is frozen, the probe is removed and the frozen tissue is allowed to thaw [11, 27, 28, 38]. This technique was first developed in middle of 19<sup>th</sup> century. James Arnott of Brigton, England was recognized as the first physician to use freezing for treatment of cancer. One of the key advantages of cryosurgery is that cell destruction is localized which minimizes damage to surrounding healthy tissue.

#### 1.4.1 Mechanism of Tissue Injury During Cryosurgery ([10, 16, 46, 81-83, 115])

During freezing as the temperature in tissue falls into the freezing range, water is crystallized. In cryosurgery, the destructive effects of freezing are due to a number of factors. These factors can be grouped into two major mechanisms, one immediate effect and another delayed one. [46]. Coldest temperature is found to be the prime factor for cell death, and -50

°C has been recommended as a guide for confirmed cell death [46]. The cause of immediate cell destruction is related to the effect of cooling and freezing, while the delayed effect of freezing injury is due to vascular stasis which can last up to several hours upon the completion of cryosurgery [16, 81-83]. The immediate mechanism of injury is the deleterious effect of freezing on the cell [10].

#### 1.4.2 Extracellular and Intracellular Ice Crystallization ([27, 83, 24])

Water is the major component of biological tissue. Thus, when the temperature in tissue falls a few degrees below 0 °C, ice crystals formation starts in extracellular space and microvasculature. The extracellular solution increases in concentration, creating a hyperosmotic environment. To achieve equilibrium, water in the cells passes out through the cell membrane by osmosis. This loss of water causes cells to shrink, damaging their membranes and constituents. Eventually, cell shrinkage reaches a maximum even though extracellular concentration continues to increase. This creates a concentration gradient between the two sides. A point in time arrives when the concentration gradient is significant and the solutes from the extracellular fluid are allowed to pass into the cell. This generates a mechanical force on the cells, which damages and destroys the cells. It is also known as "solution effect" and occurs between temperatures of -4 °C to -21 °C [24].

When cooling rates are high, there is less time for extracellular ice crystallization. Theoretically, this means that there would be a reduction in cell destruction. However, another ice formation phenomenon takes place-intracellular ice. When this occurs, water cannot leave the cells fast enough to maintain osmotic equilibrium across the cell membrane. Therefore, equilibrium is achieved by the formation of ice crystals within the cells as well as

outside. In cryobiology, heterogeneous nucleation of intracellular ice can form at temperatures of -15 °C and below, whereas homogeneous intracellular ice crystals form at temperatures of -40 °C [24]. As the temperature drops, the intracellular solution becomes thermodynamically super cooled and becomes increasingly unstable. This instability causes ice nucleation to take place, leading to the formation of ice crystals within the cell membrane. The intracellular ice crystals irreversibly rupture the cell membrane due to an expansion in volume. At the same time, it disrupts the proper functioning of cell organelles, thereby destroying the cancerous cells [24].

Solution effects injury is associated with low freezing rates, while intra-cellular ice is commonly associated with high cooling rates. Cells close to the tip are subjected to a fast cooling rate and cell death is high following intracellular ice crystallization. Further away, cooling rates are lower and fewer cells are damaged. At a certain distance, cell death reaches a minimum but starts to rise again as the cooling rate is further reduced and the "solution effect" predominates.

In both extracellular and intracellular ice crystallization, water is removed from the biological system and desiccation results in cell death. The fraction of unfrozen water is an important factor in cell survival or death [82]. Furthermore, the deleterious effects of cell shrinkage and expansion may be sufficient to explain cell death [98]

#### 1.4.3 Mathematical Formulation of Cryosurgery

As freezing front propagates from the cryoprobe outward, the extent of the tissue affected by freezing at times cannot be easily determined by the surgeon, resulting in a loss of precision and control. It is important to be able to predict and control the cooling rate over

some range of temperatures and freezing states. Heat transfer by conduction has been assumed to be the only heat transfer process during cryosurgery and fundamental Pennes [99] bioheat equation is used to formulate the mathematical model in cryosurgery and is given as

(a) In unfrozen region

$$\rho_{u}c_{u}\frac{\partial T_{u}(X,t)}{\partial t} = \nabla k_{u} \cdot \nabla T_{u}(X,t) + \left(\rho c\right)_{b} w_{b}(T_{b} - T_{u}(X,t)) + Q_{m} \qquad X \in D_{u}(t), \qquad (1.15)$$

where  $\rho_u$ ,  $k_u$ ,  $c_u$  are density, thermal conductivity and specific heat of unfrozen region.  $c_b$  is specific heat of blood;  $w_b$ , blood perfusion rate;  $T_u(X,t)$  is temperature in unfrozen region;  $T_b$ , arterial blood temperature and  $Q_m$  is the metabolic heat generation in the tissue and  $D_u(t)$  denotes the unfrozen domain at time t.

(b) In frozen region: due to absence of blood perfusion and metabolism in frozen region, the heat balance equation can be written as

$$\rho_f c_f \frac{\partial T_f(X, t)}{\partial t} = \nabla k_f \cdot \nabla T_f(X, t) \qquad X \in D_f(t), \qquad (1.16)$$

Fre  $\rho_f$ ,  $k_f$ ,  $c_f$  are density, thermal conductivity and specific heat of frozen region; X,t) is temperature in frozen region and  $D_f(t)$  denotes the unfrozen domain at the t.

The conditions at phase change interface are given by

$$T_u(X,t) = T_f(X,t) = T_{ph}(X,t)$$
  $X \in \Gamma_{ph}(t)$  (1.17a)

$$k_{f} \frac{\partial T_{f}(X,t)}{\partial n} - k_{u} \frac{\partial T_{u}(X,t)}{\partial n} = \rho L \nu_{n} \qquad X \in \Gamma_{ph}(t)$$
(1.17b)

where n denotes unit outward normal; L and  $T_{ph}$  are latent heat and freezing temperature respectively;  $\nu_n$  denotes the normal velocity to the phase change interface

and  $\Gamma_{oh}(t)$  represents position of moving interface.

#### 1.4.4 Some Terminologies

Thawing: It is the reverse process of freezing during cryosurgery. It is considered to be the other important phase of cryosurgery that causes tissue injury. During the thawing process small crystals merge together form large crystals, which readily disrupt cellular membranes. This re-crystallization may enhance tissue destruction induced by the preceding freezing [48]. Hyperthermia, in cancer treatment is to raise the temperature of diseased tissue to therapeutic value.

In vitro: It refers to the technique of performing a given experiment in a test tube, or generally, in a controlled environment outside a living organism.

In vivo means that which take place inside an organism. In science, in vivo refers to experimentation done in, or on the living tissue of a whole, living organism as opposed to a partial or dead one. Animal testing and clinical trials are forms of in vivo research.

100

#### 1. 5 SOLUTION METHODOLOGY

#### 1.5.1 Introduction:

One common feature of solidification problems is that the location of the solid-liquid interface is not known a priori and must be determined during the course of analysis. These problems are non-linear due to the existence of a moving boundary between the two phases associated with the release of latent heat. Neither position nor the velocity of the interface can be predicted in advance. Mathematical analysis becomes yet more complicated, when the physical properties of the system are temperature dependent.

#### 1.5.2 Analytical Methods

Phase change problems have a limited number of analytical solutions. These solutions are limited for one dimensional, infinite or semi-infinite region with simple boundary conditions.

These solutions are usually in the form of similarity variable and are known as similarity solutions. The first and still the most comprehensive solution is due to Neumann. It refers to a one dimensional semi-infinite region, initially occupied by a liquid at a constant temperature greater than the melting point and with one surface, subsequently maintained at a constant temperature below the melting temperature. This solution was further generalized by Carslaw et al. [18]. Lombardi et al. [75] used this method to study the thawing process with a heat flux condition at fixed boundary.

Formulation of moving boundary problems in terms of integral equations was also found useful. Evans et al. [42] used Laplace transforms to express one-phase moving boundary problems. Further Ku et al. [66] gave a generalized Laplace transform for phase hange problems. Selin et al. [121, 122] gave the solution for plane, cylindrical and spherical noving boundary using integral transform.

The use of Green's function for the solution of heat flow problems subjected to conditions prescribed on fixed boundaries is well known. Recently Liu et al. [72] used Green function to study the freezing and thawing process of biological skin. By integrating the one-dimensional heat flow equation with respect to the space variable and inserting the boundary conditions, Goodman et al. [49] produced an integral equation which expresses the overall heat balance of the system. This method is known as heat balance integral method. Muchlbaur et al. [86] and Katiyar et al. [63] used this method in the transient heat transfer

analysis of alloy solidification.

The solution of quasi-steady approximation of Stefan problem is easy to obtained, but the validity of the solution is limited, as the initial condition can not be met. Recently, Jiji et al. [61] used quasi-steady approximation to analyze the freezing and melting of phase change materials with energy generation. Caldwell et al. [17] used perturbation method to solved quasi steady approximation of Stefan problem.

#### 1.5.3 Numerical solution

Numerical methods appear to offer a more practical approach for solving phase change problems. Various methods have been proposed for the numerical solution of phase change problems [104, 108, 153, 154]. They differ primarily in the way that heat transfer on the phase boundary is modeled. Existing numerical methods can be divided into following categories [32].

Front tracking method: The front tracking methods consider the interface between solid and liquid as a boundary, distinct sets of conservation equations are solved, and additional boundary conditions are specified at the interface to couple these sets of equations. This method includes fixed finite-difference grids; modified grids using variable time steps or variable space grids; methods of lines and adaptive grid methods etc [25, 50, 51, 93, 132].

Front fixing method: In this method phase change boundaries are fixed by a change of variable that simplified the numerical work considerably. Body-fitted curvilinear coordinates and isotherm migration methods are some examples of front fixing method.

Fixed domain method: In both the front tracking and front fixing methods, it is necessary to satisfy the Stefan condition on the moving boundary. It may sometimes be difficult or even

impossible to track the moving boundary if it does not move smoothly or monotonically with time. Furthermore, the moving boundary may have sharp peaks, or double back or it may even disappear. Thus the reformulation of problem in such a way that the Stefan conditions can be bound implicitly in new form of equations, which applies over the whole of a fixed domain, is an attractive one. This reformulation is accomplished by introducing Enthalpy function or effective heat capacity [41].

#### 1.5.4 Enthalpy Method

The essential feature of the basic enthalpy methods is that the evaluation of the latent heat is accounted for by the enthalpy as well as the relationship between the enthalpy and temperature, which can be defined in terms of the latent heat release characteristics of the phase change material. This relationship is usually assumed to be a step function for isothermal phase change problems and a linear function for non-isothermal phase change cases as follows [32]

(a) For isothermal phase change

$$H = \begin{cases} c_f(T - T_m) & T \le T_m \\ c_u(T - T_m) + L & T > T_m \end{cases} , \qquad (1.18a)$$

(b) For non-isothermal phase change [12, 52]

$$H = \begin{cases} c_{f}(T - T_{ms}) & T < T_{ms} \\ (T - T_{ms}) \left(\frac{1}{2}(c_{f} + c_{u}) + \frac{L}{(T_{ml} - T_{ms})}\right) & T_{ms} \le T \le T_{ml}, \\ L + \frac{1}{2}(c_{f} + c_{u})(T_{ml} - T_{ms}) + c_{u}(T - T_{ml}) & T > T_{ml} \end{cases}$$

$$(1.18b)$$

where L is latent heat,  $T_{ml}$  and  $T_{ms}$  are liquidus and solidus temperatures respectively. Subscripts f and u are for frozen and unfrozen state respectively.

Using enthalpy, H (Equation 1.18), the equations (1.4)-(1.6) reduce to a single equation

$$\rho \frac{\partial H}{\partial t} = \nabla k . \nabla T \,, \tag{1.19}$$

while equations (1.15)-(1.17) reduce to

$$\rho \frac{\partial H}{\partial t} = \nabla k \cdot \nabla T + (\rho c)_b w_b (T_b - T) + Q_m. \tag{1.20}$$

In enthalpy formulation, enthalpy becomes dependent variable along with temperature. This method is used by many researchers in the study of phase change problems in metal casting, freezing of food, cryosurgery, thermal energy storage system, freezing and thawing of food [36, 69, 94, 124, 138-143].

The advantages of this method are [139]:

- (i) There are no conditions to be satisfied at x = S(t), where S(t) is the position of phase change interface.
- (ii) There is no need to accurately track the phase change boundary.
- (iii) There is no need to consider the regions on either side of x = S(t) separately.
- (iv) It is easy to deal with the cases where phase change occurs over a wide range rather than at a single point.
- (v) Fixed grids can be used for computation purpose.

Enthalpy methods give most accurate solution, especially for phase change problem in which a phase change occurs over a wide range [55]. In enthalpy method whole region is divided into a finite number of volume elements. Using the heat balance equation

(1.19)/(1.20), enthalpy of each element is updated. Knowing the enthalpy of an element, temperature can be calculated by inverting equation (1.18) [101].

Equation (1.19)/(1.20) can be solved using finite difference method (FDM) [37, 104], finite element method (FEM) [15, 30, 54, 89, 93,111, 145, 156, boundary element method (BEM) [35, 53] or finite volume method (FVM). The success of finite element method and boundary element method lie in their ability to handle complex geometries, but they are acknowledge to be more time consuming in terms of computing and programming. Because of their simplicity in formulation and programming, finite difference techniques are still the most popular at the present [37, 67, 68].

#### 1.5.5 Finite Difference Method

The central theme in finite difference simulation is the conversion of a physical problem involving the continuous variation of a field variable f(x, y, z, t), into an approximate numerical formulation containing discrete value of f at spatial points  $(x_i, y_i, z_i)$  and the time levels  $t_p$  [134, 136, 144]. The spatial points are called nodes of the finite difference grid. The governing differential equations of the physical problem are approximated at the nodes, to generate algebraic equations for the nodal values of f.

(i) Divide the whole domain into 'n' nodes of equal length 'h'.

Finite difference method can be explained briefly in the following steps:

(ii) Replace the derivatives of different order in differential equation by using appropriate finite difference approximation at each internal node, as follow

Forward difference

$$f' = \frac{f_{i+1} - f_i}{h} + O(h)$$
,

$$f' = \frac{f_{i+2} - f_{i+1} + f_i}{h^2} + O(h)$$
,

Backward difference:

$$f' = \frac{f_i - f_{i-1}}{h} + O(h)$$

$$f'' = \frac{f_i - f_{i-1} + f_{i-2}}{h^2} + O(h)$$

Central difference:

$$f' = \frac{f_{i+1} - f_{i-1}}{2h} + O(h^2)$$

$$f'' = \frac{f_{i+1} - f_i + f_{i-1}}{h^2} + O(h^2)$$

- (iii) Apply the boundary conditions
- (iv) Solve the discretized (algebraic) equations by a suitable matrix inversion or iterative technique.

Finite difference methods using enthalpy formulation of phase change problems include explicit method, semi implicit method, and fully implicit method. The explicit method is conditionally stable, while others are unconditional stable [100, 153].

#### 1. 6 PLAN OF THESIS

In the present thesis solidification processes occurring in cryosurgery and alloy have been studied. Explicit finite difference method has been used to solve the Stefan equation using enthalpy and effective heat capacity formulation. A computer code has been developed using C++ programming language and MATLAB (version 7.01). Results obtained are inter-

preted and are plotted in the form of graphs.

The thesis consists six chapters as per following details:

# Chapter 1

This chapter is introductory in nature and gives a brief account for solidification process, its mathematical formulation and numerical solution in biology and alloy. At the end of the chapter, summary of the whole work embodied in the thesis is given.

# Chapter 2

The factors affecting cell injury during cryosurgery include the coolest temperature in the tissue, the duration of frozen cycle, the rate of freezing front propagation, the thawing rate and the freezing/thawing cycles etc.[48, 128]. The factors which affects necrosis such as the lowest temperature in the tissue or the rate of freezing front propagation depends on the biophysical parameter that are present in a given cryosurgical procedure. These parameters include the temperature and duration of freezing-thawing process, the shape and size of cryoprobe, the heat capacity, the thermal conductivity of the tissue, the rate of blood flow and rate of metabolism in the involved tissue [3].

In this chapter the effect of cryoprobe diameter, cryoprobe temperature and heat generation due to metabolism and blood perfusion, on phase change heat transfer process during cryosurgery in lung tumor has been analyzed numerically. Results show that (i) increase in cryoprobe diameter, (ii) decrease in cryoprobe freezing temperature, lead to increase in minimum temperature, freezing rate, freezing area in tissue and decrease in tumor freezing time. Further decrease in minimum temperature, cooling rate, freezing area and an increase in time to freeze tumor has been observed with the presence of heat source term compared to the case where heat source term was not included.

# Chapter 3

Freezing immediately followed by a rapid and strong heating of targeted tissue can significantly improve the treatment effect by providing double chance to possibly kill tissues; further subsequent freezing of the tumor treated by hyperthermia will help to reduce the chance of bleeding from the tissue [73, 74]. This suggests the combined use of these therapies. Due to large differences in thermal properties of the dense tumor tissue and low dense surrounding lung tissue, the physical phenomena associated with heat transfer during cryosurgery and hyperthermia in lung are interesting and unique [11]. In present chapter Pennes bioheat Equation is used to find transient temperature profile, freezing and thawing interface during combined cryosurgery and hyperthermia treatment of lung. Three blood reflow patterns when (i) blood vessel take very short time to resume its function on thawing (Case 1), (ii) blood vessel are completely destroyed (Case 2) and (iii) blood vessel need a time delay to resume on thawing (Case 3), the frozen tissue, were also taken into account [157]. The temperature rising in tissue has been found highest for case 1 and least for case 2. Temperature profiles and phase change interfaces are obtained for all cases. Information obtained are beneficial to know whether the tumor has been damaged or not, and to minimize the damage to neighboring healthy lung tissue by over-freezing and overheating, and hence to optimize the treatment planning.

# Chapter 4

Thawing is the reverse process of freezing. It is an essential part of cryosurgery and cryopreservation. In cryosurgery during freezing, some healthy tissues may also freeze. These frozen tissues can resume their state due to heat supply by body metabolism and blood perfusion, but if freezing is deep then tissue will remain in frozen state for a longer time and

hence may damage, in this case external heating is needed to warm them. Further, in cryopreservation to obtain an optimal recovery of skin, quantitative evaluation of the temperature history during the phase change is highly desirable [72]. In this chapter transient temperature profile and position of phase change interfaces are obtained numerically, which is important to apply cryosurgery precisely. Informations from this study are significant for the operation of a successful cryosurgical treatment and can also be applied to cryopreserved living organ.

# Chapter 5

Biological tissues can be treated as porous media as it is composed of dispersed cell separated by connective voids which allow flow of nutrients, minerals etc. to reach all cell within the tissue [64]. In present chapter, a mathematical model has been developed to study the phase change phenomena during freezing and thawing process in biological tissues considered as porous media. Numerical simulation is used to study the effect of porosity, on the motion of freezing and thawing front and transient temperature distribution in tissue. It is observed that porosity has significant effect on transient temp profile and phase change interfaces, further decrease in freezing and heating rate has been found with increased value of porosity.

# Chapter 6

The effects of volumetric energy generation on phase change problem are important for many engineering application including casting of nuclear waste materials, vivo freezing of biological tissues and solar collectors etc. Recently Jiji et al. [61] gave a quasi-steady analysis of heat generation effect on freezing and melting process in phase change material. In general there is a need of transient study of system [80]. In this chapter, transient heat

transfer analysis has been done to study the effect of volumetric heat generation on one-dimensional solidification in finite media with convective cooling. The whole process is divided in four different stages [63]. It is found that motion of freezing interface slows down with increase in heat generation rate, while it accelerates with respect to increased rate of convective cooling.

# Chapter 2

# A PARAMETRIC STUDY ON PHASE CHANGE HEAT TRANSFER PROCESS DURING CRYOSURGERY OF LUNG TUMOR

# 2.1 INTRODUCTION

The primary goal of cryosurgery is to maximize all mechanism that produces maximal destruction to undesired tissues while minimizing damage to surrounding healthy tissue [11, 24]. The factors affecting cell injury during cryosurgery include the lowest temperature in the tissue, the duration of frozen cycle, the rate of freezing front propagation, the thawing rate and the freezing/thawing cycles etc. [46-48, 56, 84, 109, 128, 133]. The factors which affect necrosis such as the lowest temperature in the tissue or the rate of freezing front propagation depend on the biophysical parameters, that are present in a given cryosurgical procedure, some of which may be selected and controlled by the surgeons. These parameters include the temperature and duration of freezing-thawing process, the shape and size of cryoprobe, the heat capacity, the thermal conductivity of the tissue, the rate of blood flow and rate of metabolic heat generatio in the involved tissue [3].

In this regard, *in vitro* experiments were made by Augustynowicz et al. [4] to study the thermal relationship between the temperature of probe and the tissue in contact with the probe. In another experiment Gage et al. [48] investigated the effect of varying freezing rate, duration of freezing and thawing on cell destruction in dog skin. They suggested that the use of a probe as cold as possible, speeds freezing, expedites and increases the frozen volume of

the tissue. Blood perfusion and metabolic heat generation also have significant effect on heat transfer in tissues [106, 107, 158]. Negligence of these terms can result up to 20% error in the result for the radius of the frozen zone [29]. The literature reveals that mathematical study on the effect of these parameters on phase change heat transfer process during cryosurgery is rare.

Due to large differences in thermal properties of the dense tumor tissue and low dense surrounding lung tissue, the physical phenomena associated with heat transfer during cryosurgery in lung are interesting and unique. Bischof et al. [11] studied the freezing behavior of lung and tumor embedded in lung analytically and numerically. Lee and Bastacky [70] compared the freezing behavior of solid and lung tissues at macroscopic and microscopic level mathematically. They concluded that at macroscopic level freezing behavior of lung and solid tissues is same, while at microscopic level, surface of lung achieve ultra rapid rate twice than those of solid tissue. Further minimum cooling rate is found twice order of magnitude faster in lung tissues than in solid tissues. In another study Schweikert et al. [120] investigated cryosurgical freezing of dense lung tumors within healthy lung tissue using numerical and order of magnitude analysis. In above studies of lung cancer, simple heat equation is used and the heat generation due to metabolism and blood perfusion is also not considered, that is an essential part of *in vivo* study.

In order to apply cryosurgery effectively, the knowledge of temperature transients in tumor and normal tissues as well as position of freezing interfaces are needed, to say whether the tumor is damaged or not and to minimize the injury to healthy tissues.

In the present chapter a numerical study on the phase change heat transfer process during cryosurgery in lung tumor is presented. Penees bioheat equation [99] is used to study

the effect of cryoprobe radius, cryoprobe temperature, heat source term due to blood perfusion and metabolism on freezing process of tissues. Non-ideal property of tissues has been used. Finite difference method using enthalpy approach is used to solve the mathematical model.

# 2. 2 PROBLEM DESCRIPTION

The schematic presentation of the physical problem is shown in Figure 2.1. Tumor of radius b=1.5 cm is embedded in lung of radius a=4.0 cm. Cryoprobe of radius  $r_c$  with freezing temperature  $T_c$  is placed at r=0.

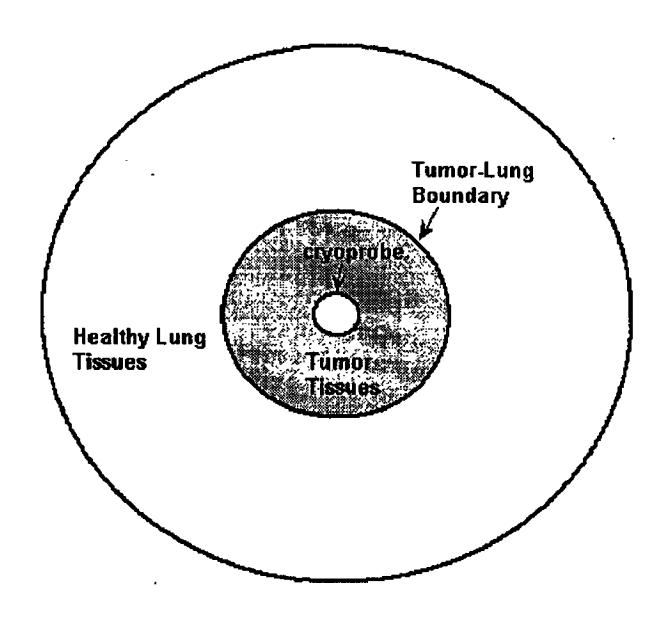


Figure 2.1 Schematic representation of physical problem

# 2.3 MATHEMATICAL MODEL

# 2.3.1 Governing Equation

Enthalpy formulation of bio-heat equation for phase change problem is given as

$$\rho \frac{\partial H}{\partial t} = \frac{1}{r} \frac{\partial}{\partial r} \left( kr \frac{\partial T}{\partial r} \right) + w_b \rho_b c_b (T_b - T) + Q_m, \qquad (2.1)$$

where  $\rho$  is density of tissue; H, enthalpy; k, thermal conductivity;  $c_b$ , specific heat of blood;  $w_b$ , blood perfusion rate; T, temperature; t, time; r, radial coordinate;  $T_b$ , arterial blood temperature and  $Q_m$  is the metabolic heat generation in the tissue. Enthalpy and tissue temperature are related as [12, 52]

$$H = \begin{cases} c_{f}(T - T_{ms}) & T < T_{ms} \\ (T - T_{ms}) \left(\frac{1}{2}(c_{f} + c_{u}) + \frac{L}{(T_{ml} - T_{ms})}\right) & T_{ms} \le T \le T_{ml} , \\ L + \frac{1}{2}(c_{f} + c_{u})(T_{ml} - T_{ms}) + c_{u}(T - T_{ml}) & T > T_{ml} \end{cases}$$
(2.2)

where  $T_{ml}$  and  $T_{ms}$  are liquidus (-1°C) and solidus (-8 °C) temperatures. L, is latent heat, subscripts f and u are for frozen and unfrozen state respectively.

# 2.3.2 Assumptions

Following assumptions have been made to solve the bio-heat transfer model:

- (i) Heat transfer is purely by conduction [14].
- (ii) Non-ideal property of tissues is used with liquidus and solidus temperature as -1°C and -8 °C respectively [103].
- (iii) Thermo-physical properties are different in frozen and unfrozen region.
- (iv) Thermal properties of tumor and lung tissues are different [11, 35, 120].

# 2.3.3 Initial and Boundary Conditions

(i) Initially whole region is assumed at body core temperature (37 °C), i.e.

$$T(r,t) = 37$$
 °C at  $t = 0$ ,

(ii) Outer boundary of the lung region is far away from cryoprobe and in contact with body, so temperature at this is taken equal to body core temperature, i.e.

$$T(r,t) = 37$$
 °C at  $r = a$ ,

- (iii) At  $r = r_c$ , where  $r_c$  is probe radius, constant cryoprobe temperature  $T_c$  is taken, i.e.  $T(r,t) = T_c$ , at  $r = r_c$ ,
- (iv) Continuity of temperature and flux on tumor-lung boundary

$$k_t \frac{\partial T_i(r,t)}{\partial x} = k_l \frac{\partial T_l(r,t)}{\partial x}$$
 and  $T_t = T_l$  at  $r = b$ ;

where subscripts t and l are for tumor and lung tissues respectively.

# 2.4 NUMERICAL SOLUTION

Taking  $r_i = i\Delta r$ ,  $t_p = p\Delta t$  and using central difference for space derivative and forward difference for time derivative, finite difference explicit scheme [52] for equation (2.1)

$$H_{i}^{p+1} = H_{i}^{p} + \frac{\Delta t \, k_{i}^{p}}{(\Delta r)^{2} \, \rho_{i}^{p}} \left\{ \left( 1 + \frac{1}{2i} \right) T_{i+1}^{p} - 2 T_{i}^{p} + \left( 1 - \frac{1}{2i} \right) T_{i-1}^{p} \right\} + \frac{\Delta t}{\rho_{i}^{k}} \left\{ \left( Q_{m} \right)_{i}^{p} + \left( w_{b} \right)_{i}^{p} \, \rho_{b} c_{b} \left( T_{b} - T_{i}^{p} \right) \right\}.$$

$$(2.3)$$

Where, i and k are space and time step respectively.  $\Delta r$  and  $\Delta t$  are the increment in space and time respectively. To satisfy the stability criteria,  $\alpha_{\max} \frac{\Delta t}{(\Delta r)^2} \leq \frac{1}{2}$ , where  $\alpha_{\max}$  is the maximum value of thermal diffusivity [52], space and time increments are taken as 0.05 cm and 0.001 sec respectively.

After calculating enthalpy at  $(p+1)^{th}$  time level, temperature distribution at  $(p+1)^{th}$  time level is calculated by reverting equation (2.2). Once the new temperature field is

obtained from enthalpy, the process repeats. Isotherms at -1°C and -8 °C give the position of upper and lower phase change interfaces s(t) respectively. The values of thermo-physical parameters used are listed in table 2.1.

Table 2.1: Thermal properties of tissues [11, 35, 120]

Parameter	Value
Density of unfrozen lung tissue (kg/m³)	161
Density of frozen lung tissue (kg/m³)	149
Density of unfrozen tumor tissue (kg/m³)	998
Density of frozen tumor tissue (kg/m³)	921
Density of blood (kg/m <sup>3</sup> )	1005
Specific heat of unfrozen lung tissue (J/kg °C)	4174
Specific heat of frozen lung tissue (J/kg °C)	1221
Specific heat of unfrozen tumor tissue (J/kg °C)	4200
Specific heat of frozen tumor tissue (J/kg °C)	1230
Thermal conductivity of unfrozen lung tissue (W/m °C)	0.11
Thermal conductivity of frozen lung tissue (W/m °C)	0.38
Thermal conductivity of unfrozen tumor tissue (W/m °C)	0.552
Thermal conductivity of frozen tumor tissue (W/m °C)	2.25
Latent heat (KJ/kg)	333
Metabolic heat generation in lung (W/m <sup>3</sup> )	672
Metabolic heat generation in tumor (W/m³)	42000
Blood perfusion in lung (ml/s/ml)	0.0005
Blood perfusion in tumor (ml/s/ml)	0.002
The upper limit of phase change (°C)	-1.
The lower limit of phase change (°C)	-8
Arterial blood temperature (°C)	37

# 2. 5 RESULTS AND DISCUSSION

The temperature distribution and propagation of freezing interface in tissue are important to monitor the tumor damage and sparing healthy tissue. The effect of various parameters on cell destruction, temperature profile and freezing extent has been obtained.

# 2. 5. 1 Effect of Cryoprobe Radius

To study the effect of cryoprobe radius on cell destruction, cryoprobe of 3, 5 and 8 mm in diameter [24] with freezing temperature -196 °C are simulated to freeze the tissue for 900 sec. Temperature profiles in tissue for three cryoprobe at t = 300 sec, 700 sec and 900 sec are shown in figure 2.2. It is found that temperature profiles for all the cryoprobe have similar shape, but increase in minimum temperature is observed with increase in diameter. It indicates that the larger diameter of cryoprobe corresponds to the lower freezing temperature in tissue.

Figure 2.3 represents the position of freezing interfaces with respect to time. Freezing interfaces move fast and produce larger freezing region for 8 mm cryoprobe compared to 3

Table 2.2: Position of freezing interfaces after 900 sec freezing for cryoprobes with 3 mm, 5 mm and 8 mm diameter

Cryoprobe	3 mm		5 mm		8mm	
Diameter	3 11111		J IIIII			
Freezing	Time	Position	Time	Position	Time	Position
Interface	(sec)	(cm)	(sec)	(cm)	(sec)	(cm)
Upper	883.0	2.1	879.45	2.45	873.70	2.70
Lower	896.30	2.0	864.35	2.35	860.9	2.60

and 5 mm cryoprobe. Position of freezing interfaces after  $t = 900 \,\mathrm{sec}$  is listed in table 2.2. It is observed from table 2.2, that cryoprobe with 5 mm and 8 mm diameter penetrates 0.35 cm and 0.60 cm more distance as compared to 3 mm cryoprobe. The reduction in time to freeze the tumor is found 236.0 sec and 417.1 sec for 5 and 8 mm cryoprobe compared to 3 mm cryoprobe (Table 2.3).

Simulation results show that 8 mm cryoprobe produces lowest temperature and maximum freezing area in tissue. The reason is that cryoprobe of larger diameter provides greater physical area between its surface and tissue, hence larger heat is removed by cryoprobe producing better—freezing potential and freezing range.

Table 2.3: Time to reach freezing interface at tumor-lung boundary for cryoprobes with 3 mm, 5 mm and 8 mm diameter

Cryoprobe Diameter	3 mm (base case for comparison)		5 mm		8mm	
Freezing Interface	Upper	Lower	Upper	Lower	Upper	Lower
Time (sec)	630.5	698.0	408.9	462	247.4	280.9
Decrease in Time (sec)	_	-	221.6	236.0	383.1	417.1

# 2. 5. 2 Effect of Cryoprobe Temperature

Cryoprobes with 3 mm diameter with freezing temperature  $T_s = -196 \,^{\circ}\text{C}$ ,  $-150 \,^{\circ}\text{C}$  and  $-120 \,^{\circ}\text{C}$  are used to study the effect of cryoprobe temperature on temperature profile and freezing front position in tissue. Freezing time is taken as 2000 sec.

Figure 2.4 shows the temperature profile in tissue for different cryoprobe temperature at  $t=500\,$  sec, 1000 sec, 1500 sec and 2000 sec. At  $t=500\,$  sec temperature profiles have same shape for all  $T_s$ , But at  $t=1000\,$  sec temperature profile corresponding to  $T_s=-120\,$  °C and -150 °C have similar shape while profile for  $T_s=-196\,$  °C differs from these two, the reason is that cryoprobe with  $T_s=-196\,$  °C produces fast cooling resulting in fast freezing of the lung tissues. Frozen lung tissue has different thermo-physical properties. Due to the change in thermo-physical properties of frozen lung tissues the freezing accelerates, hence producing fast temperature gradient compared to  $T_s=-120\,$  °C and  $T_s=-196\,$  °C. Same is the case for different profile corresponding to  $T_s=-120\,$  °C than  $T_s=-150\,$  °C and  $T_s=-196\,$  °C at time  $t=1500\,$  sec. At

**Table 2.4:** Position of freezing interfaces after 2000 sec freezing for cryoprobes with  $T_s = -120 \,^{\circ}\text{C}, -150 \,^{\circ}\text{C}$  and  $-196 \,^{\circ}\text{C}$ 

Cryoprobe	-120 °C		-150 °C		-196 ℃		141
Temperature							
Freezing	Time	Position	Time	Position	Time	Position	
Interface	(sec)	(cm)	(sec)	(cm)	(sec)	(cm)	
Upper	1947.10	2.0	1909.2	2.40	1863.85	2.75	
Lower	1932.15	1.9	1909.55	2.30	1867.10	2.65	

t=2000 sec temperature profiles again have same shape. It is also observed that minimum temperature in tissue increases with decrease in  $T_s$  and least corresponds to  $T_s=-196\,^{\circ}\mathrm{C}$ .

**Table 2.5:** Time to reach freezing interface at tumor-lung boundary for cryoprobes with  $T_c = -120 \,^{\circ}\text{C}, -150 \,^{\circ}\text{C}$  and  $-196 \,^{\circ}\text{C}$ 

Cryoprobe Temperature	-120 °C (base case for comparison)		-150 °C		-196 °C	
Freezing Interface	Upper	Lower	Upper	Lower	Upper	Lower
Time (sec)	1464.10	1617.40	943.95	1047.02	630.50	698.0
Decrease in Time (sec)	_	-	520.15	570.38	830.60	919.40

The position of freezing fronts for different  $T_s$  is shown in Figure 2.5. The cryoprobe with  $T_s = -196\,^{\circ}\text{C}$  produces 39.47% and 15.22% increase in freezing region compared to  $T_s = -120\,^{\circ}\text{C}$  and  $T_s = -150\,^{\circ}\text{C}$  respectively (Table 2.4). Also from Table 2.5, cryoprobe with  $T_s = -150\,^{\circ}\text{C}$  and  $-196\,^{\circ}\text{C}$  take 570.38 sec and 919.4 sec lesser time respectively, than  $T_s = -120\,^{\circ}\text{C}$  to freeze the tumor. Reason is that cryoprobe with lowest temperature removes maximum heat from tissue thus results in lowest temperature, fast cooling and largest freezing extent.

# 2. 5. 3 Effect of Metabolism and Blood Perfusion

To study the effect of heat source term  $q = w_b \rho_b c_b (T_b - T) + Q_m$ , cryoprobe of 3 mm diameter with  $T_c = -196$ °C is used to freeze the tissue for 900 sec. Lower temperature is observed in tissue for the case without heat source term compared to the case with heat source term (Figure 2. 6).

Figure 2.7 shows the freezing front position for the case with and without heat source

term. It is observed that freezing interfaces move fast and produce larger freezing area for the case of without q than the case with q. After 900 sec freezing upper and lower freezing interface cover a distance 2.4 cm and 2.3 cm respectively in tissue for the case without q respectively, while they reaches at a distance 2.1 cm and 2.0 cm for the case with q. Also time taken to freeze the tumor is 564.70 sec and 698.0 sec for the case without q and with q respectively.

The presence of heat source term increases the difficulty of freezing the targeted tissue, the freezing rate and the minimum temperature in tissue. Thus metabolic heat generation and blood perfusion have a significant effect on temperature profile, freezing interface propagation in tissue.

# 2.6 CONCLUSION

The effect of cryoprobe diameter, cryoprobe temperature and heat generation due to metabolism and blood perfusion on phase change heat transfer process during cryosurgery in lung tumor has been analyzed numerically. Results show that (i) increase in cryoprobe diameter (ii) decrease in cryoprobe freezing temperature, lead to increase in minimum temperature, freezing rate, freezing area in tissue and decrease in time to freeze the tumor. Further decrease in minimum temperature, cooling rate, freezing area and increase in time to freeze tumor has been observed with the presence of heat source term compared to the case where heat source term was not included. Results obtained are expected to be helpful in preselecting the parameters to optimize the freezing protocols.

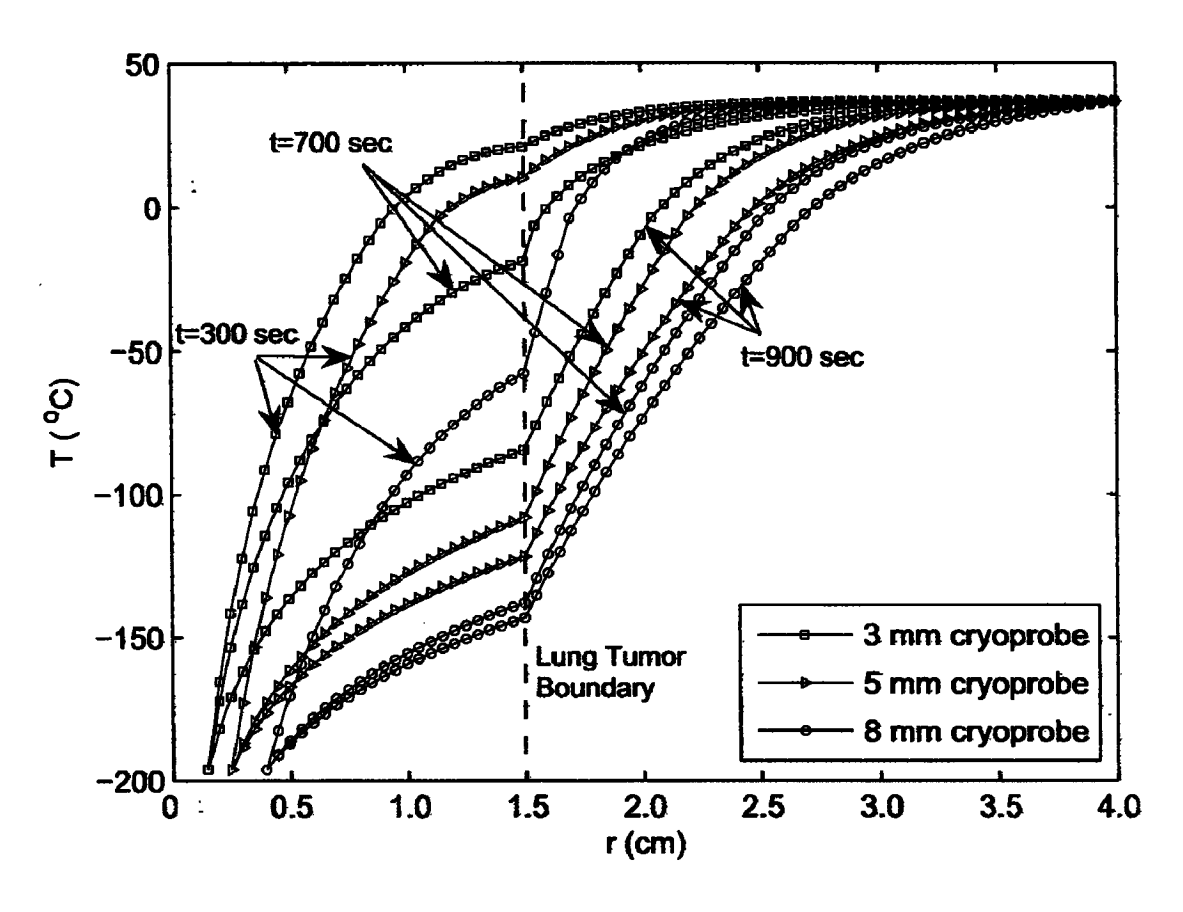


Figure 2.2: Temperature profile for cryoprobe of 3, 5 and 8 mm diameter.

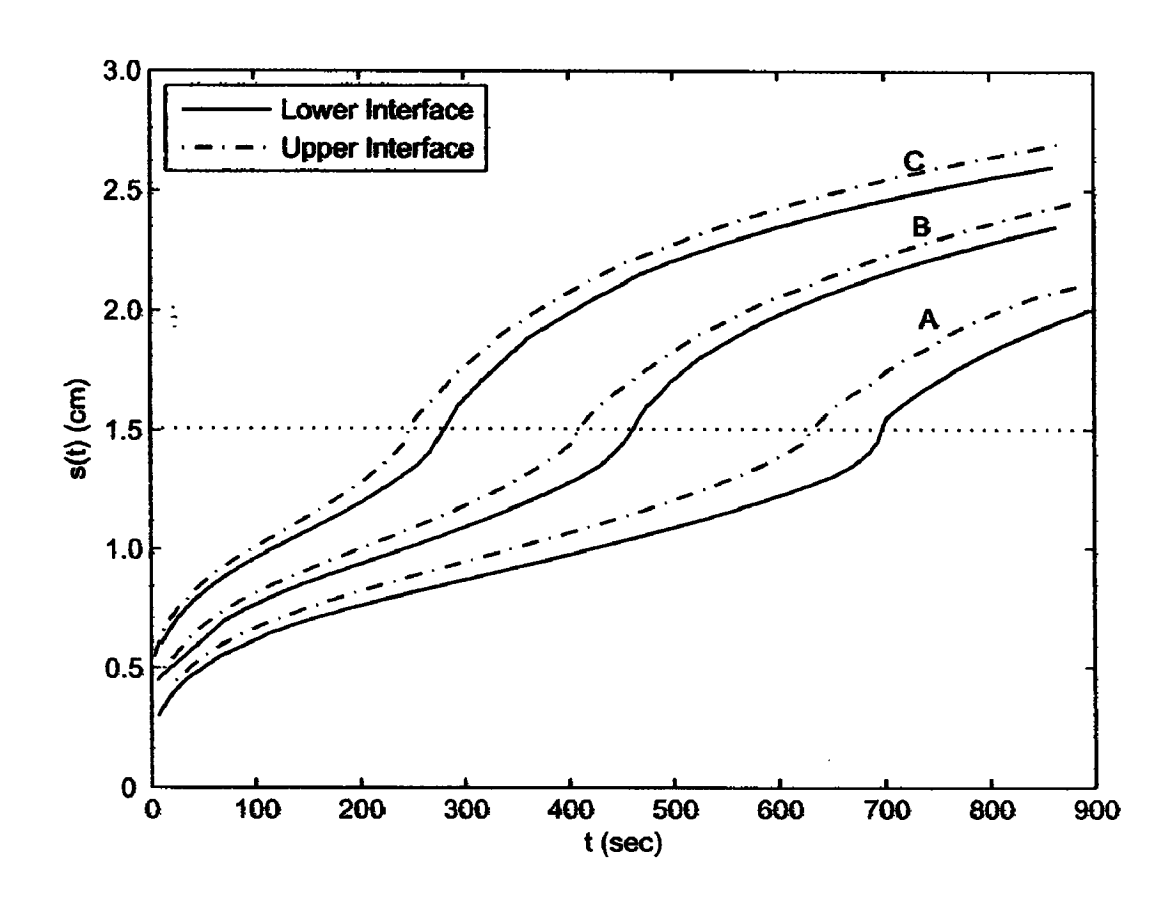


Figure 2.3: Phase change interfaces for cryoprobe of (A) 3 mm, (B) 5 mm and (C) 8 mm diameter.

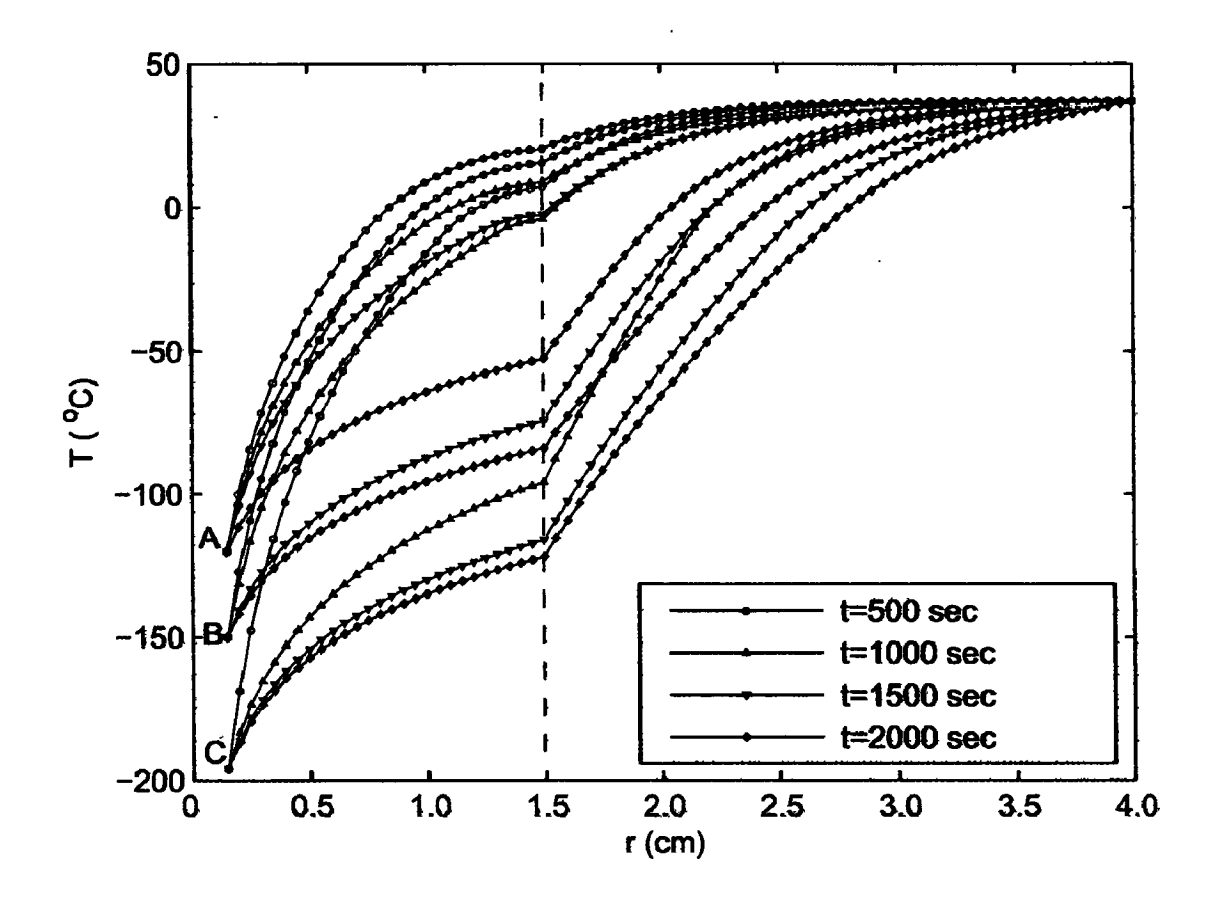


Figure 2.4: Temperature profile for cryoprobe freezing temperature (A) -120 °C, (B) -150 °C and (C) -196 °C.

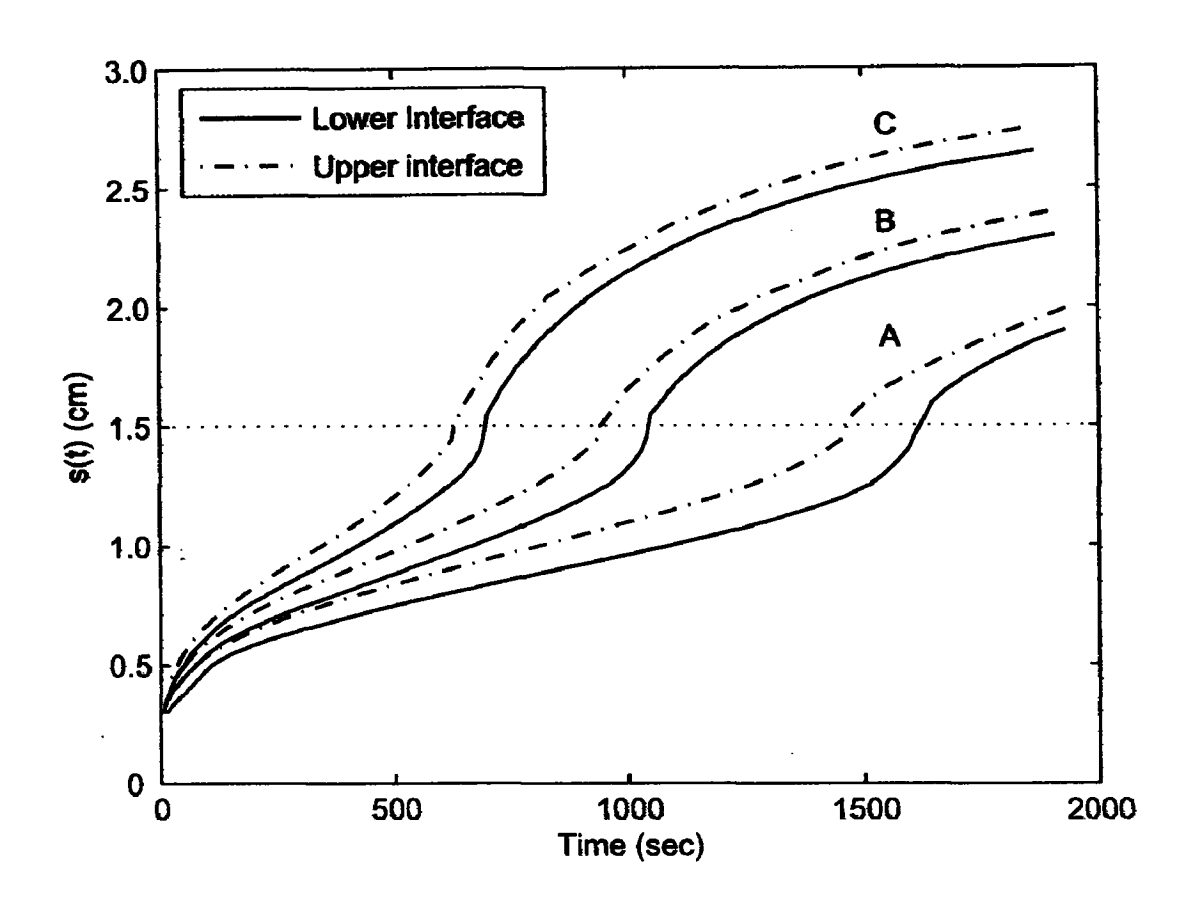


Figure 2.5: Phase change interfaces for cryoprobe freezing temperature (A)  $-120\,^oC,$  (B)  $-150\,^oC$  and (C)  $-196\,^oC.$ 

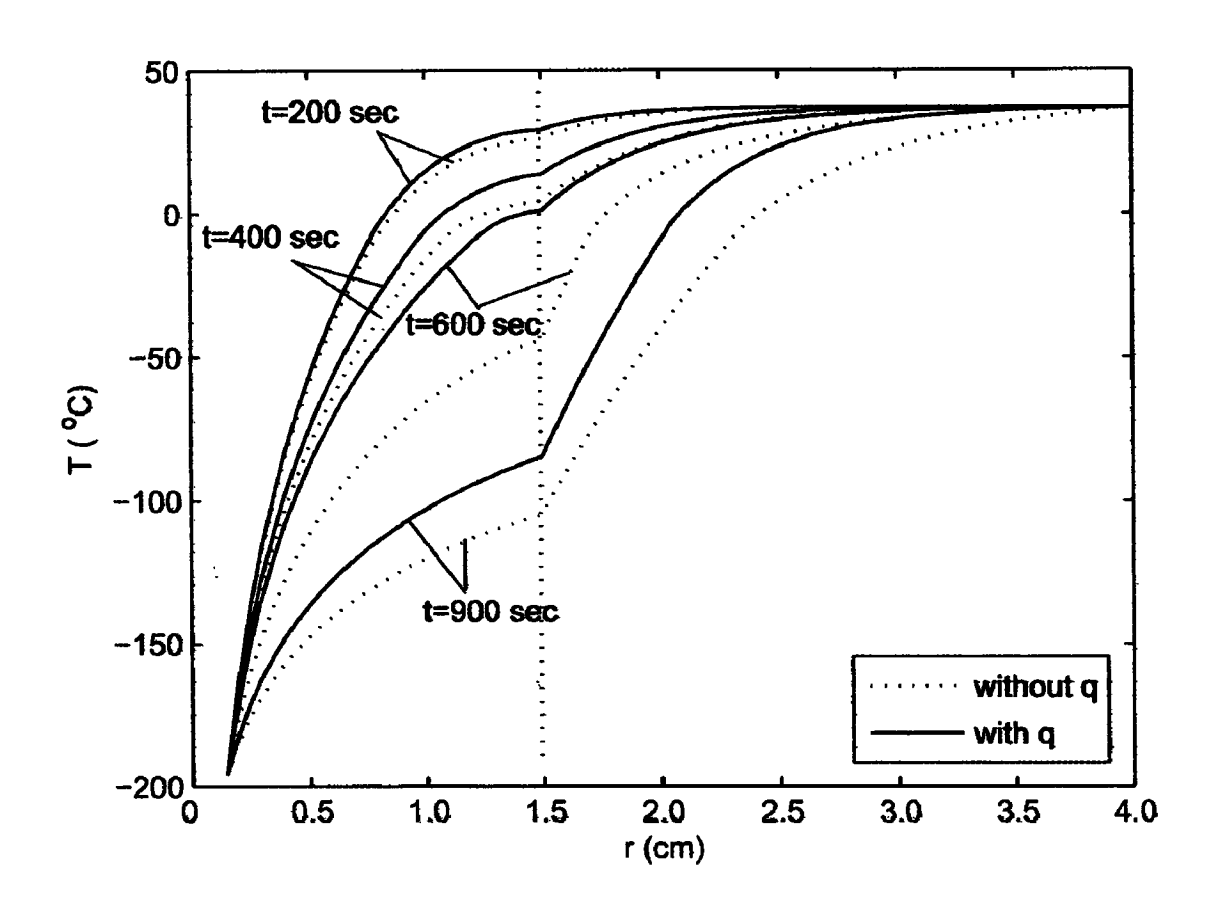


Figure 2.6: Temperature profile for the case with and without heat source term (q).

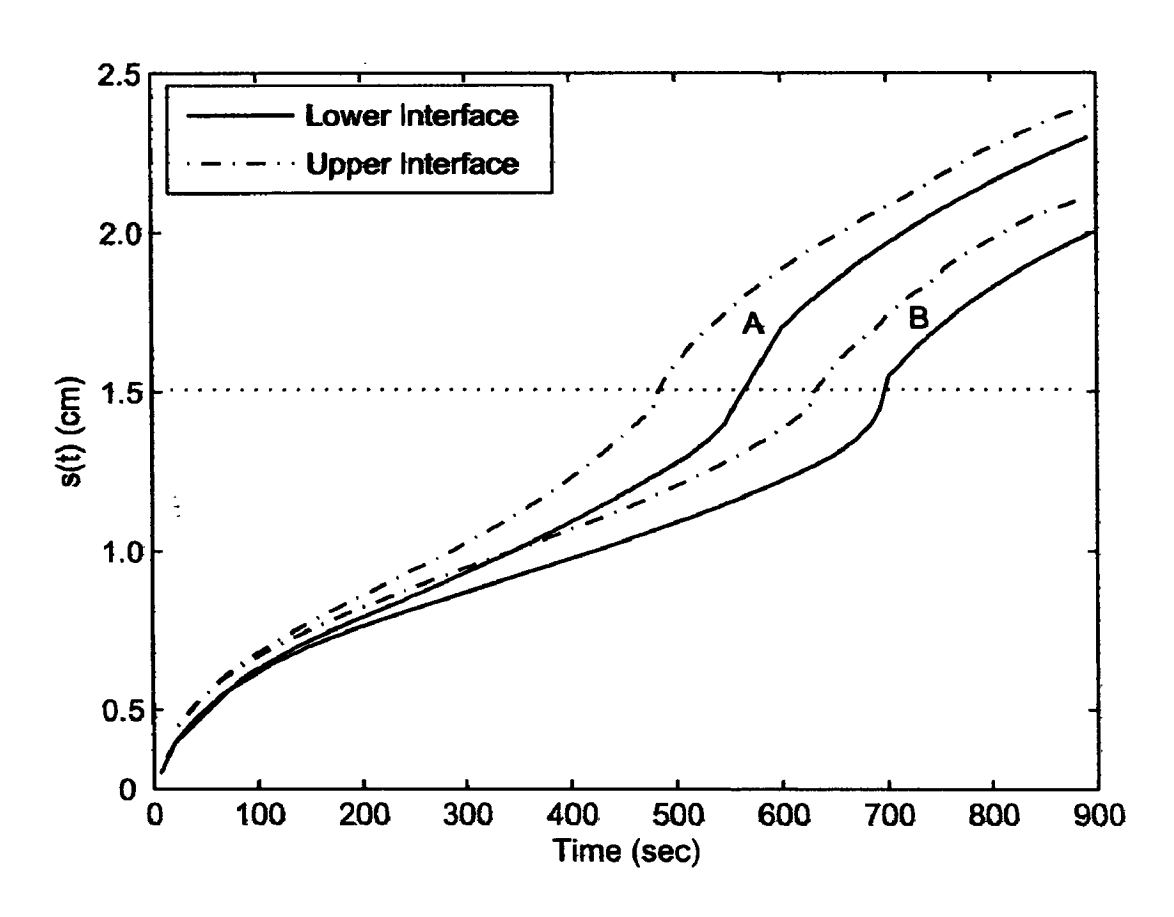


Figure 2.7: Phase change interfaces for the cases (A) without q and (B) with q.



•

# **Chapter 3**

# NUMERICAL STUDY ON COMBINED HYPERTHERMIA AND CRYOSURGICAL TREATMENT OF LUNG CANCER

# 3.1 INTRODUCTION

Lung cancer is the most common cancer worldwide accounting for 1.2 million new cases annually and is responsible for 17.8% of all cancer deaths [149]. Cryosurgery, chemotherapy, hyperthermia and radiotherapy etc. are the medical techniques to treat them. Cryosurgery is use of extremely low temperature with an instrument called as cryoprobe to abalate the targeted tissues [9], while hyperthermia in cancer therapy is to raise the temperature of cancerous tissue above therapeutic value (42 °C) [44]

Liu et al. [73, 74] carried out that freezing immediately followed by a rapid and strong heating of targeted tissues can significantly improve the treatment effect by providing double chance to possibly kill them. Further subsequent freezing of the tumor treated by hyperthermia will help to reduce the chance of bleeding from the tissues [34]. This suggests the combined use of these therapies.

In order to apply cryosurgery effectively, the knowledge of temperature transients in tumor and normal tissues, as well as position of freezing/thawing interface are important to say whether the tumor is damaged or not and to minimize the injury to healthy tissues. Numerous experimental and analytical studies have been done on cryosurgery and hyperthermia therapy alone in various types of cancer [3, 11, 31, 52, 70, 76, 79, 112, 114, 116 120, 160], but little is available on the combined effects of these two. Only Deng and Liu [35]

used effective heat capacity method to perform comprehensive analysis on freezing/thawing behavior of skin tissues with tumor, during combined cryosurgery and hyperthermia.

In present study, Pennes bioheat equation with phase change has been used to find transient temperature profiles, freezing and thawing interfaces during combined cryosurgery and hyperthermia treatment of lung cancer. Non-ideal property of tissues, metabolic heat generation and blood perfusion has been taken into account. Three blood re-flow patterns, when (i) blood vessels take very short time to resume their functioning on thawing; (ii) blood vessels are completely destroyed, and (iii) blood vessels need a time delay to resume on thawing the frozen tissue, were also taken into account [157]. Enthalpy method is used to solve the mathematical model.

#### 3.2 PROBLEM DESCRIPTION

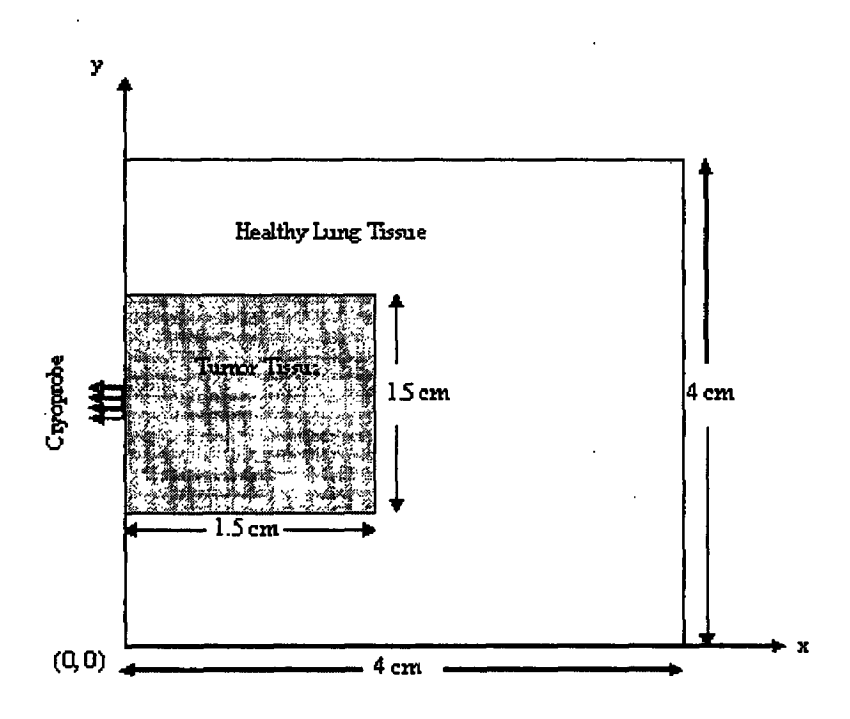


Figure 3.1: Schematic representation of physical problem

Figure 3.1 shows the schematic presentation of the physical problem. Tumor of dimension 1.5 cm×1.5 cm is embedded in lung of dimension 4.0 cm×4.0 cm. Tumor domain is  $0 \le x \le 1.5$  cm, 1.25 cm  $\le y \le 2.75$  cm. Cryoprobe is placed at x = 0, 1.18 cm  $\le y \le 2.2$  cm.

#### 3.3 MATHEMATICAL MODEL

# 3.3.1 Governing Equation

Enthalpy formulation of bio-heat equation for phase change problem associated with freezing and heating is given as [99]

$$\rho \frac{\partial H}{\partial t} = \frac{\partial}{\partial x} (k \frac{\partial T}{\partial x}) + \frac{\partial}{\partial y} (k \frac{\partial T}{\partial y}) + w_b \rho_b c_b (T_b - T) + Q_m, \qquad (3.1)$$

where  $\rho$  is density of tissue; H, enthalpy; k, thermal conductivity;  $c_b$ , specific heat of blood;  $w_b$ , blood perfusion rate; T, temperature; t, time;  $T_b$ , arterial blood temperature and  $Q_m$ , the metabolic heat generation in the tissue. Enthalpy and tissue temperature are related as [52]

$$H = \begin{cases} c_{f}(T - T_{ms}) & T < T_{ms} \\ (T - T_{ms}) \left(\frac{1}{2}(c_{f} + c_{u}) + \frac{L}{(T_{ml} - T_{ms})}\right) & T_{ms} \le T \le T_{ml}, \\ L + \frac{1}{2}(c_{f} + c_{u})(T_{ml} - T_{ms}) + c_{u}(T - T_{ml}) & T > T_{ml} \end{cases}$$
(3.2)

where  $T_{ml}$  and  $T_{ms}$  are liquidus (-1 °C) and solidus (-8 °C) temperatures. Subscripts f and u are for frozen and unfrozen state respectively.

# 3.3.2 Assumptions

Following assumptions have been made to solve the bio-heat transfer model

- (i) Heat transfer is purely by conduction. [14].
- (ii) Non-ideal property of tissues is used with liquidus and solidus temperature as -1 °C and -8 °C respectively [103].
- (iii) Heat source due to metabolism and blood perfusion is present only when tissue is in unfrozen/unburned state [34].
- (iv) Thermo-physical properties in frozen and unfrozen region are different but constant.
- (v) Thermal properties of tumor and healthy lung tissues are different [11, 34, 120].
- (vi) Thawing is assumed to occur over the same temperature range as for freezing, and complete thawing is obtained when temperature everywhere in the domain has exceed the upper phase change limit [102].

# 3.3.3 Initial and Boundary Conditions

(i) Initially whole region is at body core temperature, i.e.

$$T(x, y, t) = 37 \,^{\circ}C$$
 at  $t = 0$ ,

(i) Cryoprobe is placed at x = 0, 1.8 cm  $\le y \le 2.2$  cm, i.e.

$$T(x, y, t) = T_c$$
 at  $x = 0, 1.8 \text{ cm} \le y \le 2.2 \text{ cm}$ ,

(ii) At x = 0,  $0 \le y \le 1.8$  cm and 2.2 cm  $\le y \le 4.0$  cm, adiabatic condition has been assumed, i.e.

$$\frac{\partial T(x,y,t)}{\partial x} = 0 \text{ at } x = 0, \ 0 \le y \le 1.8 \text{ cm} \text{ and } 2.2 \text{ cm} \le y \le 4.0 \text{ cm},$$

(iii) Outer boundary is far away from cryoprobe, so assumed at body core temperature i.e.

$$T(x, y, t) = 37$$
 °C at  $0 \le x \le 4.0$  cm,  $y = 0$  and  $y = 4.0$  cm;  $x = 4.0$  cm,  $0 \le y \le 4.0$  cm,

(iv) Continuity of flux and temperature at lung-tumor boundary i.e.

 $k_t \frac{\partial T_t(x, y, t)}{\partial x} = k_t \frac{\partial T_l(x, y, t)}{\partial x}$  and  $T_t = T_l$  at  $0 \le x \le 1.5 \,\text{cm}$ ,  $y = 1.25 \,\text{cm}$  and  $y = 2.75 \,\text{cm}$ ;  $x = 1.5 \,\text{cm}$ ,  $1.25 \,\text{cm} \le y \le 2.75 \,\text{cm}$ , where subscripts t and t are for tumor and healthy lung tissues respectively.

# 3.4 NUMERICAL SOLUTION

Finite difference explicit scheme is used to solve the above mathematical model. Taking  $x_i = i\Delta x$ ,  $y_j = j\Delta y$  ( $\Delta x = \Delta y$ ) and  $t_p = p\Delta t$ ; the enthalpy at time step (p+1) has been given as

$$H_{i,j}^{p+1} = H_{i,j}^{p} + \frac{\Delta t \, k_{i,j}^{p}}{(\Delta x)^{2} \, \rho_{i,j}^{p}} \left\{ T_{l+1,j}^{p} + T_{l,j+1}^{p} - 4 T_{l,j}^{p} + T_{l-1,j}^{p} + T_{l-1,j}^{p} \right\} + \frac{\Delta t}{\rho_{i,l}^{p}} \left\{ \left( Q_{m} \right)_{i,j}^{p} + \left( w_{b} \right)_{i,j}^{p} \, \rho_{b} c_{b} \left( T_{b} - T_{i,j}^{p} \right) \right\},$$

$$(3.3)$$

where i, j are space step in x and y direction respectively and p is time step.  $\Delta x$ ,  $\Delta y$  and  $\Delta t$  are the increment in x-axis, y-axis and time respectively. Time and space increments are adjusted in such a way that they satisfy the stability criteria

$$\max \left\{ \alpha_{\max} \frac{\Delta t}{(\Delta x)^2}, \alpha_{\max} \frac{\Delta t}{(\Delta y)^2} \right\} \leq \frac{1}{4},$$

where  $\alpha_{\text{max}}$  is the maximum value of thermal diffusivity [52]. After calculating enthalpy at  $(p+1)^{th}$  time level, temperature distribution at  $(p+1)^{th}$  time level is calculated by reverting equation (3.2). Once the new temperature field is obtained from enthalpy, the process repeats. Isotherms at -1 °C and -8 °C give the position of upper and lower phase change (freezing/thawing) interfaces respectively.

# 3. 5 RESULTS AND DISCUSSION

To study the freezing and heating process the cryoprobe temperature has been taken -196 °C for  $0 \le t \le 800$  sec during freezing and 80 °C for 800 sec  $\le t \le 2100$  sec during heating. Parameters and thermo-physical properties of tumor and lung are listed in Table 2.1. Figure 3.2 shows the position of phase change interface in x-direction at y = 2.0 cm during freezing. The lower interface reaches at x = 1.95 cm at t = 800 sec, while upper interface reaches at x = 2.10 cm at t = 785.0 sec. Due to smaller thermal conductivity of lung than tumor, a higher thermal gradient is required in it for the requirement of heat flux continuity at tumor-lung boundary. Thus interfaces accelerate as they leave the tumor and enter the surrounding low dense healthy lung tissues. This confirms the earlier work of Bischof et al. [11].

Figure 3.3 shows the temperature profile at t = 200 sec, 400 sec, 600 sec and 800 sec, during freezing. After 800 sec, the maximum temperature in tumor region is -60.77 °C, which is much lower than lethal temperature (-30 °C). The positions of freezing interfaces are shown in Figure 3.4. That is important to know the freezing necrosis extent in tumor. These informations are beneficial to control the freezing and hence to minimize the damage to healthy lung tissues, because over-freezing may cause an irreversible injury to the neighboring lung tissues.

Subsequently strong heating with  $T_c = 80$  °C is applied after 800 sec freezing. During the heating process, thawing interfaces move in two directions, one toward the cryoprobe from body core due to the heat supply by blood perfusion and another inside the tissue from cryoprobe due to the heating of cryoprobe. When these two interfaces meet, the tissue is supposed to be fully thawed. Figure 3.5 shows the position of thawing interfaces in

x-direction at y = 2.0 cm, the upper interfaces meet at t = 1350 sec at a distance x = 1.45 cm, while lower interfaces meet at t = 1136 sec at a distance x = 1.30 cm. Figure 3.6 shows the position of thawing interfaces in 2-D. At t = 1350 sec the frozen region is fully thawed. Temperature distribution at t = 900 sec, t = 1136 sec and t = 1350 sec during thawing are shown in Figure 3.7.

Three typical blood re-flow patterns have been considered after thawing, case 1: when blood vessels take very short time to resume their functioning on thawing; case 2: blood vessels are completely destroyed during freezing, and case 3: blood vessels need a time delay to resume on thawing [157].

Figure 3.8, 3.9 and 3.10 show the temperature contours for case 1, 2 and 3 respectively. Minimum temperature in the tumor region after t = 2100 sec has been found 44.065 °C, 43.935 °C and 44.024 °C for case 1, 2 and 3 respectively, which is greater than burn threshold (40 °C). Thus there is double chance to kill the tumor by using freezing followed by strong heating and hence improving the treatment effect.

To study the effect of three blood re-flow patterns, temperature during the heating process at a point P(1.75 cm, 2.0 cm) is listed in table 3.1. It is clear that the temperature at P is highest for case 1 and least for case 2. It is because of largest heat supplied by blood vessels as they resume quickly on thawing in case 1, while no heat is supplied by blood vessels in case 2. In case 3, there is time delay in resuming the functioning of the blood vessels, so temperature at point P for case 3 is greater than case 2 but lower than case 1. These three blood flow patterns result different temperature profiles in tissue.

**Table 3.1:** Temperature at point P for three blood re-flow patterns during heating

Time (sec)	Temperature (°C)					
1 ime (sec)	case1	case2	case3			
1350	3.78246	3.78246	3.78246			
1400	13.0673	12.6047	12.7978			
1450	19.3683	18.9463	19.1584			
1500	24.1619	23.7692	23.9920			
1550	27.9866	27.6223	27.8466			
1600	31.1113	30.7764	30.9946			
1650	33.7022	33.3981	33.6040			
1700	35.8747	35.6018	35.7915			
1750	37.7135	37.4717	37.6425			
1800	39.2807	39.0694	39.2198			
1850	40.6127	40.4293	40.5603			
1900	41.8090	41.6392	41.7598			
1950	42.9576	42.7953	42.9102			
2000	44.0577	43.9038	44.0125			
2050	45.1033	44.9578	45.0604			
2100	46.0926	45.9552	46.0520			

# 3.6 CONCLUSION

In the present study combined cryosurgery and hyperthermia treatment, which has double chance to kill the tumor by lowering its temperature to necrosis temperature and raising it to burn threshold has been numerically analyzed. Non-ideal property of biological tissue, heat generation due to metabolism and blood perfusion has been taken into account. Three blood re-flow patterns during heating have been studied. The temperature raising has been found highest for case 1 and least for case 2. Temperature profiles and phase change interfaces are obtained for all cases. These information are beneficial to know whether the

tumor has been damaged or not and to minimize the damage to neighboring healthy lung tissue by over-freezing and overheating and hence to optimize the treatment planning.

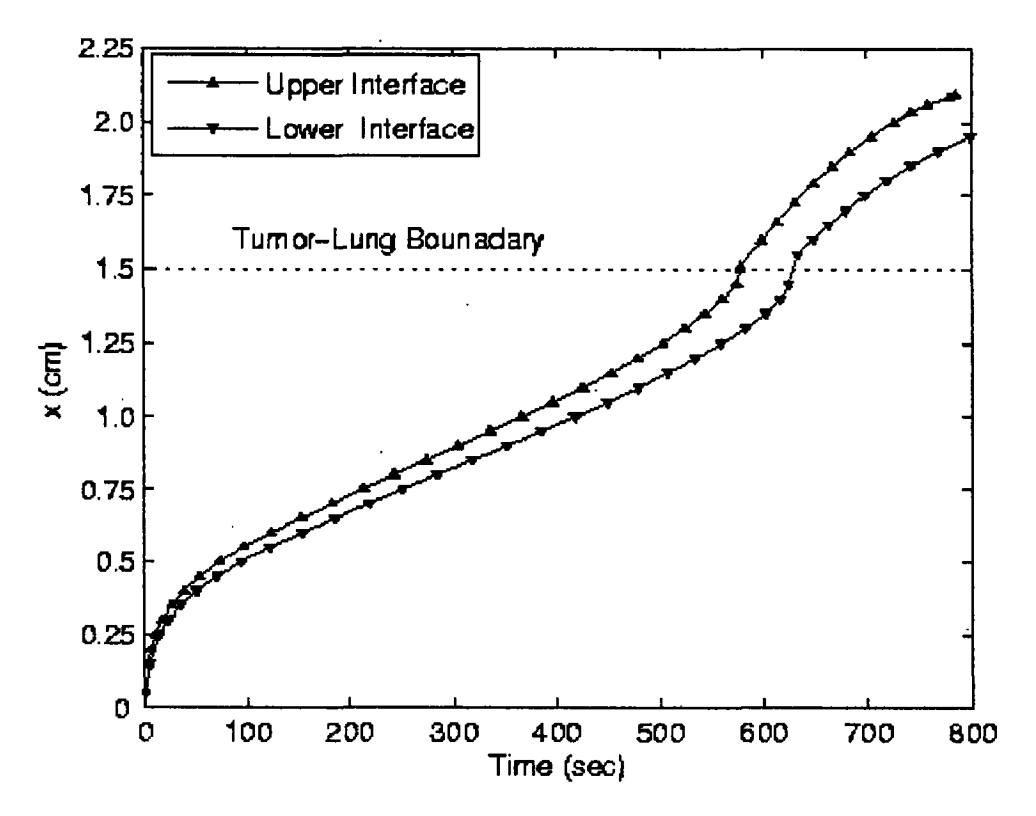


Figure 3.2 Phase change interface during freezing at y = 2.0 cm.

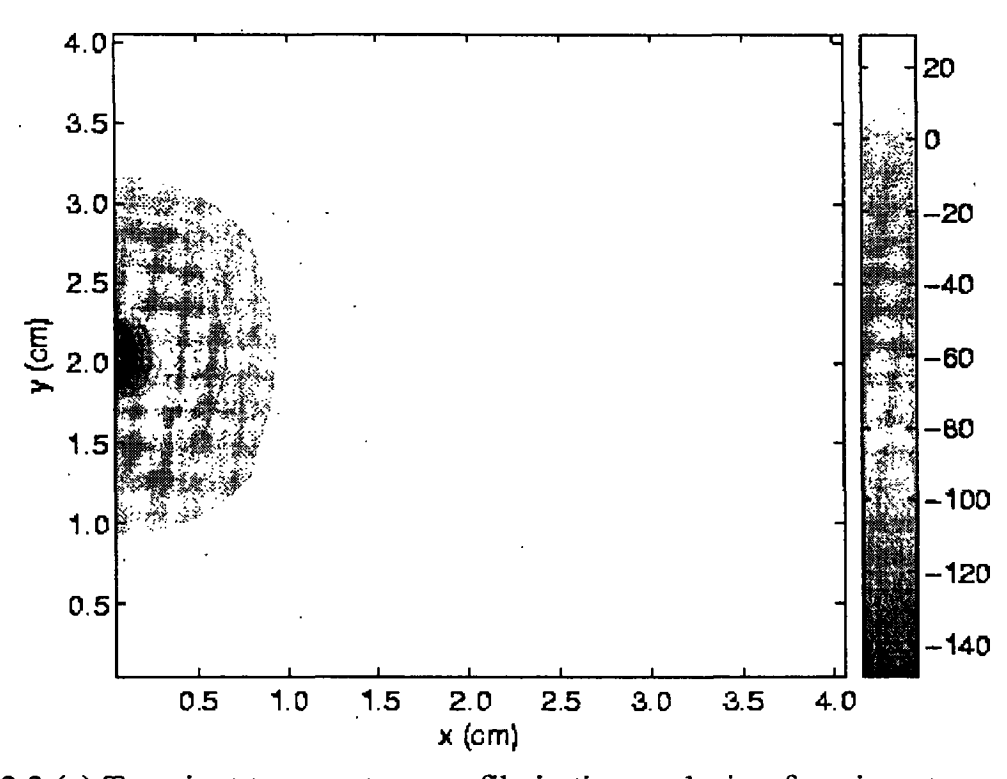


Figure 3.3 (a) Transient temperature profile in tissues during freezing at  $t = 200 \,\mathrm{sec}$ .

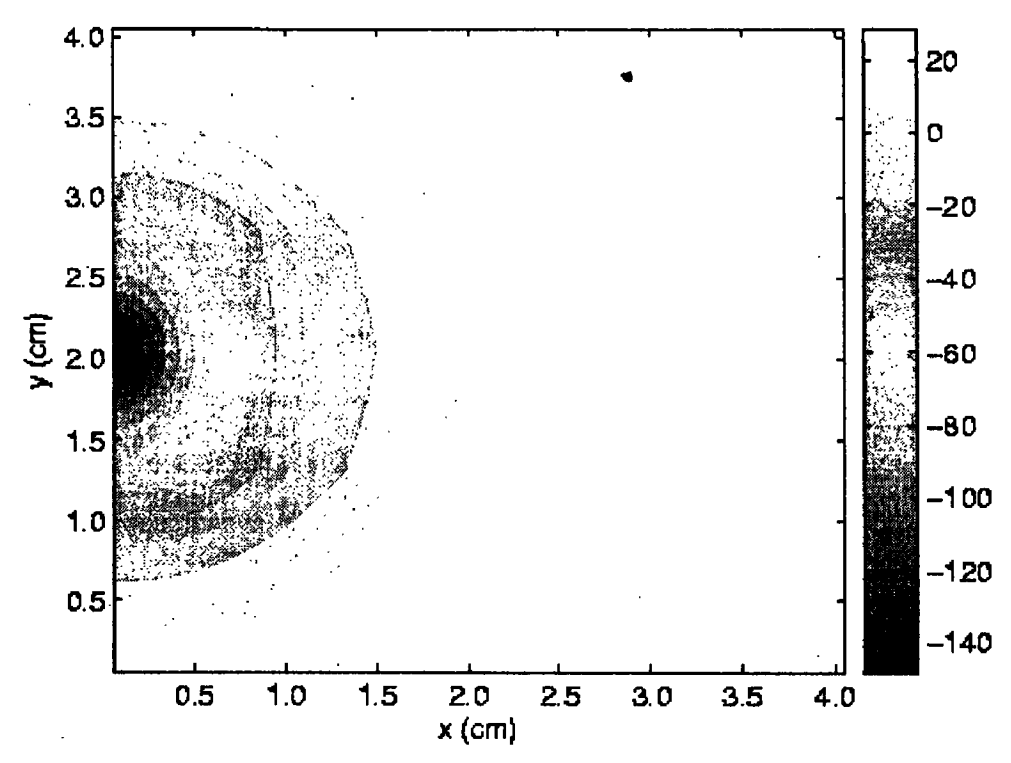


Figure 3.3 (b) Transient temperature profile in tissues during freezing at t = 400 sec.

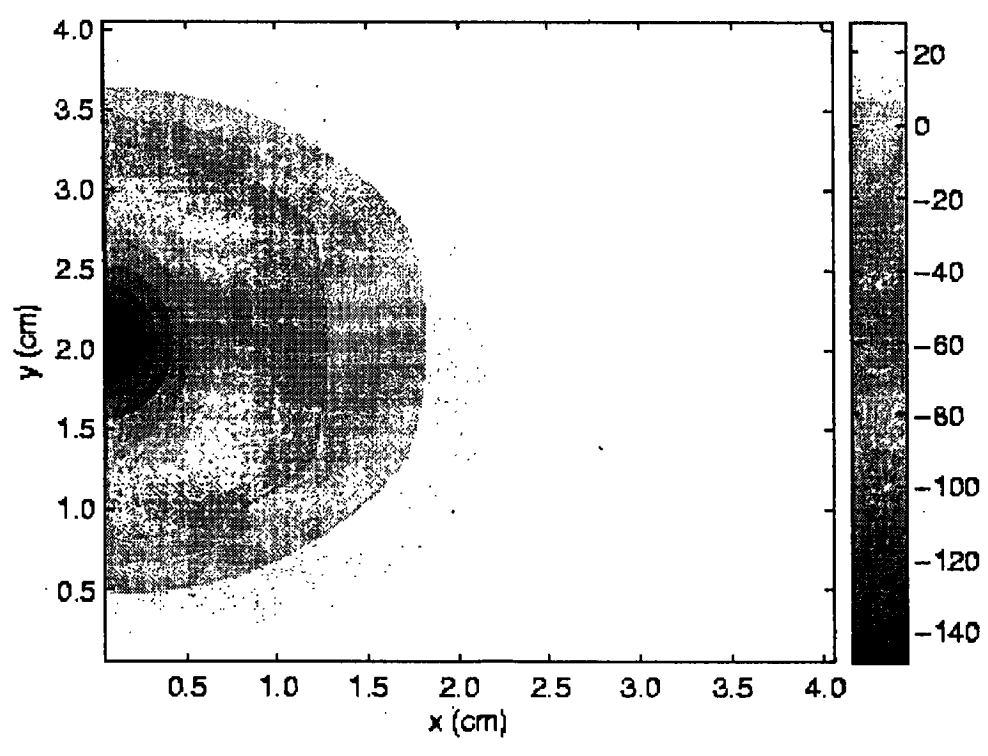


Figure 3.3 (c) Transient temperature profile in tissues during freezing at  $t = 600 \,\mathrm{sec}$ .

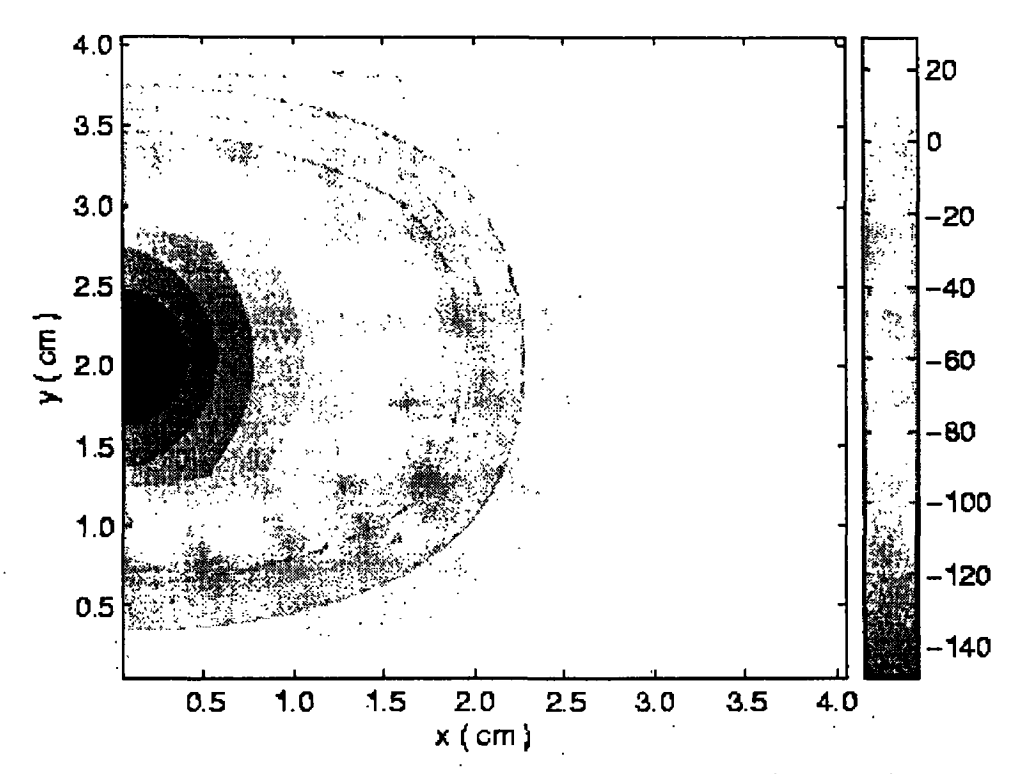


Fig 3.3 (d) Transient temperature profile in tissues during freezing at t = 800 sec.

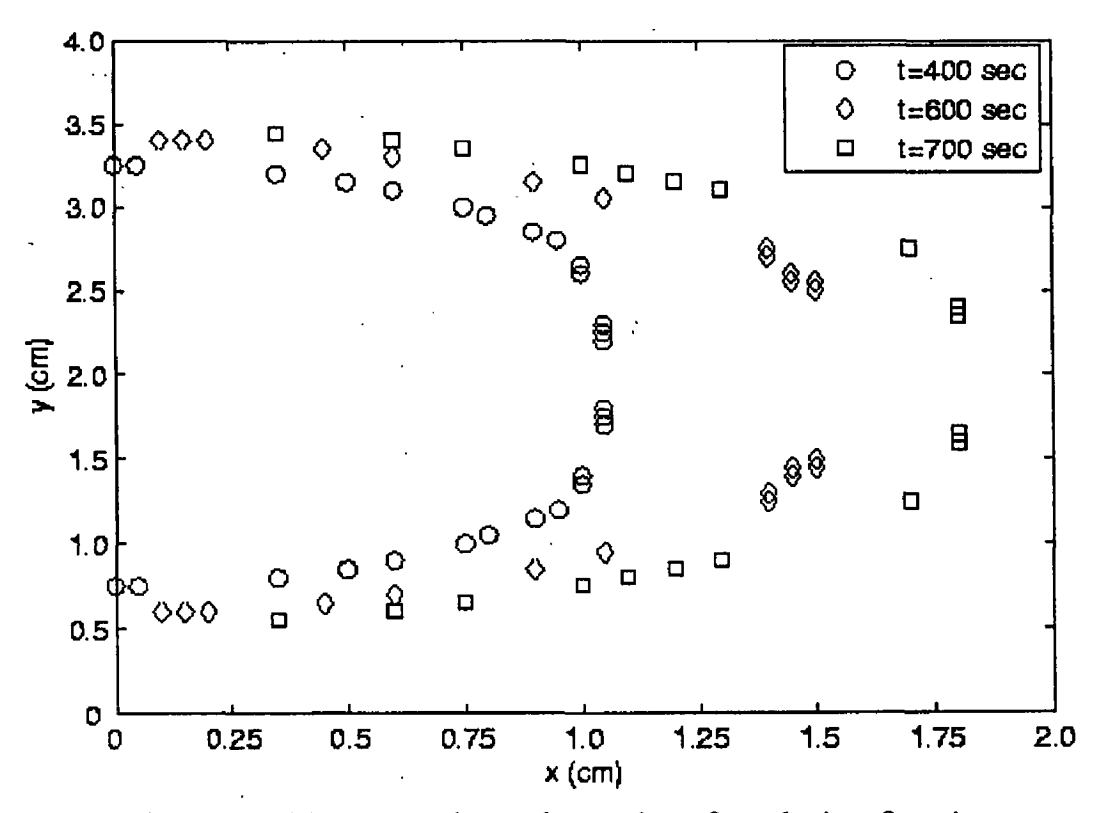


Figure 3.4 (a) Lower phase change interface during freezing.

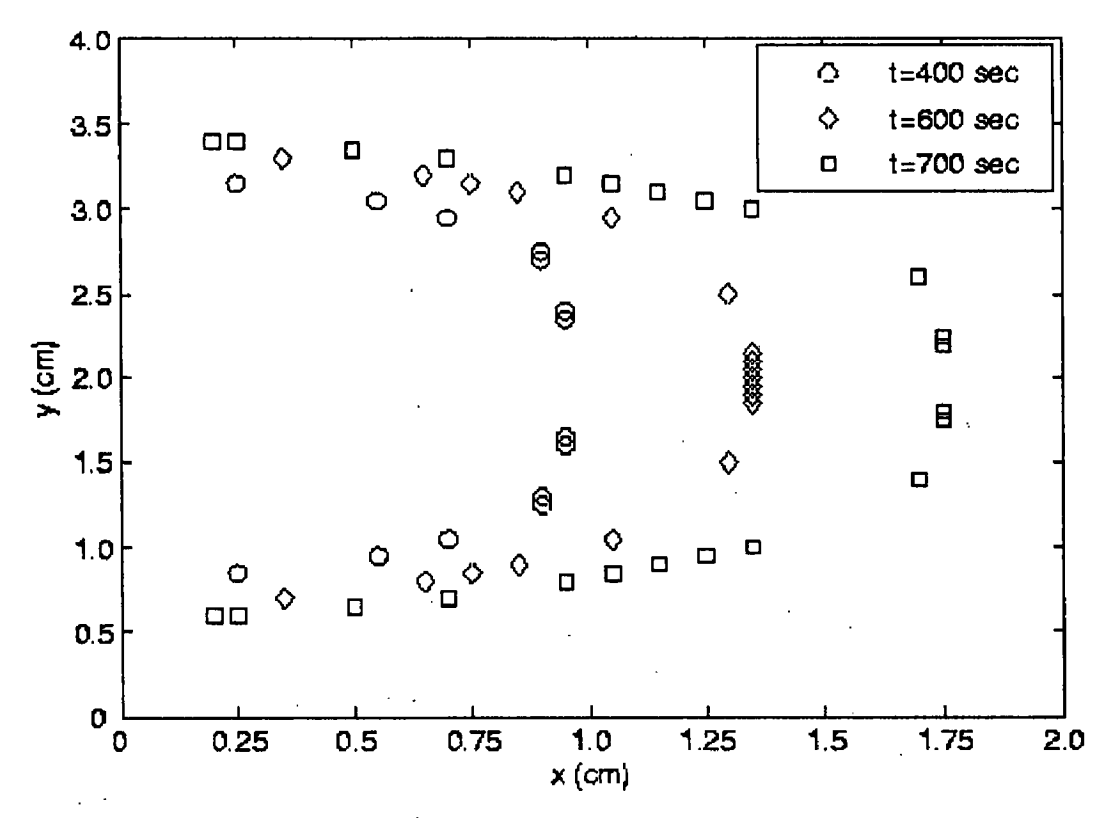


Figure 3.4 (b) Upper phase change interface during freezing.

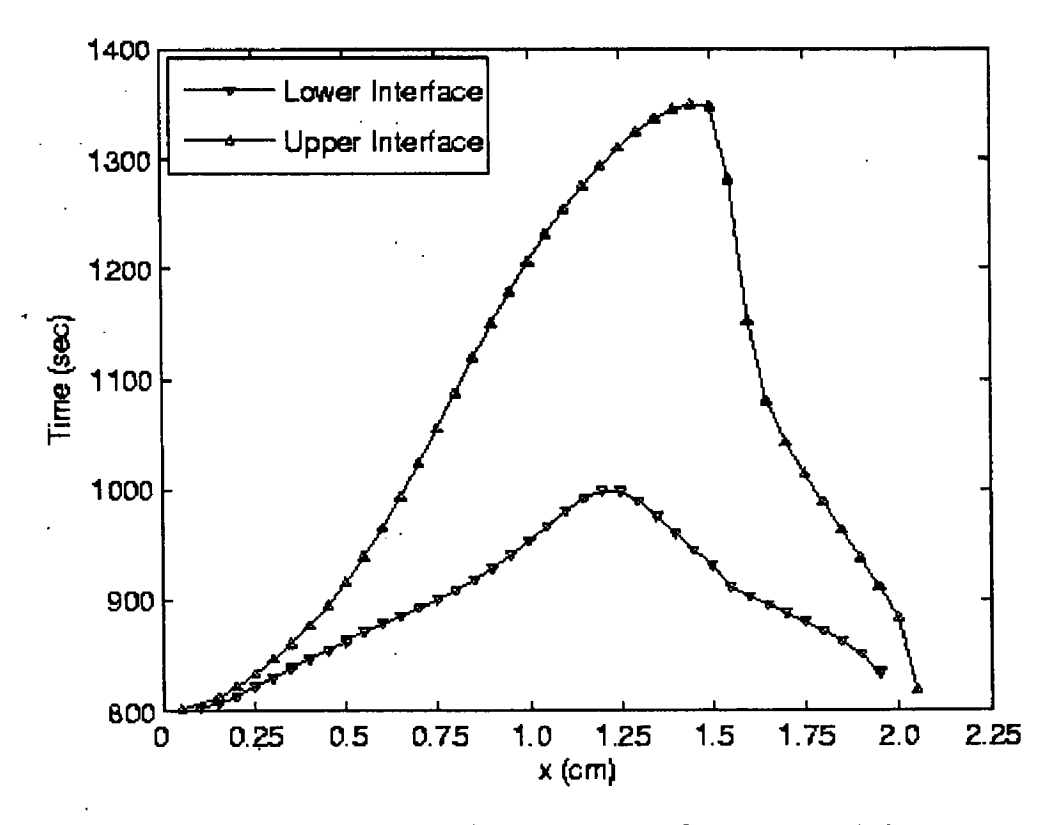


Figure 3.5 Position of thawing interfaces at y = 2.0 cm.

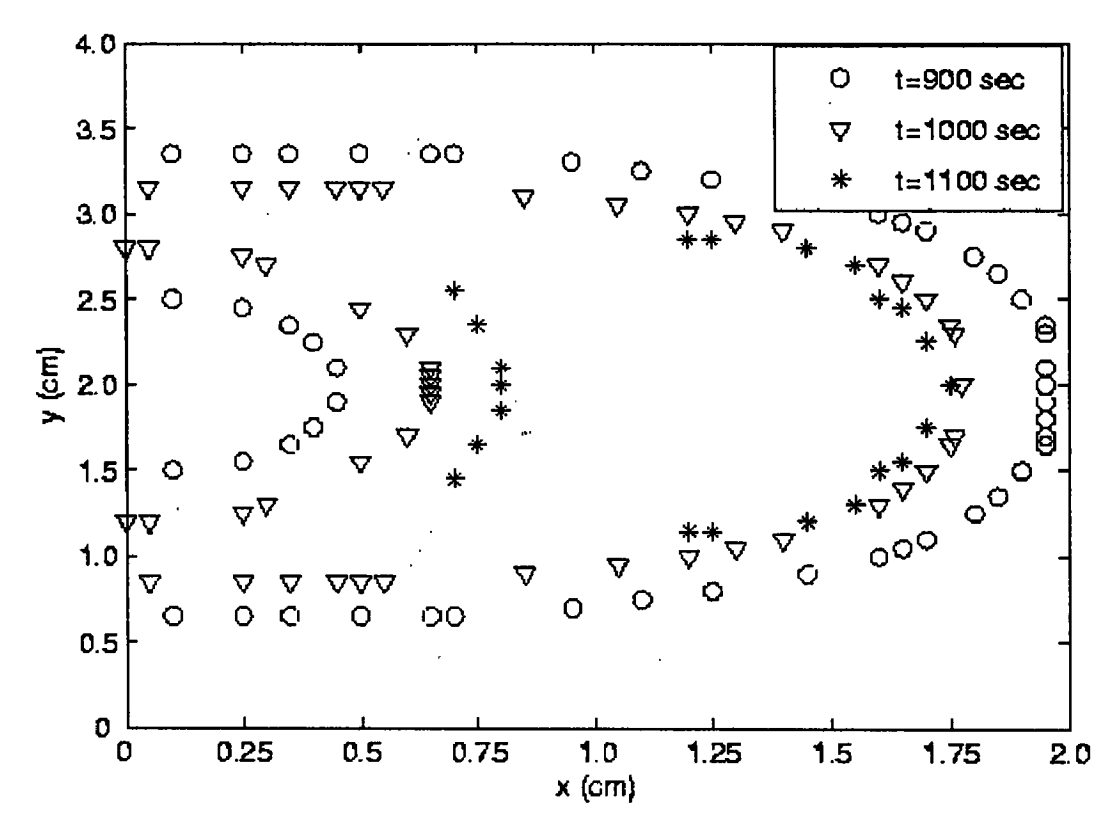


Figure 3.6 (a) Upper phase change interface during thawing.

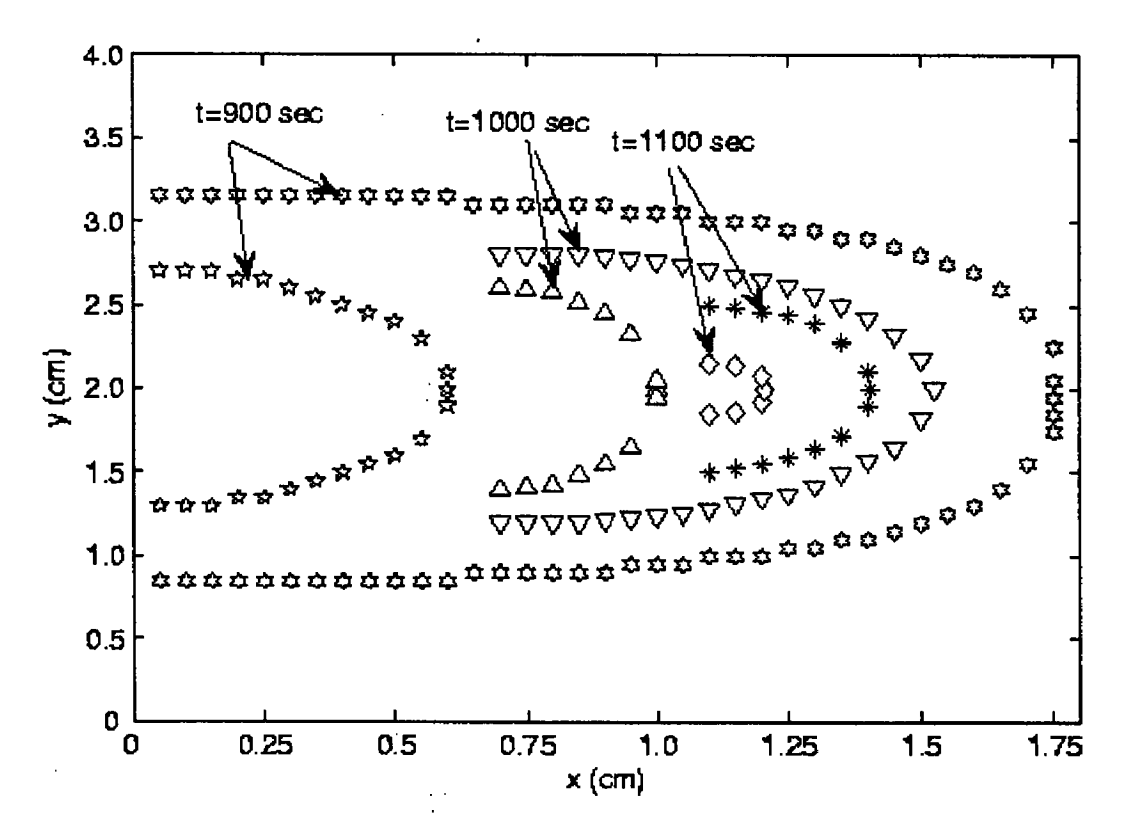


Figure 3.6 (b) Lower phase change interface during thawing.

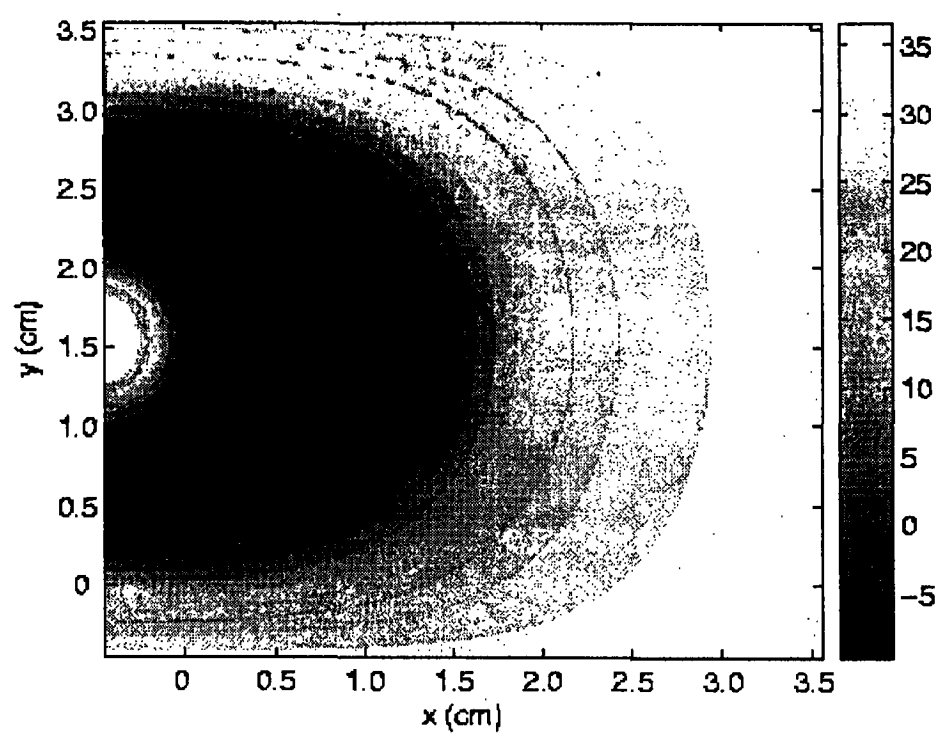


Figure 3.7 (a) Transient temperature profile during thawing at t = 900 sec.

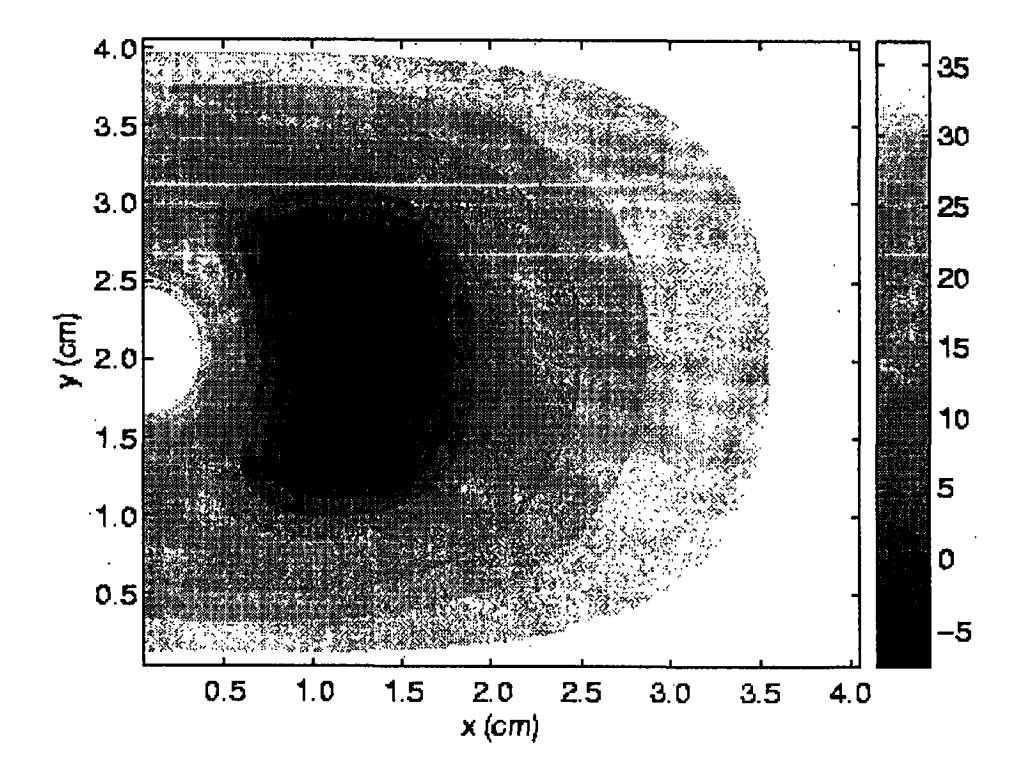


Figure 3.7 (b) Transient temperature profile during thawing at at t = 1136 sec.

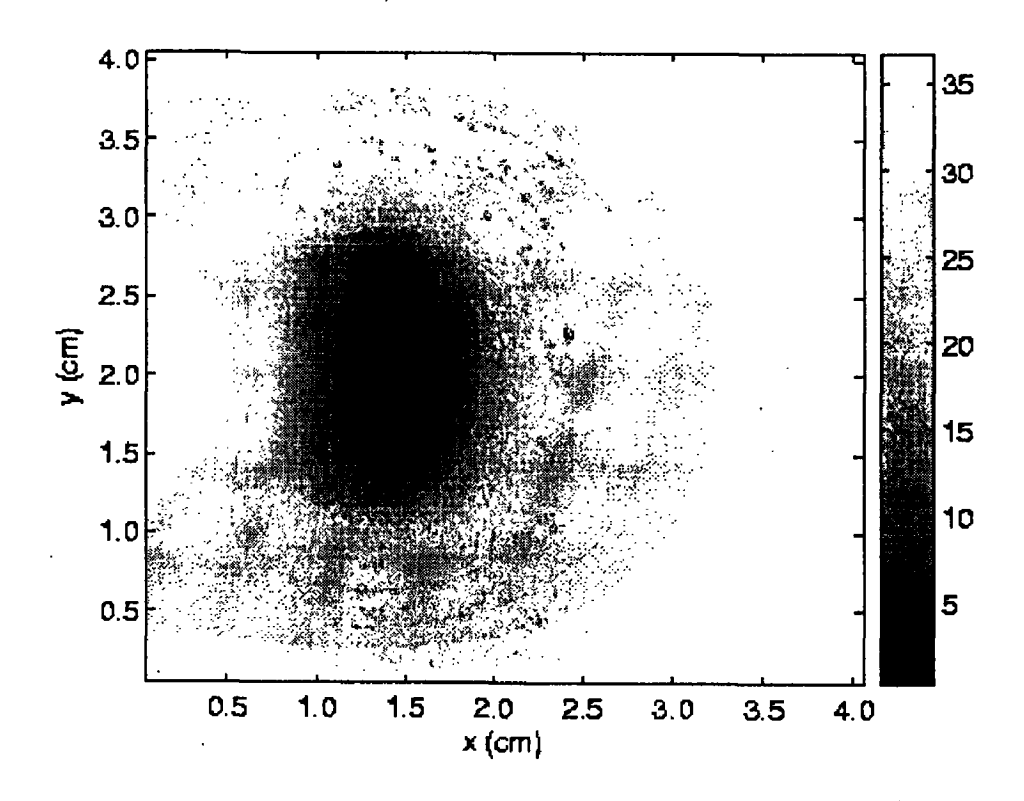


Figure 3.7 (c) Transient temperature profile during thawing at at t = 1350 sec.

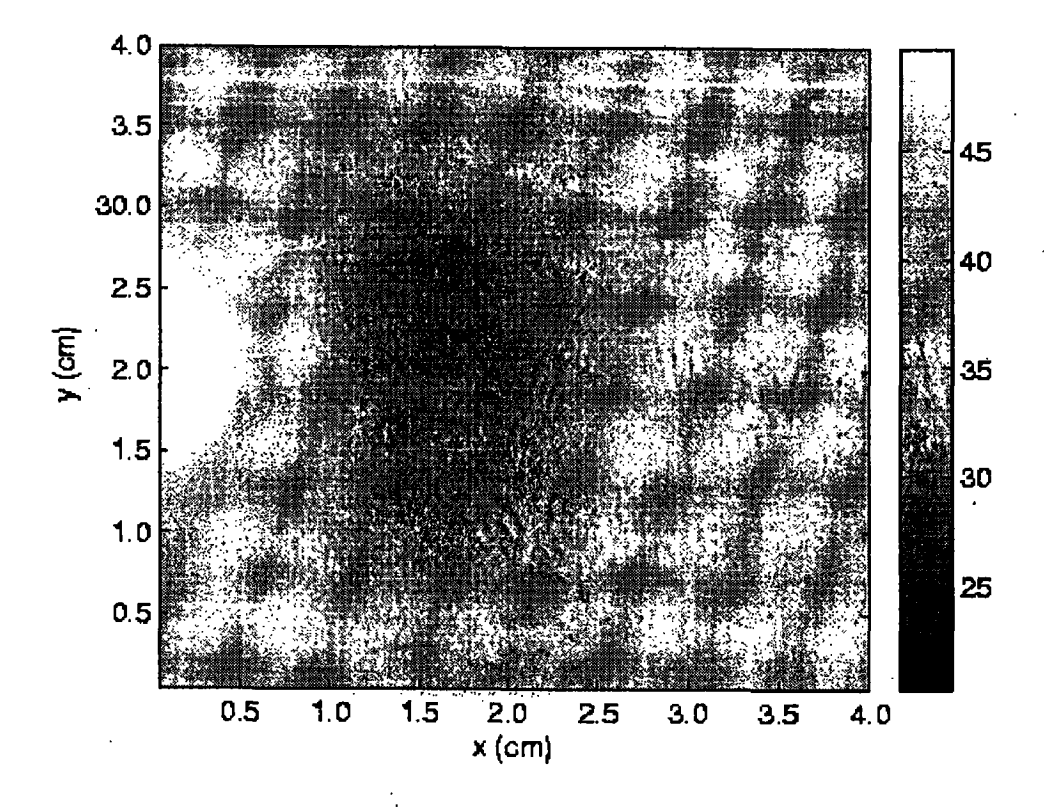


Figure 3.8 (a) Transient temperature profile for case1 during heating at t = 1600 sec.

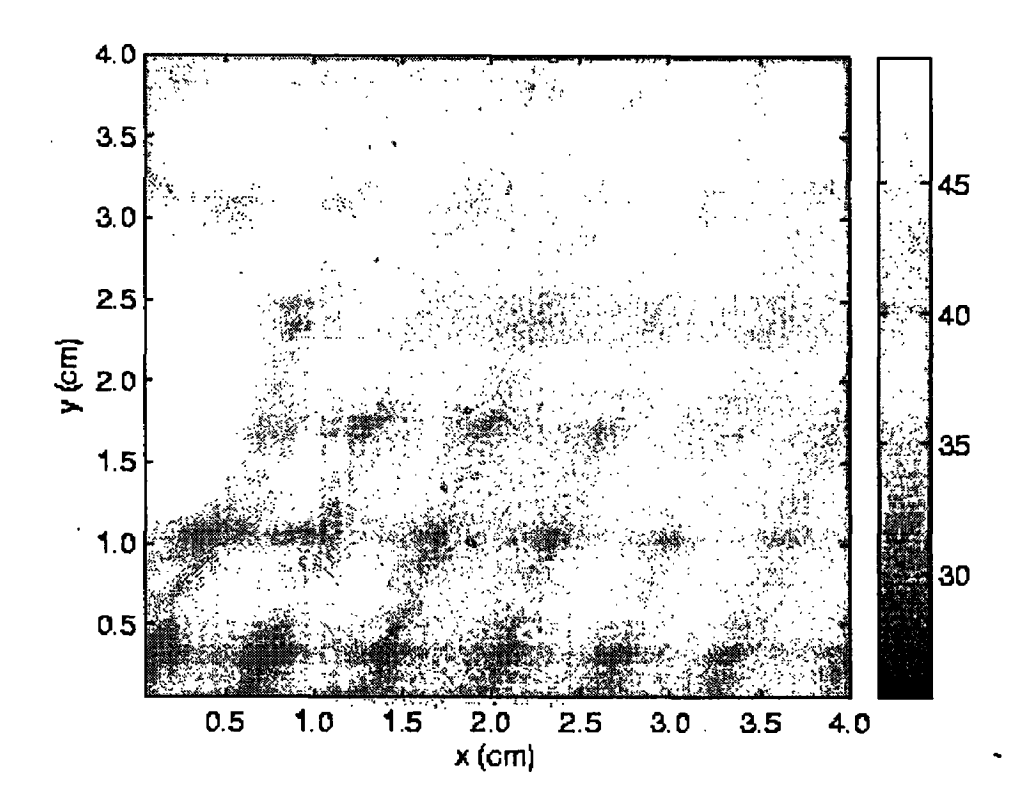


Figure 3.8 (b) Transient temperature profile for case1 during heating at t = 1800 sec.

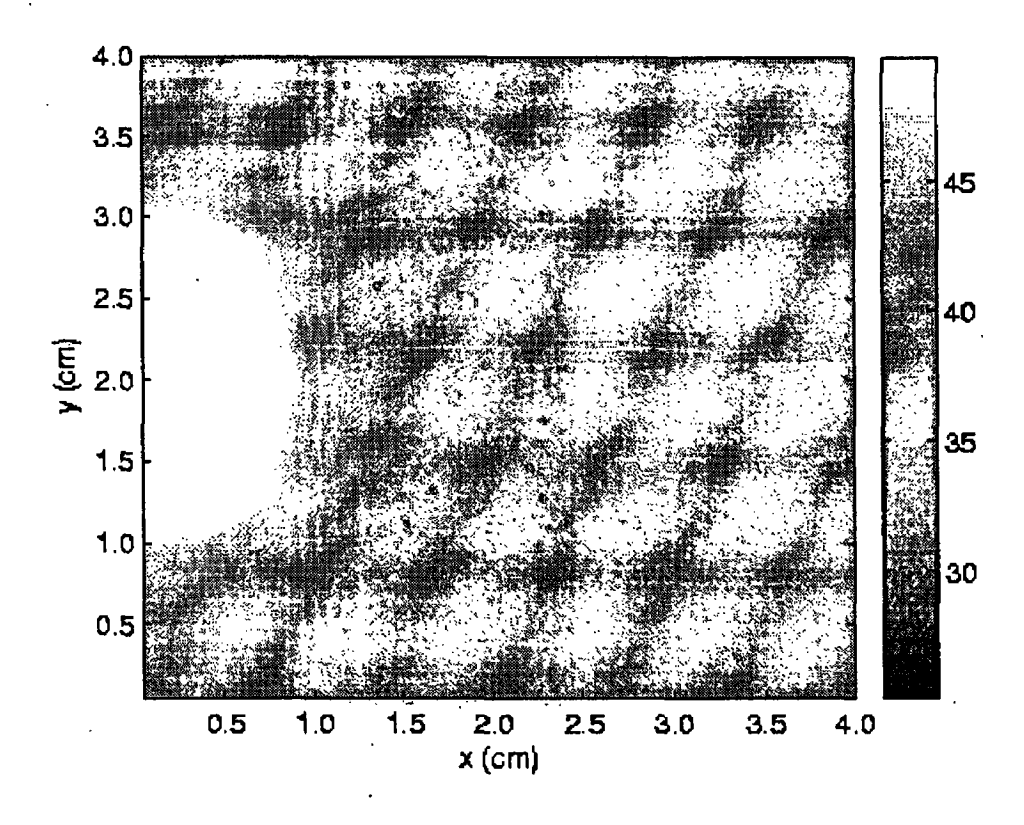


Figure 3.8 (c) Transient temperature profile for case1 during heating at t = 1950 sec

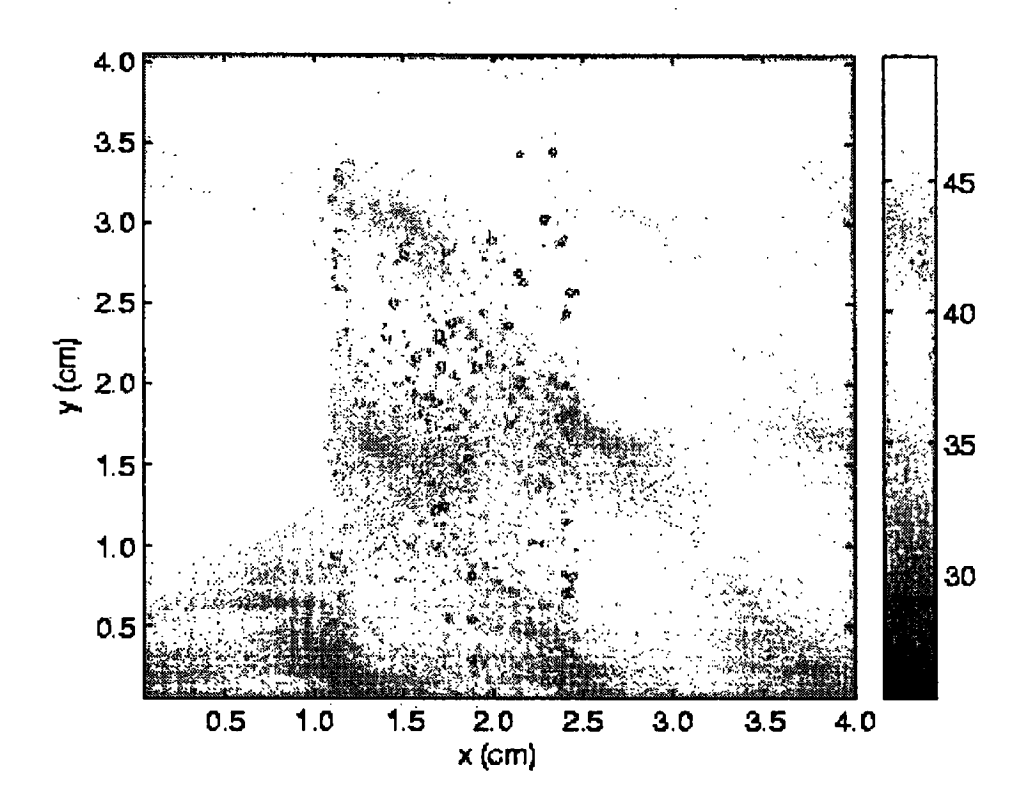


Figure 3.8 (d) Transient temperature profile for case1 during heating at t = 2100 sec.

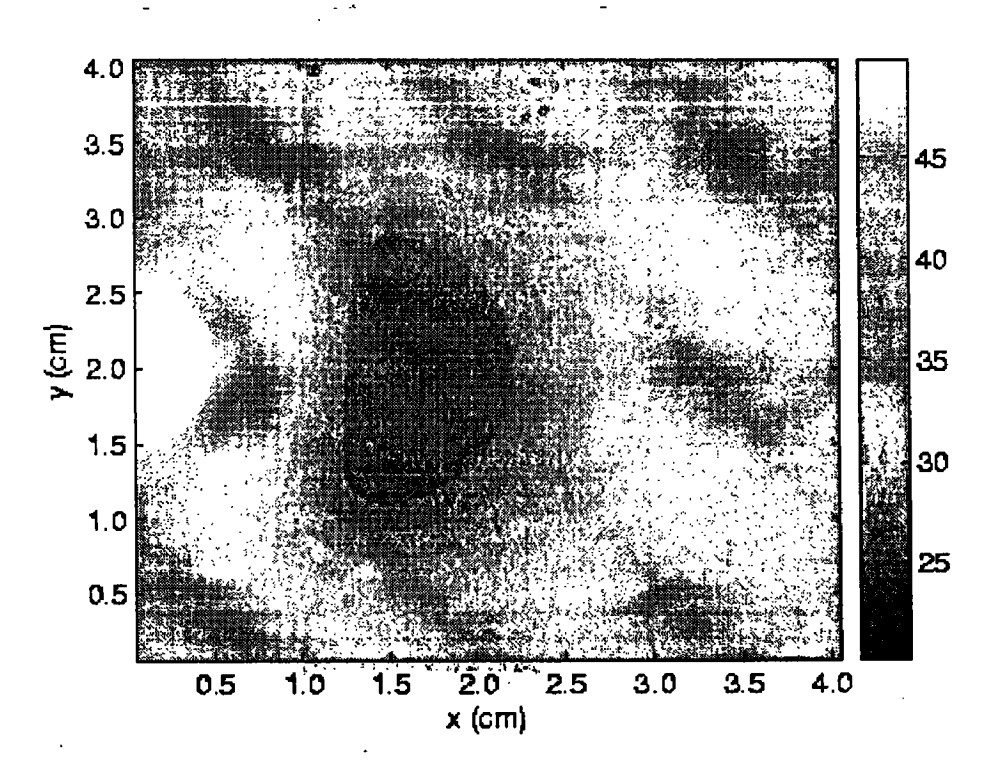


Figure 3.9 (a) Transient temperature profile for case 2 during heating at t = 1600 sec.

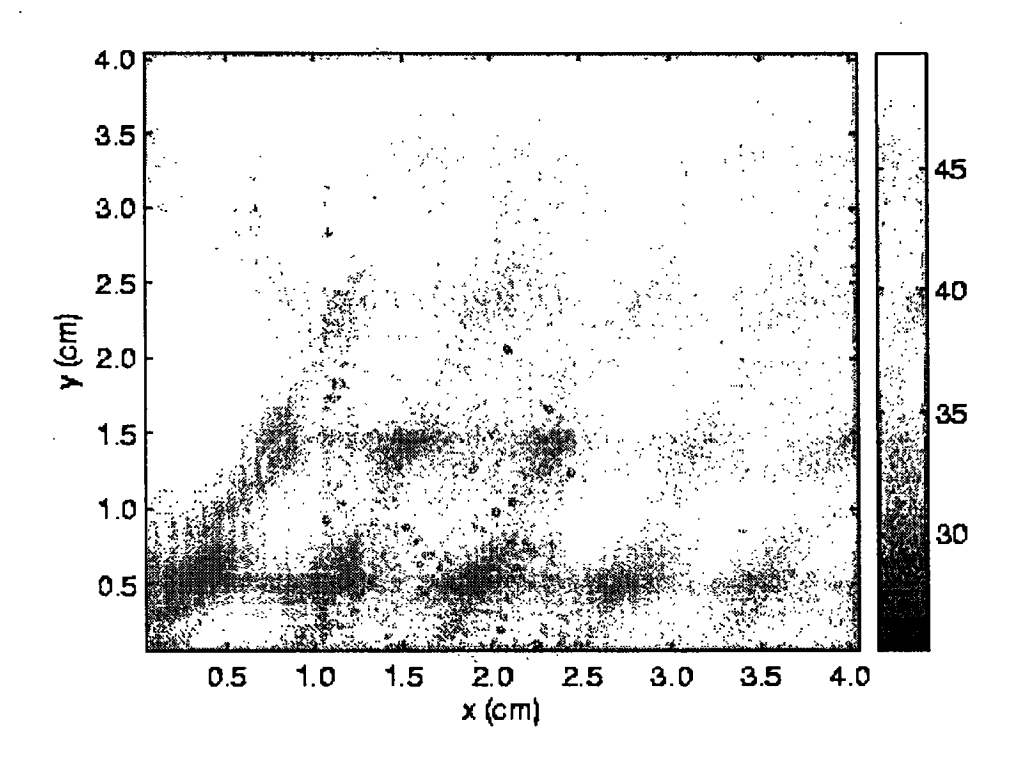


Figure 3.9 (b) Transient temperature profile for case 2 during heating at t = 1800 sec.

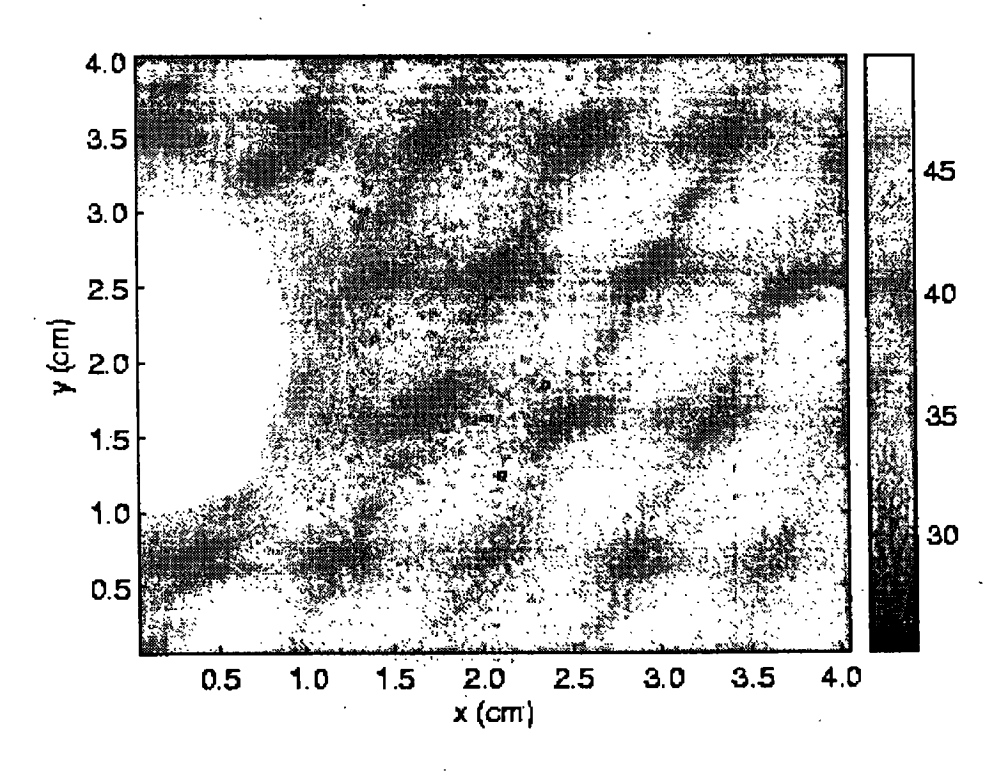


Figure 3.9 (c) Transient temperature profile for case2 during heating at t = 1950 sec.

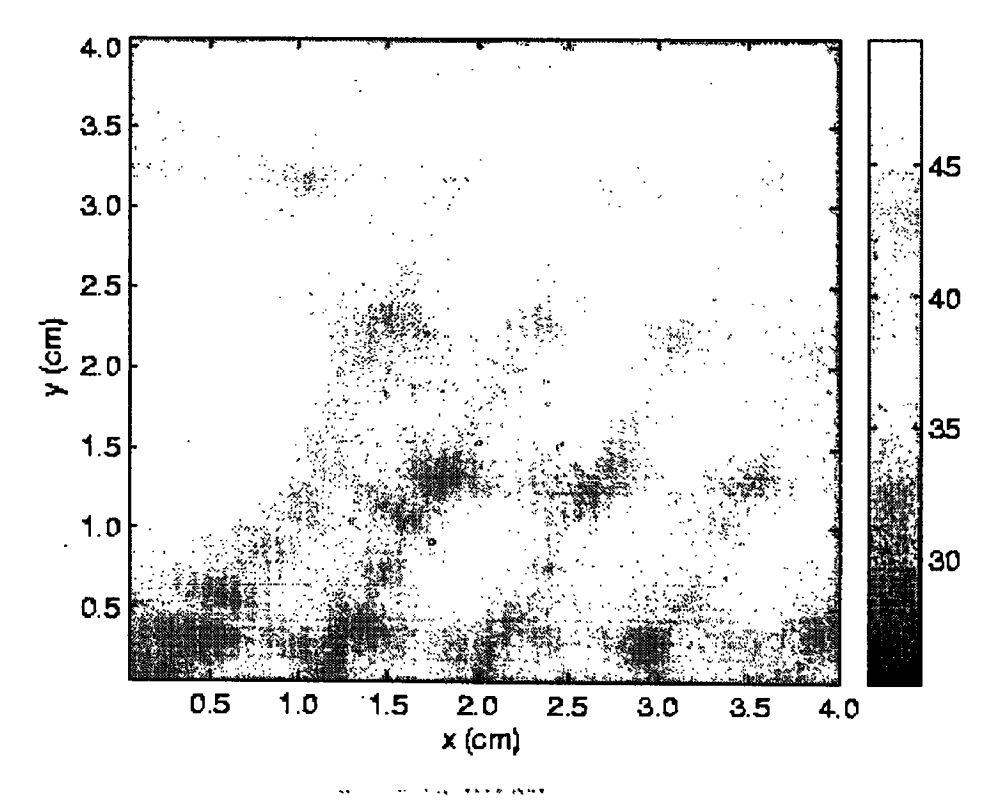


Figure 3.9 (d) Transient temperature profile for case 2 during heating at t = 2100 sec.

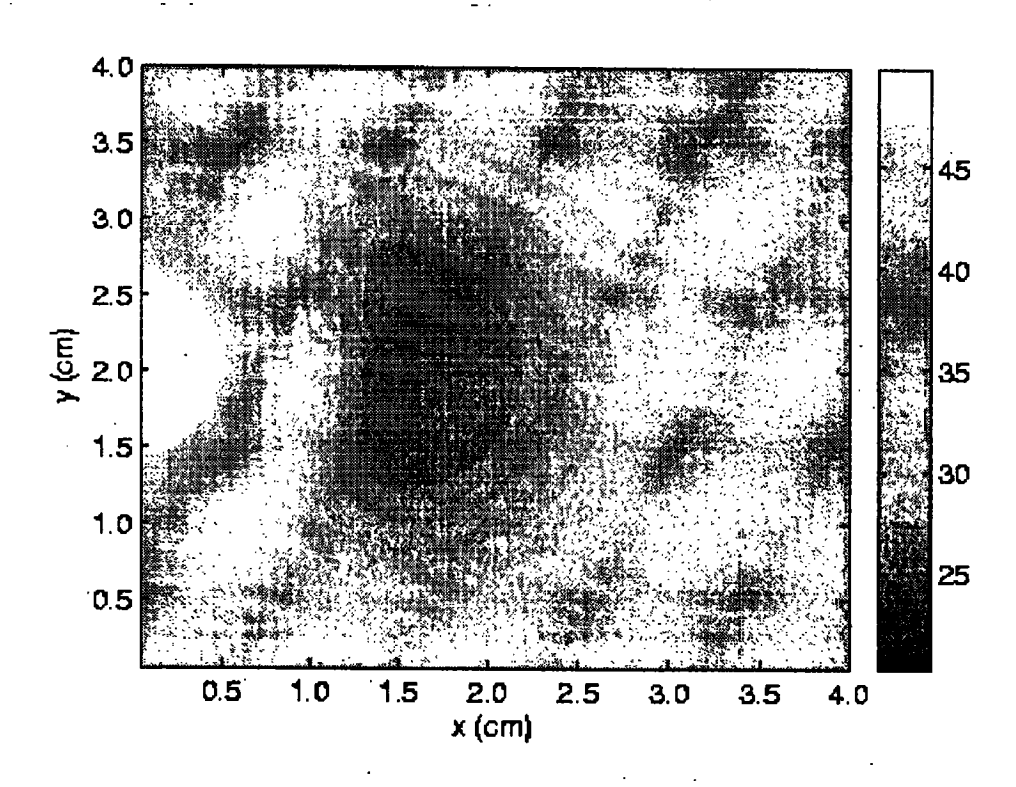


Figure 3.10 (a) Transient temperature profile for case 3 during heating at t = 1600 sec.

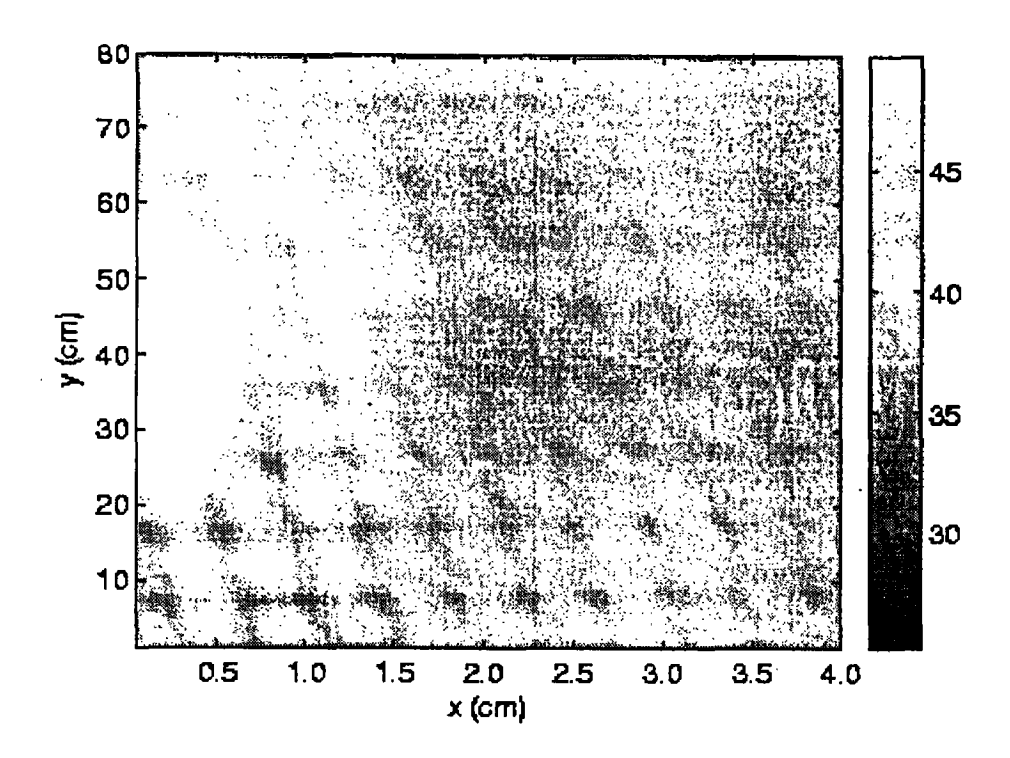


Figure 3.10 (b) Transient temperature profile for case 3 during heating at t = 1800 sec.

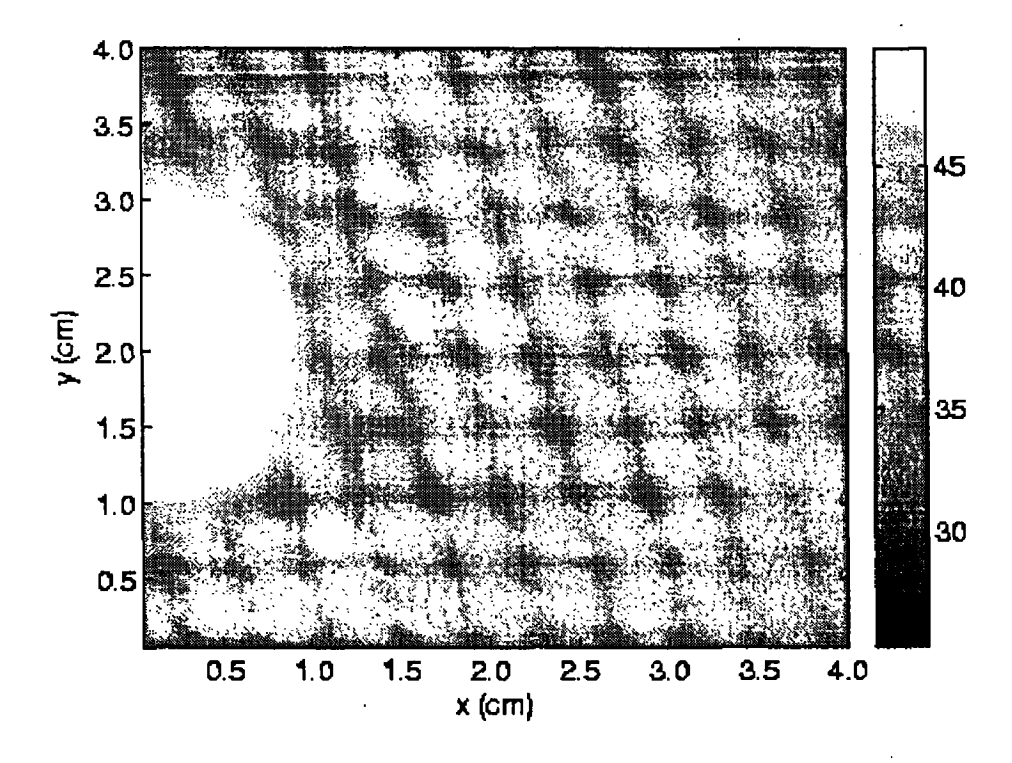


Figure 3.10 (c) Transient temperature profile for case 3 during heating at t = 1950 sec.

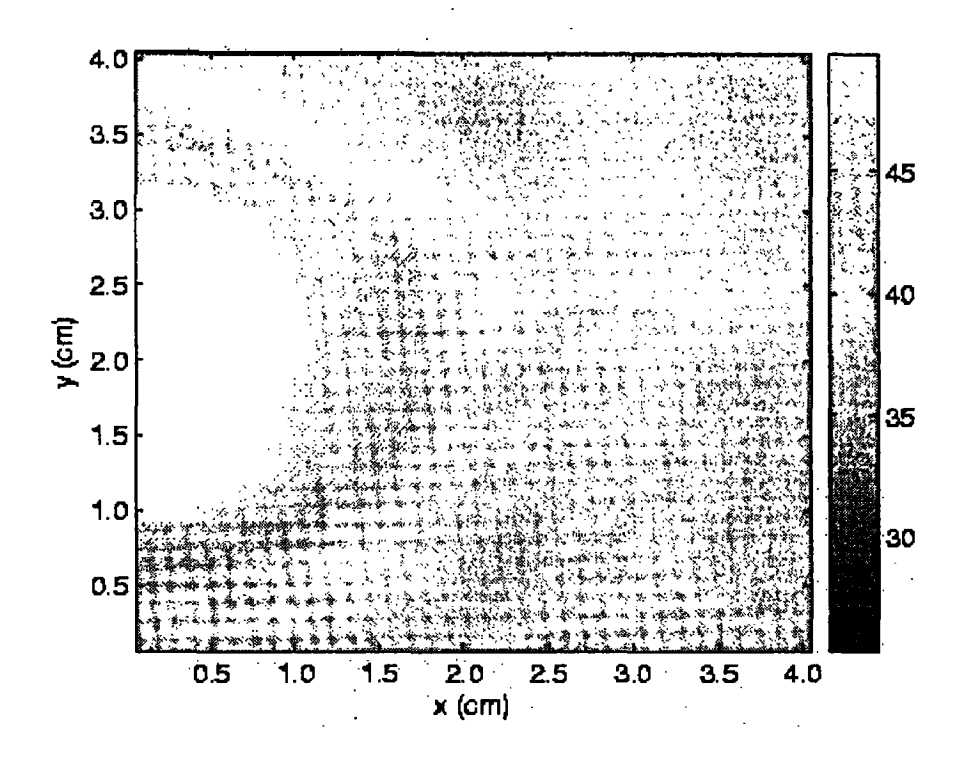


Figure 3.10 (d) Transient temperature profile for case3 during heating at t = 2100 sec.

## Chapter 4

## NUMERICAL STUDY ON FREEZING AND THAWING OF

SKIN: A THREE-LAYER MODEL

#### 4.1 INTRODUCTION

Thawing is the reverse process of freezing. It is an essential part of cryosurgery and cryopreservation. In cryosurgery during freezing, some healthy tissues may also freeze. These frozen tissues can resume their state due to heat supply by body metabolism and blood perfusion, but if freezing is deep then tissues will remain in frozen state for a longer time and hence may damage, in this case external heating is needed to warm them. Further in cryopreservation to obtain an optimal recovery of skin, quantitative evaluation of the temperature history during the phase change is highly desirable. Furthermore, in cryosurgey, during the thawing process small crystals merge together to form large crystals, which readily disrupt cellular membranes. This re-crystallization may enhance tissue destruction induced by the preceding freezing. Knowledge of the thawing front and the transient temperature are critical for adjusting the heating power to reduce healthy cell destruction [72].

To a date a great deal of research is focused on the study of freezing and thawing process alone. Zhang et al. [157] gave a mathematical analysis to study the thawing process in three regions during cryosurgical re-warming. Zho et al. [159] presented a numerical study on the thawing of frozen biological tissues caused by laser irradiation using Monte-Carlo and effective heat capacity method. Liu et al. [72] used Green's function method to solve the

phase change problem of biological skin with finite thickness. Some other studies were also done regarding the freezing of human skin [87].

In all the above models, skin is treated as a single layer, while the human skin consists of three layers epidermis, dermal and sub-cutaneous tissues. The epidermis consists of mainly dead tissues in the form of stratum corneum [95-97, 117-119]. The dermis is composed of matter masses of connective tissues and elastic fibers through which numerous blood vessels, lymphatics and nerves pass. The sub-dermal part contains fat cells, connective tissues, blood vessels, lymphatics and nerves. There is no blood vessel in epidermis. The density of blood vessels increases in dermis and becomes almost uniform in sub-dermal part. This causes in the variation in the thermal properties like thermal conductivity, density and specific heat etc. in these regions. Therefore three-layer classification will be more realistic rather considering skin as single layer. Tovi et al. [137] used this three layer model for heat transfer in human skin subjected to a flash fire.

Phase-change problems simultaneously involving the freezing and heating behaviors of biological tissues are much more complex than when only single freezing is applied, because many more phase change interfaces will be produced during the alteration of freezing and thawing.

In the present paper enthalpy formulation of Pennes bioheat equation [99] is used to study the phase change problem during freezing and thawing process in human skin considering skin as three layer model (Fig 4.1 [137]), to calculate the transient temperature profile and position of freezing and thawing front in skin.

## 4. 2 PROBLEM DESCRIPTION

Figure 4.1 shows the physical description of human skin, outer layer, i.e. epidermis layer is 0.08 mm in thickness. The thickness of dermis and sub-cutaneous layers are 2 mm and 10 mm respectively. Cryoprobe with temperature  $T_c$  is applied at x = 0, while the surface x = l is assumed at body core temperature.

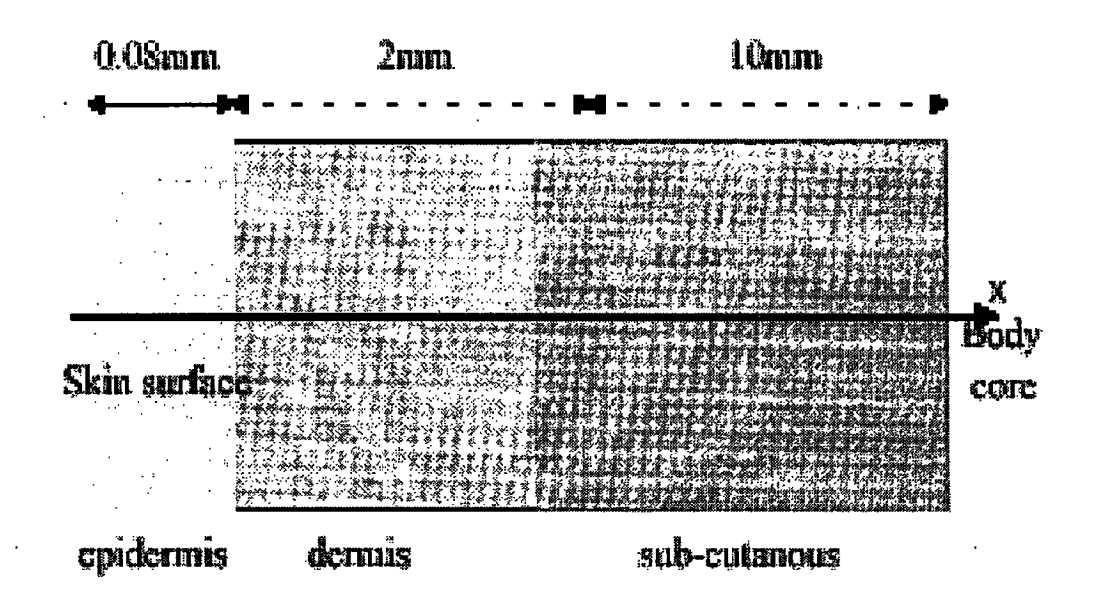


Figure 4.1: Schematic geometry of three-layer skin model

· Š.

## 4.3 MATHEMATICAL MODEL

## 4.3.1 Assumptions

Following assumptions are made to study the freezing and thawing process

- (i) Heat flow is purely by conduction only [14].
- (ii) The thermal conductivity, specific heat and density are different in all the three regions are constant, but different
- (iii) Thermo-physical properties are different in different states for epidermis dermis and sub-cutaneous layer.
- (iv) Initial temperature distribution is taken as 37°C.

- (v) Non-ideal property of biological tissues is taken with liquidus temperature  $T_{ml} = -1 \,^{\circ}C$  and solidus temperature as  $T_{ms} = -8 \,^{\circ}C$ . [103]
- (vi) Thermal conductivity and specific heat are same in frozen state for all layers
- (vii) In unfrozen state, blood perfusion and metabolic heat generation in dermal and subcutaneous part is taken same and constant, while zero in epidermis region.
- (viii) Blood perfusion and metabolism heat generation is taken zero in frozen and mushy state.

## 4.3.2 Governing Equation

Based on the above assumptions the enthalpy formulation of the phase change problem using Pennes bioheat Equation is given as

$$\rho_{k} \frac{\partial H_{k}(T)}{\partial t} = K_{k} \left( T \right) \frac{\partial^{2} T_{k}(x,t)}{\partial x^{2}} + w_{b} \left( T \right) c_{b} \left( T_{b} - T_{k}(x,t) \right) + Q_{m}(T), \tag{4.1}$$

where  $\rho$ , H, K(T),  $w_b$ ,  $c_b$ ,  $T_b$ ,  $Q_m(T)$  and T are effective density, enthalpy, effective thermal conductivity, effective blood flow rate, specific heat of blood, arterial temperature, effective metabolic heat generation and temperature respectively. k = e, d, s for epidermis, dermis and sub-cutaneous layer.

## 4.3.3 Initial and Boundary Conditions

(i) Initialy tissue is on body core temperature, i.e.

$$T_{\nu}(x,0) = 37 \,^{\circ}C$$
, (4.2)

(ii) Cryoprobe at x = 0, i.e.

$$T_{e}(0,t) = T_{c}$$
 at  $x = 0$ , (4.3)

(iii) At epidermis and dermis boundary

$$K_{e}(T)\frac{\partial T_{e}}{\partial x} = K_{d}\frac{\partial T_{d}}{\partial x}$$

$$T_{e} = T_{d}$$

$$at x = l_{1},$$

$$(4.4)$$

(iv) At dermis and sub-cutaneous boundary

$$K_{d}(T)\frac{\partial T_{d}}{\partial x} = K_{5}\frac{\partial T_{s}}{\partial x}$$

$$T_{d} = T_{s}$$

$$at x = l_{2},$$

$$(4.5)$$

(v) At body core

$$T_s(l,t) = 37 \, ^{\circ}C \,, \tag{4.6}$$

where,

$$H = \begin{cases} c_{kf} (T_k - T_{ms}) & T < T_{ms} \\ (T_k - T_{ms}) \left( \frac{1}{2} (c_{kf} + c_{ku}) + \frac{L}{(T_{ml} - T_{ms})} \right) & T_{ms} \le T \le T_{ml} \\ L + \frac{1}{2} (c_{kf} + c_{ku}) (T_{ml} - T_{ms}) + c_{ku} (T_k - T_{ml}) & T > T_{ml} \end{cases}$$

$$(4.7)$$

$$K(T) = \begin{cases} K_f & T < T_{ms} \\ \frac{(K_f + K_u)}{2} & T_{ms} \le T \le T_{ml} \\ K_u & T > T_{ml} \end{cases}$$
(4.8)

$$w_{b_k}\left(T\right) = \begin{cases} 0 & T_k \le T_{ml} \\ w_b & T_k > T_{ml} \end{cases},\tag{4.9}$$

$$Q_{m_k}\left(T\right) = \begin{cases} 0 & T_i \le T_{ml} \\ q_m & T_i > T_{ml} \end{cases}$$
 (4.10)

where c, L, k,  $w_b$ ,  $q_m$ ,  $T_c$ ,  $T_{ms}$ ,  $T_{ml}$  are specific heat, latent heat, thermal conductivity, blood perfusion, cryoprobe temperature at skin surface, liquidus and solidus

temperature respectively. Subscripts f and u are for frozen and unfrozen states.  $l_1$  and  $l_2$  are epidermis-dermis and dermis-subcutaneous boundary respectively, and k = e, d and s is for epidermis, dermis and sub-cutaneous layers.

## 4.4 NUMERICAL SOLUTION

Finite difference explicit scheme is used to solve Eq. (4.1) – Eq. (4.10). Taking  $x_j = j\Delta x$  and  $t_p = p\Delta t$ , the enthalpy at time step p+1 is given by

$$(H_{k})_{j}^{p+1} = (H_{k})_{j}^{p} + \frac{\Delta t (K_{k})_{j}^{p}}{(\Delta x)^{2} (\rho_{k})_{j}^{p}} \{ (T_{k})_{j+1}^{p} - 2 (T_{k})_{j}^{p} + (T_{k})_{j-1}^{p} \}$$

$$+ \frac{\Delta t}{(\rho_{k})_{j}^{p}} \{ (w_{b_{k}})_{j}^{p} c_{b} (T_{b} - (T_{k})_{j}^{p}) + (Q_{m_{k}})_{j}^{p} \},$$

$$(4.11)$$

where j and p are axial and time steps respectively and  $\Delta x$  and  $\Delta t$  are the axial and time increments respectively. The time and space increments are adjusted in such a way, that they satisfy the stability criteria,  $\frac{\alpha_{\max} \Delta t}{(\Delta x)^2} \le \frac{1}{2}$ , where  $\alpha_{\max}$  is maximum value of thermal diffusivity.

After calculating enthalpy at (p+1) level, temperature is calculated by reverting Eq. (4.7). Once the new temperature field is obtained from the enthalpy, the process repeats for next time steps. The values of thermal parameters used in simulation are listed in Table 4.1[137, 157].

### 4. 5 RESULTS AND DISCUSSION

To study the freezing and heating process a constant cooling  $T_c = -196$  °C for t < 1500 sec and constant heating  $T_c = 40$  °C for 1500 sec  $\le t \le 2000$  sec is applied at skin surface. To apply cryosurgery precisely, it is important to know the extent of tissue freezing

and the thermal history in the tissues. In this regards temperature profile in tissues at t = 250 sec, 750 sec, 1000 sec and 1500 sec are shown in Figure 4.2.

The position of two phase change interfaces with respect to time is shown in Figure 4.3. At t = 1500 sec upper interface reaches at x = 1.25 mm while lower interface covers a distance 1.20 mm inside the body.

Table 4.1: Properties of Three-Layer Skin model [Zhang, 2002, Tovi, 1999]

Thermal Parameters	Epidermis	Dermis	Sub-cutaneous	
Density in frozen state (kg/m³)	921.00	921.00	921.00	
Density in unfrozen state (kg/m³)	1200.00	1200.00	1000.00	
Specific heat in unfrozen state (J/kg°C)	3600.00	3400.00	3060.00	
Specific heat in frozen state(J/kg°C)	1800.00	1800.00	1800.00	
Thermal conductivity in unfrozen state	0.26	0.52	0.21	
(W/m°C)				
Thermal conductivity in frozen state	2.0	2.0	2.0	
(W/m°C)				
Blood perfusion rate (Kg/m³s)	0.0	0.5	0.5	
Metabolic heat generation (W/m³)	0.0	2500.00	2500.00	
Latent heat (kJ/kg)	250.00	250.00	250.00	
Specific heat of blood (J/kg°C)		1230.00		

At t = 1500 sec cooling is removed and a constant heating  $T_c = 40$  °C is applied at x = 0, now thawing process starts from two sides one from skin surface due to heating, towards body core and another, due to heat supply from the body core toward skin surface.

The position of upper and lower interfaces during thawing with respect to time is

given in figure 4.4. The upper interface meets at t = 1931 sec at a distance 0.76 mm from skin surface while lower interface meets at t = 1696 sec at a distance 0.70 mm from skin surface.

Figure 4.5 shows the transient temperature profile during heating of tissues at time t = 1510 sec, 1590 sec, 1696 sec and 1931 sec. It is clear that there is a significant rise in temperature of tissues with respect to time during heating.

### 4.6 CONCLUSIONS

In this paper a multi-layer human skin model is used to study the freezing and thawing process during cryosurgery. To solve the phase-change problem enthalpy formulation is used. Non-ideal property of biological tissues, blood perfusion and metabolic heat generation is taken into account in the model. Transient temperature profile and position of freezing/thawing interfaces are obtained numerically which is important to apply cryosurgery precisely. Information from this paper is significant for the operation of a successful cryosurgical treatment planning and can also be applied to cryo-preserved living organ.

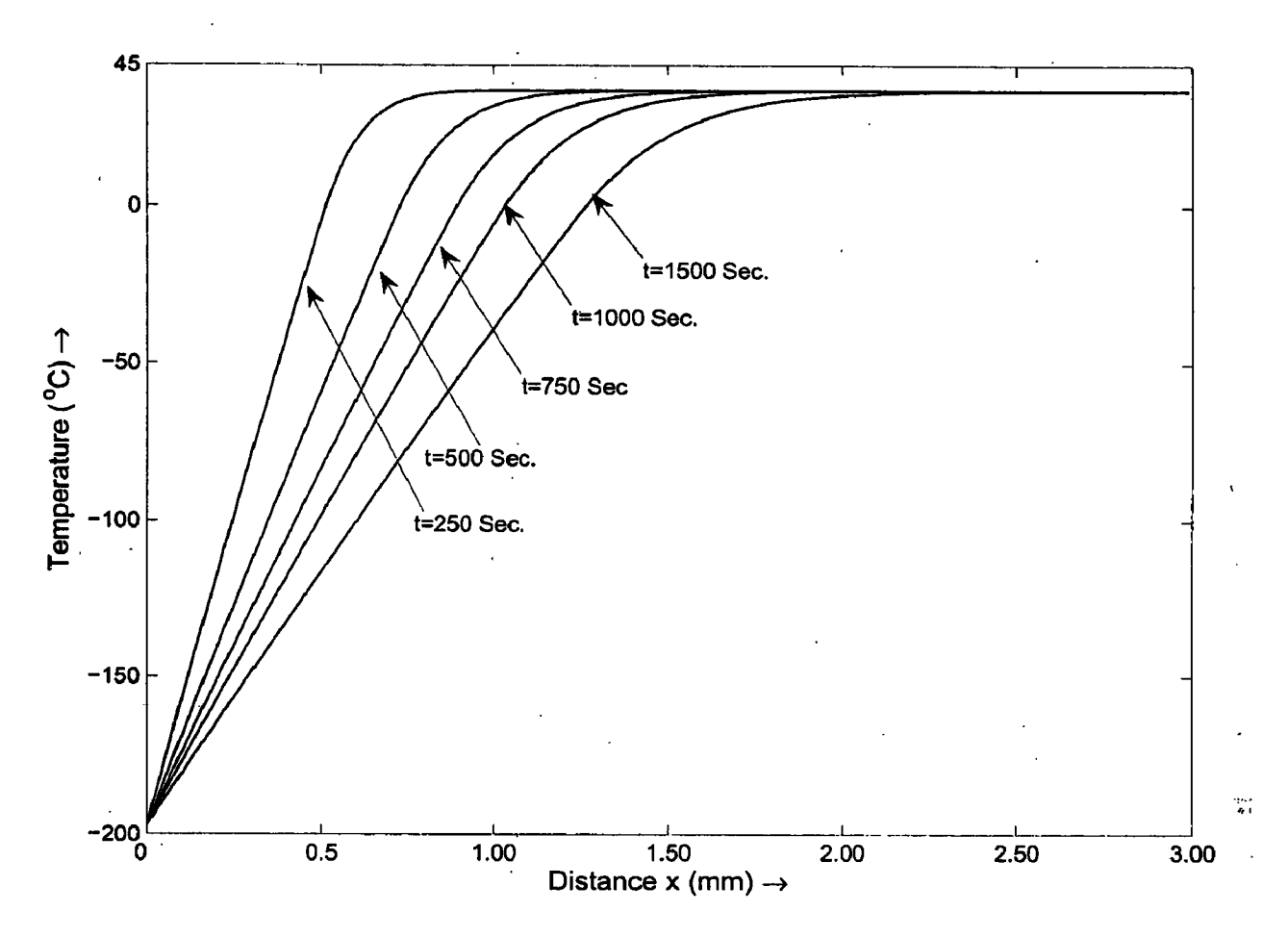


Figure 4.2: Transient temperatures for t  $\leq$  1500 sec.

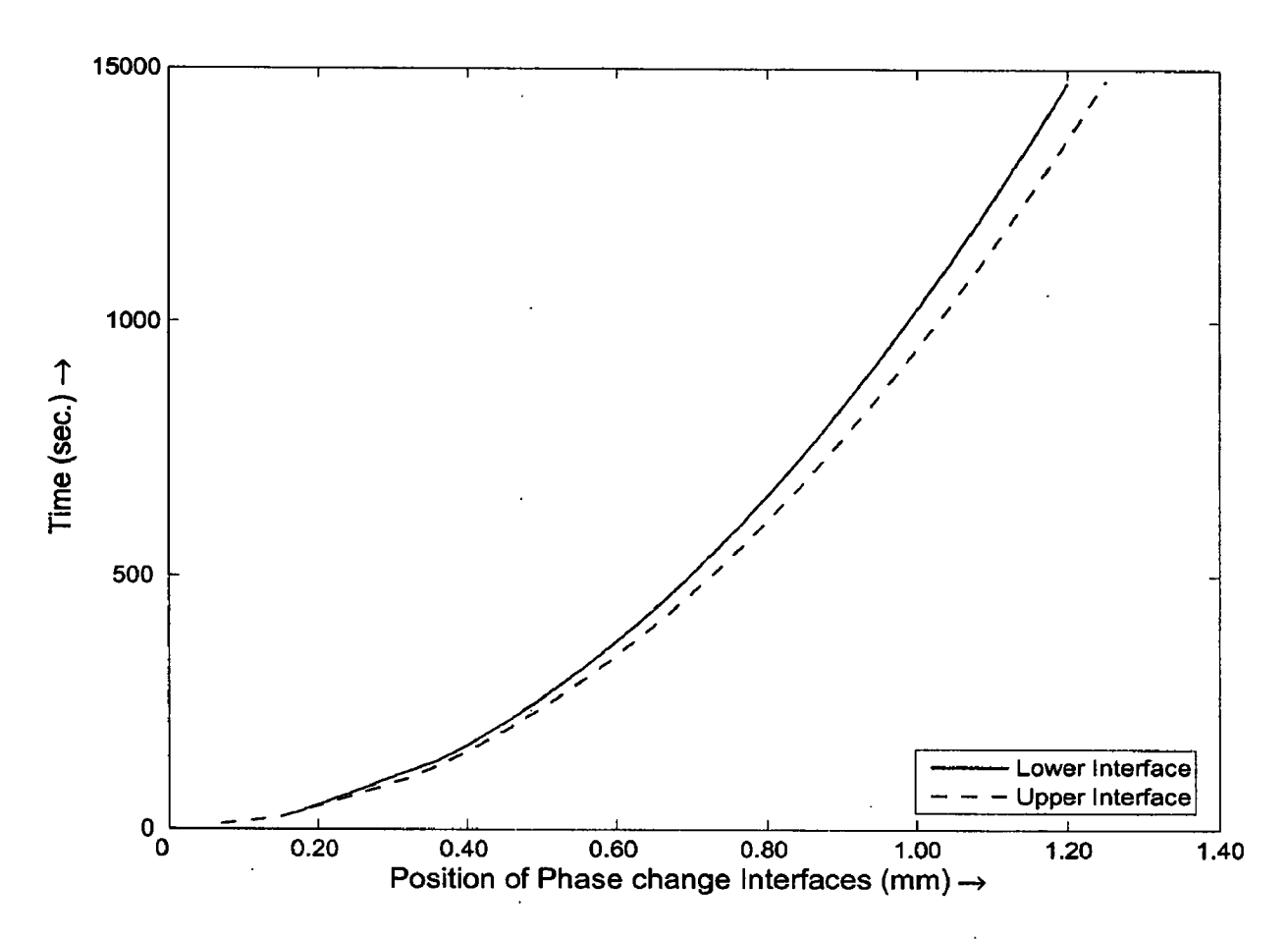


Figure 4.3: Position of phase change interfaces during freezing.

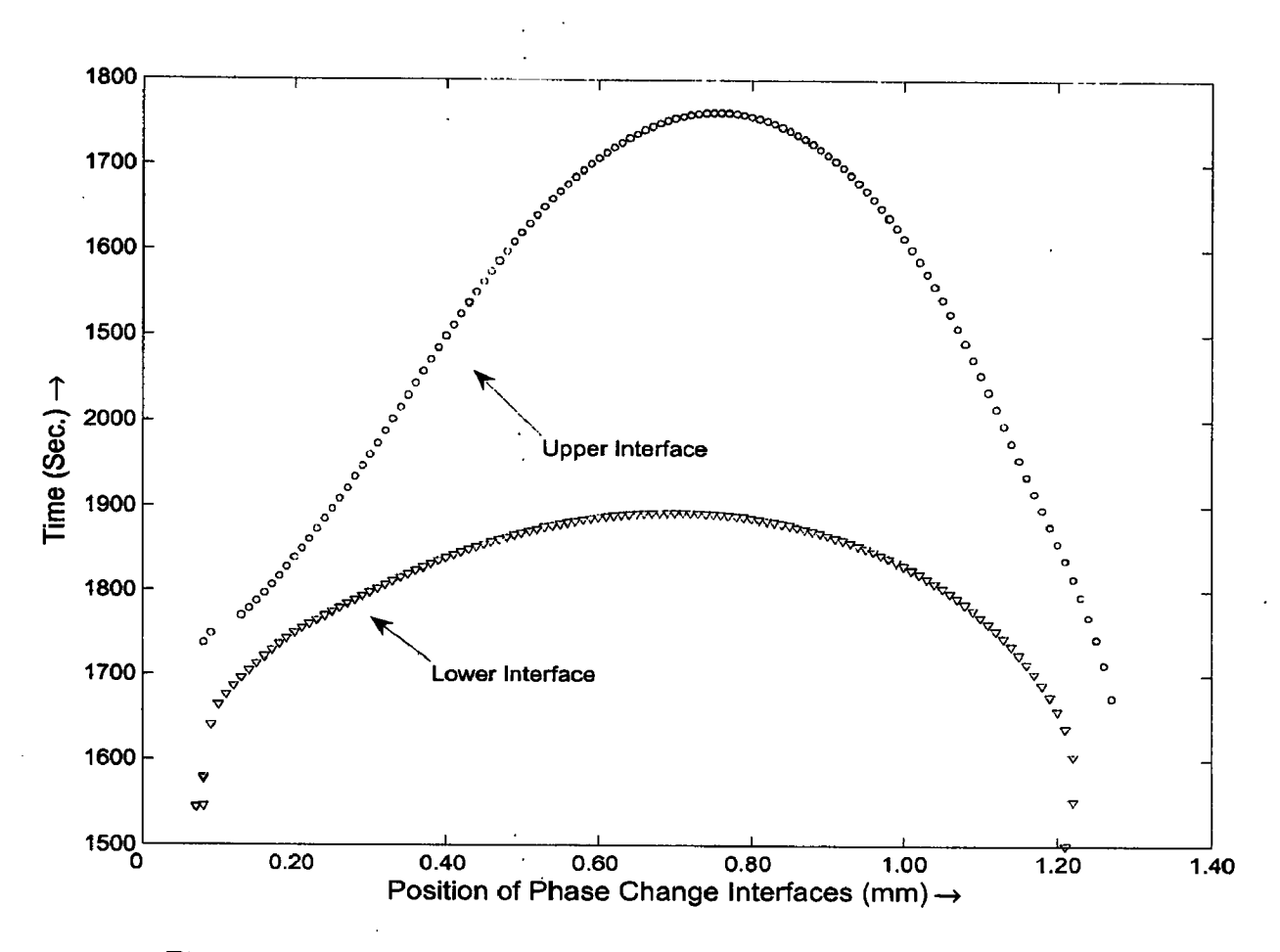


Figure 4.4: Position of phase change interfaces during thawing.

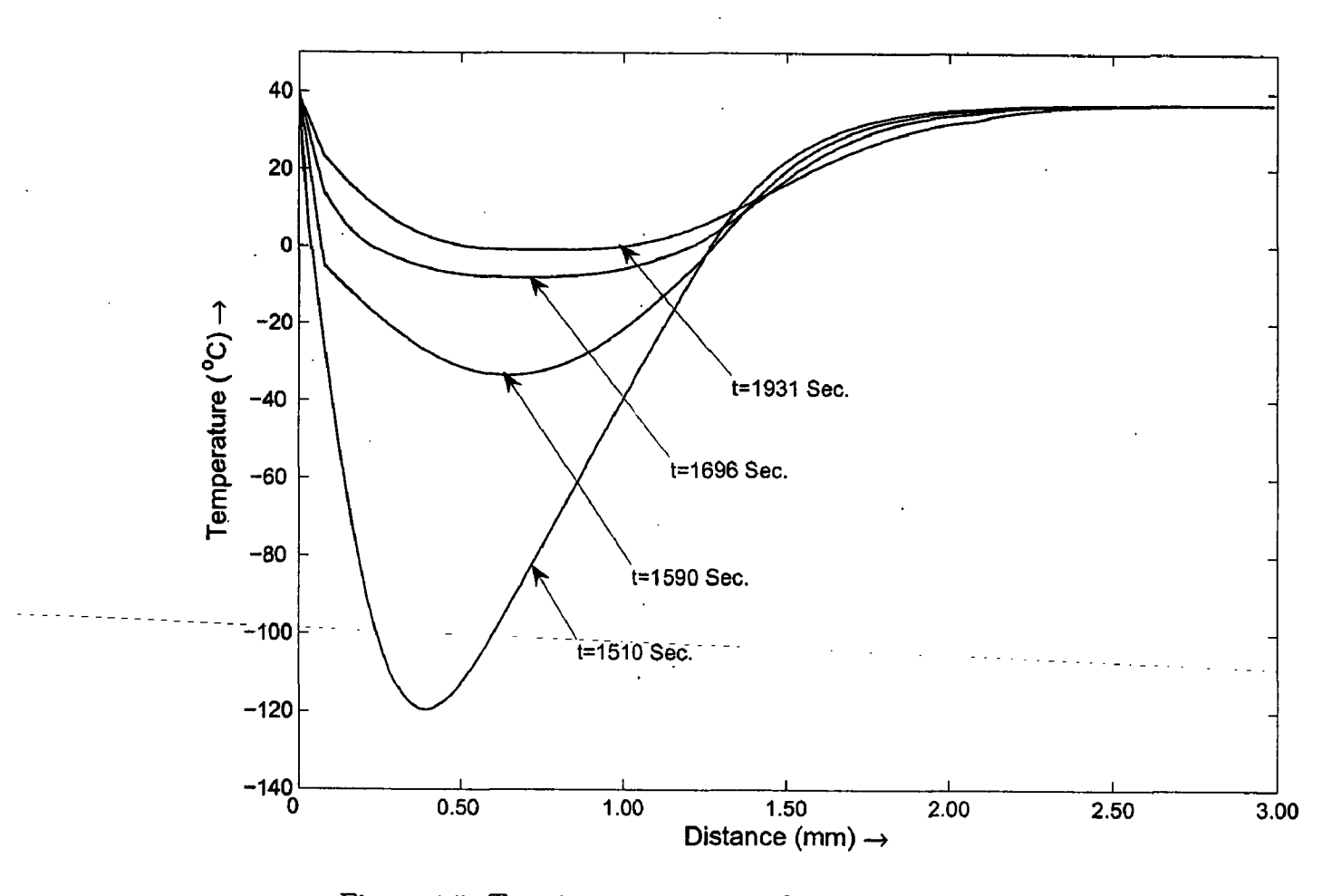


Figure 4.5: Transient temperature for  $1500 \le t \le 2100$  sec.

## **Chapter 5**

# MATHEMATICAL MODELLING OF FREEZING AND THAWING PROCESS IN TISSUES AS A POROUS MEDIA

## 5.1 INTRODUCTION

A material volume consisting of solid matrix with an interconnected void is defined as porous media. The ratio of void space to the total volume of the medium is defined as its porosity. The development of transport models in porous media has a bearing in the progress of several applications such as geology, chemical reactors, drying and liquid composite modeling, combustion and biological applications.

The blood perfused tissue volume, including blood flow in micro-vascular bed character, contain many vessels and can be treated as a porous structure consisting of a tissue fully filled with blood (Figure 5.1 [64]). Blood enters these tissues through vessels, referred to as arteries and perfuse to the tissue cells via blood capillaries. Returning blood from the capillaries gets accumulated in veins where the blood is pumped back to the heart.

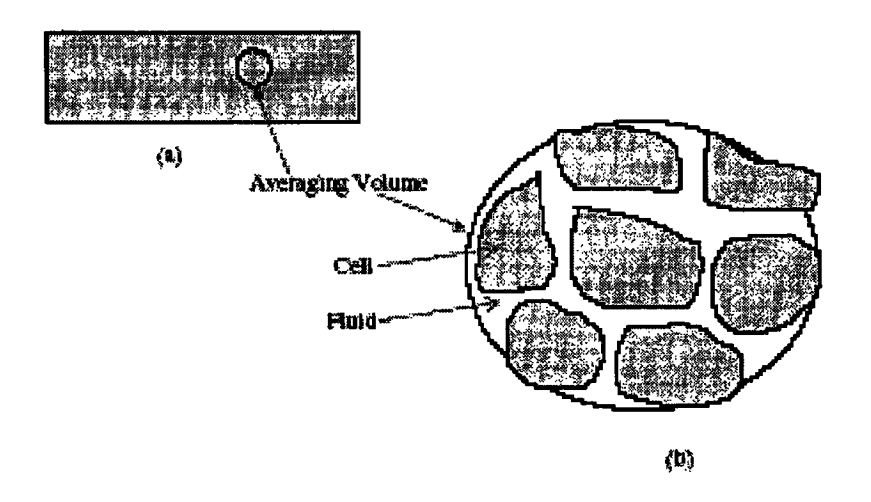


Figure 5.1: Schematic diagram for a tissue: (a) tissue and (b) averaging volume

Energy transport in the tissue is due to thermal conduction, blood perfusion and heat generation. The energy transport in biological system is usually expressed by bioheat equation, as proposed by Pennes [99]. Some other models are also proposed to model energy transport in biological tissue by Weinbaum, Jiji and Lemons [62]; Weinbaum and Jiji [146] and Chen and Holmes [23] etc.

The real application of the porous media models and bioheat transfer in human tissue is relatively recent. In this regard a system of two energy equations, containing one equation for the blood and the other for the peripheral skeletal tissue has been proposed by Xuan and Roetzel [150, 151] using porous media concept to model the tissue blood system composed mainly of tissue cells (solid particles) and interconnected voids. The interconnected voids contain either arterial or venous blood. They used the principle of local thermal non-equilibrium between the tissue and blood to formulate the thermal energy exchange in the tissue.

Recently, Shih et al. [125] proposed a modified transient bioheat transfer equation based on porous media property. The scalar effective thermal conductivity and directional effect of blood flow were also included, but the metabolic heat generation term was not considered in the energy equation. A review article on the role of porous media in modeling flow and heat transfer in biological tissues has been given by Khaled and Vafai [64].

In biological tissues, freezing and thawing phenomena are associated with cryosurgery and cryopreservation. Plenty of publications have been devoted to the thermal modeling of phase change problem during freezing and thawing using Pennes bioheat equation. But to the best of author's knowledge, study on freezing and thawing of biological tissues considering it as porous media is rare.

In the present study an attempt has been made to incorporate the porous media concept in the study of freezing and thawing of biological tissues. Effective heat capacity approach has been used to model the phase change phenomena. Resulting mathematical model is solved using finite difference method. Moreover, non-ideal property of tissues and metabolic heat generation in tissues has also been taken into account. It is observed that freezing and thawing processes slow down with increase in porosity.

## 5.2 MATHEMATICAL MODEL

The vascular volume of tissue is fully occupied with blood flow i.e. vascular volume of tissue is equal to the blood volume. The energy equation in tissue and blood can be written as [125]:

(a) In tissue:

$$\rho_{t}c_{t}\frac{\partial T_{t}}{\partial t} = \nabla \cdot (k_{t}\nabla T) + w_{b}\rho_{b}c_{b}(T_{b} - T) + Q_{m}, \qquad (5.1)$$

(b) In blood

$$\rho_b c_b \left( \frac{\partial T_b}{\partial t} + u_b \cdot \nabla T_b \right) = \nabla \cdot (k_b \nabla T_b), \tag{5.2}$$

where  $\rho$  is density of tissue; c, specific heat; k, thermal conductivity;  $w_b$ , blood perfusion rate; T, temperature; t, time; u, blood velocity;  $T_b$ , arterial blood temperature and  $Q_m$  is the metabolic heat generation in the tissue. Subscripts t and b stands for tissue and blood respectively. Combining and rearranging equations (5.1) and (5.2) using the volume averaging conservation principal, the one dimensional energy transport equation in biological tissue, regarded as homogeneous porous media, is obtained as [125]

$$\left(\phi \rho_b c_b + \left(1 - \phi\right) \rho_i c_i\right) \frac{\partial T(x, t)}{\partial t} + \phi \rho_b c_b u \frac{\partial T(x, t)}{\partial x} = \frac{\partial}{\partial x} \left(K \frac{\partial T(x, t)}{\partial x}\right) + (1 - \phi) \left\{w_b \rho_b c_b (T_b - T(x, t)) + Q_m\right\}$$

$$(5.3)$$

where  $K = \phi k_b + (1 - \phi)k_t$ ; u is blood velocity along x - direction and  $\phi$  is porosity of the medium.

When modeling the effect of freezing and thawing this equation should include three phases: Matrix (tissue cells), fluid (blood) and ice. For this the following volume fractions are defined [85]

$$\phi_m = \phi$$
,  $\phi_{bu} = \phi \Theta$ ,  $\phi_{bf} = \phi - \phi_{bu}$ ,

where subscripts m, bu and bf stands for tissue (solid matrix), blood (fluid) and ice respectively.

 $\phi_m + \phi_{bu} + \phi_{bf} = 1$ , implies that pore space is saturated and

$$\Theta = \begin{cases} \exp\left[-\left(\frac{T - T_{ml}}{\eta}\right)^{2}\right] & T < T_{ml} \\ 1 & T \ge T_{ml} \end{cases}$$
(5.4)

The thermal conductivity could be approximated as [113]

$$K(\phi_{m,bu,bf},T) = \left[\phi_{m}\sqrt{k_{m}(T)} + \phi_{bu}\sqrt{k_{bu}(T)} + \phi_{bf}\sqrt{k_{bf}(T)}\right]^{2}$$
(5.5)

## **Initial and Boundary Conditions**

(i). Initially whole tissue is at body core temperature (37 °C), i.e.

$$T(x,t) = 37 \,^{\circ}\text{C}$$
 at  $t = 0$ , (5.6a)

(ii). At x = 0,

$$T(x,t) = -196 \,^{\circ}\text{C}$$
, (During freezing) (5.6b)

$$T(x,t) = 40 \,^{\circ}\text{C}$$
, (During heating) (5.6c)

(iii). At other end of tissue, adiabatic condition has been taken, i.e.

$$\frac{T(x,t)}{\partial x} = 0 \text{ at } x = l, \qquad (5.6d)$$

## 5.3 NUMERICAL SOLUTION

Using effective heat capacity method the energy transport equation (5.3) for 1-D phase change problem during freezing and thawing may be written as

$$C_a \frac{\partial T}{\partial t} = \frac{\partial}{\partial x} \left( K \frac{\partial T(x,t)}{\partial x} \right) - u \frac{\partial T}{\partial x} + (1 - \phi) \rho_b c_b w_b \left( T_b - T(x,t) \right) + (1 - \phi) Q_m, \tag{5.7}$$

where effective heat capacity  $C_a$  is defined as:

$$C_{a} = \begin{cases} \phi_{bu} \rho_{bu} c_{bu} & T > T_{ml} \\ \phi_{bu} \rho_{bu} c_{bu} + \phi_{bf} \rho_{bf} c_{bf} - \rho L \frac{d\phi_{bf}}{dT} & T_{ms} \leq T \leq T_{ml} \\ \phi_{bf} \rho_{bf} c_{bf} & T < T_{ms} \end{cases}$$

$$(5.8)$$

Using forward finite difference for time derivative and central finite difference for space derivative, temperature at p+1 time step is given by:

$$T_i^{p+1} = (1 - 2F_o - W\Delta t)T_i^p + (F_o - \tilde{u})T_{i+1}^p + (F_o + \tilde{u})T_{i-1}^p + (WT_b + \tilde{Q}_m)\Delta t,$$
 (5.9)

where

$$F_o = \frac{K \, \Delta t}{C_a (\Delta x)^2} \,,$$

$$W = \frac{\left(1 - \phi\right) \rho_b c_b w_b}{C_a},$$

$$\tilde{u} = \frac{u(x_i, t)}{\Delta x \, C_a} \,,$$

$$\tilde{Q}_m = \frac{(1-\phi)Q_m}{C_a}.$$

Value of  $\Delta x$  and  $\Delta t$  are adjusted in such a way that stability criteria  $(1-2F_o-W\Delta t)\geq 0$  is satisfied. The position of upper and lower freezing interfaces are determined by the isotherms of  $T_{ms}$  and  $T_{ml}$ .

## 5. 4 RESULTS AND DISCUSSION

Thermal properties used for simulation are listed in table 5.1. During the freezing process a constant temperature -196 °C is applied at x = 0 for  $0 \le t \le 400$ . The positions of lower and upper interface with respect to time for different value of porosity have been plotted in figure 5.2 and figure 5.3 respectively.

Table 5.1 Thermal properties of tissue [[102, 103, 125]]

Property	Tissue	Blood	Ice
Thermal conductivity (W/m-°C)	0.5	0.5	2.0
Density (Kg/m <sup>3</sup> )	1050	1050	921
Specific heat (J/kg-°C)	3770	3770	1800
Latent heat (L)	333.6 kJ/l	cg	
Blood perfusion $(\rho_b c_b)$	0.5 kg/m <sup>3</sup> sec		
Blood velocity (u)	0.0005 m/sec		
Metabolic heat generation $(Q_m)$	2.5 kW/m <sup>3</sup>		

It is found that lower interface penetrates 4.1 cm, 4.2 cm, 4.3 cm, and 4.3 cm. for  $\phi = 0.2$ , 0.4, 0.6, 0.8 respectively, while the upper interface penetrates 4.3 cm, 4.4 cm, 4.5 cm, 4.5 cm for  $\phi = 0.2$ , 0.4, 0.6, 0.8 respectively during the freezing process (table 5.2) It is observed that freezing interfaces decelerate with increased value of porosity.

To study the effect of porosity on transient temperature profile in tissue, the temperature at two points  $A(x=1.5\,\mathrm{cm})$  and  $B(x=3.5\,\mathrm{cm})$  have been plotted in figure 5.4 and figure 5.5. The rate of temperature lowering, decreases with increase in  $\phi$ . Highest rate is found for  $\phi=0.2$  and least for  $\phi=0.8$ .

It is observed that when tissue is in unfrozen state the temperature decreases rapidly. When region is in mushy state, the temperature decrease slows down, because of latent heat release. This latent heat effect increases with increase in porosity.

**Table 5.2:** Penetration distance and time of freezing interfaces for different values of  $\phi$ 

	Lower Interface		Upper Interface	
Porosity	Position (cm)	Time (Sec)	Position (cm)	Time (Sec)
0.2	4.1	95.5	4.3	119.5
0.4	4.2	185.0	4.4	198.3
0.6	4.3	279.4	4.5	293.7
0.8	4.3	299.8	4.5	303.4

During the thawing process, thawing a constant temperature 40 °C is applied at x = 0 for  $400 \le t \le 1050$ . At this stage, the freezing interfaces start moving in two directions, one from x = 0 towards the body core and another from body core towards x = 0.

Figure 5.6 and 5.7 show the position of lower and upper thawing interfaces with respect to time for different values of  $\phi$ . Similar to freezing process, it is observed that thawing interfaces slow down with increase in porosity. The melting position and time of these interfaces for different values of porosity are listed in table 5.3.

Table 5.3: Meeting position and time of thawing interfaces for different values of porosity.

	Lower Interface		Upper Interface	
Porosity	Position (cm)	Time (Sec)	Position (cm)	Time (Sec)
0.2	2.5	814.9	3.0	862.8
0.4	2.6	832.7	3.4	926.2
0.6	2.7	853.0	. 3.7	975.3
0.8	2.8	876.3	4.1	1009.3

An increased value of porosity corresponds to a greater vascular volume i.e. large number of blood vessels. Thus the heat supplied by blood vessels increase with increase in porosity. Due to an increase in heat supply by the blood vessels, the freezing process slows down during freezing with increase in porosity.

During freezing all the blood vessels are frozen, so there is no heat supply by vessels on thawing. The amount of ice formed in tissue during freezing increases with increased value of porosity, so large amount of heat is required to thaw it. Thus the thawing process slows down with increased value of porosity.

#### 5. 5 CONCLUSION

In the present study, an attempt has been made to model the freezing and thawing process in biological tissues considering them as porous media. Non-ideal property and heat

generation due to metabolism has been taken into account. Effective heat capacity approach is used to incorporate the latent heat effect. Finite difference method is used to solve mathematical model. It is observed that porosity has significant effect on transient temperature profile and phase change interfaces. A decrease in freezing and thawing process is observed with increased value of porosity. This study warrants future theoretical and experimental investigations in this direction.

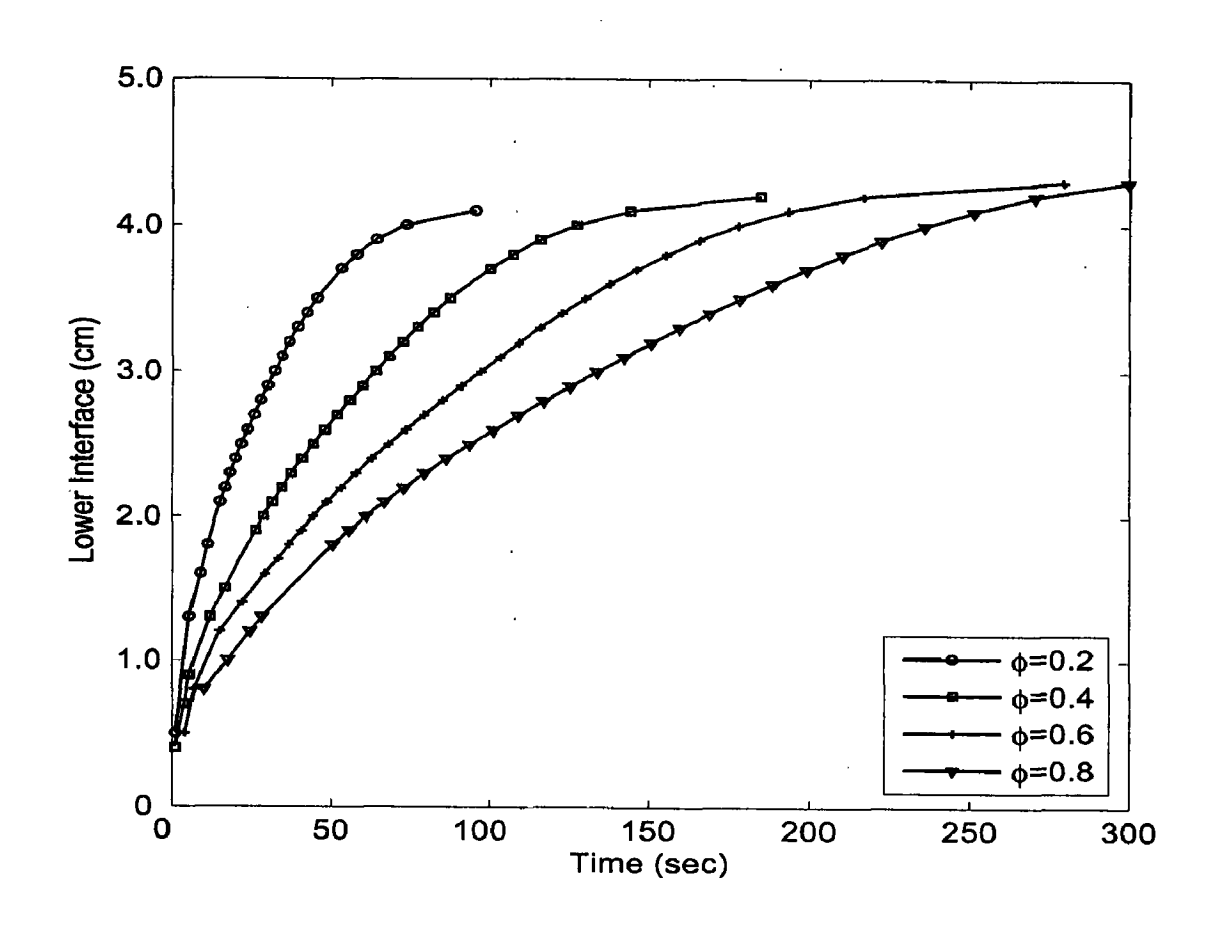


Figure 5.2: Position of lower interface during freezing for different value of porosity.

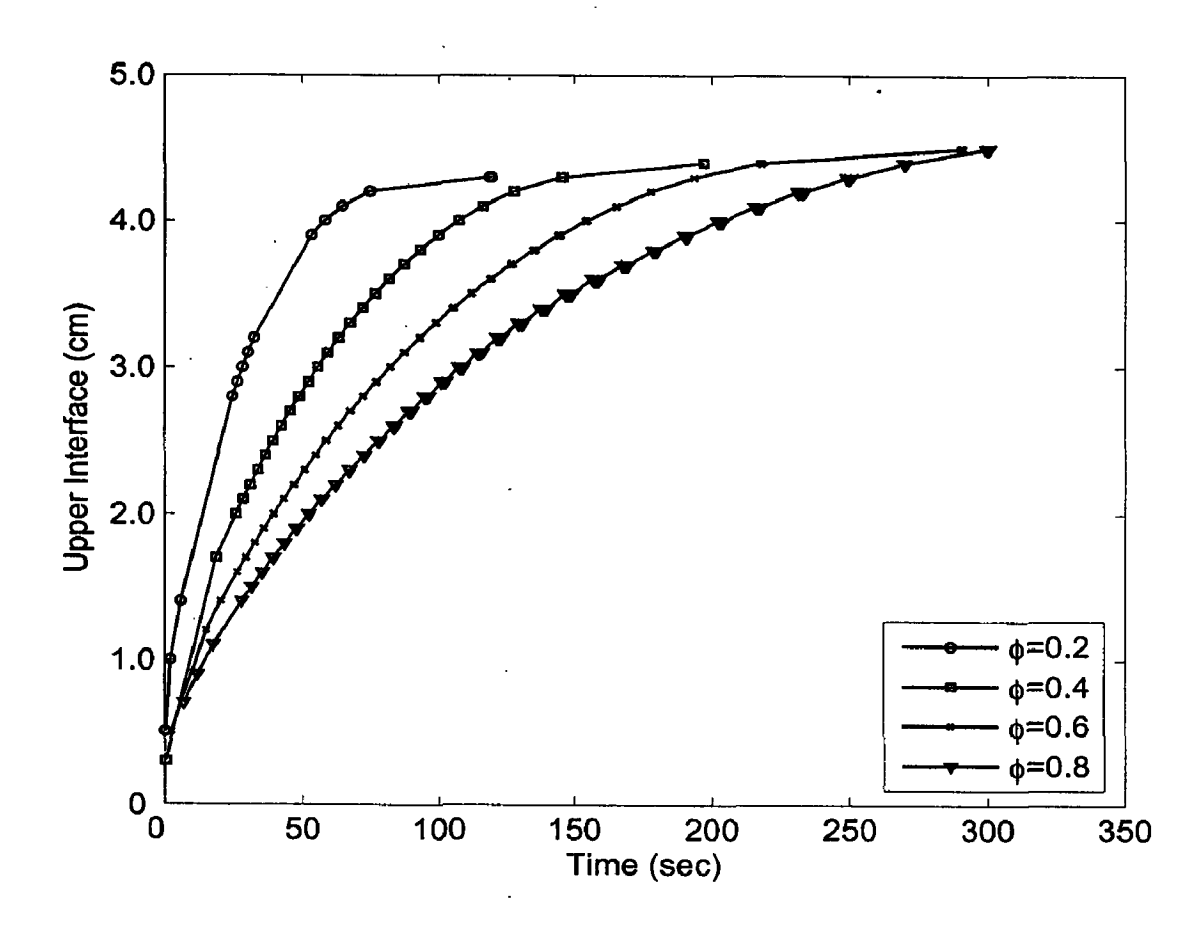


Figure 5.3: Position of upper interface during freezing for different value of porosity.

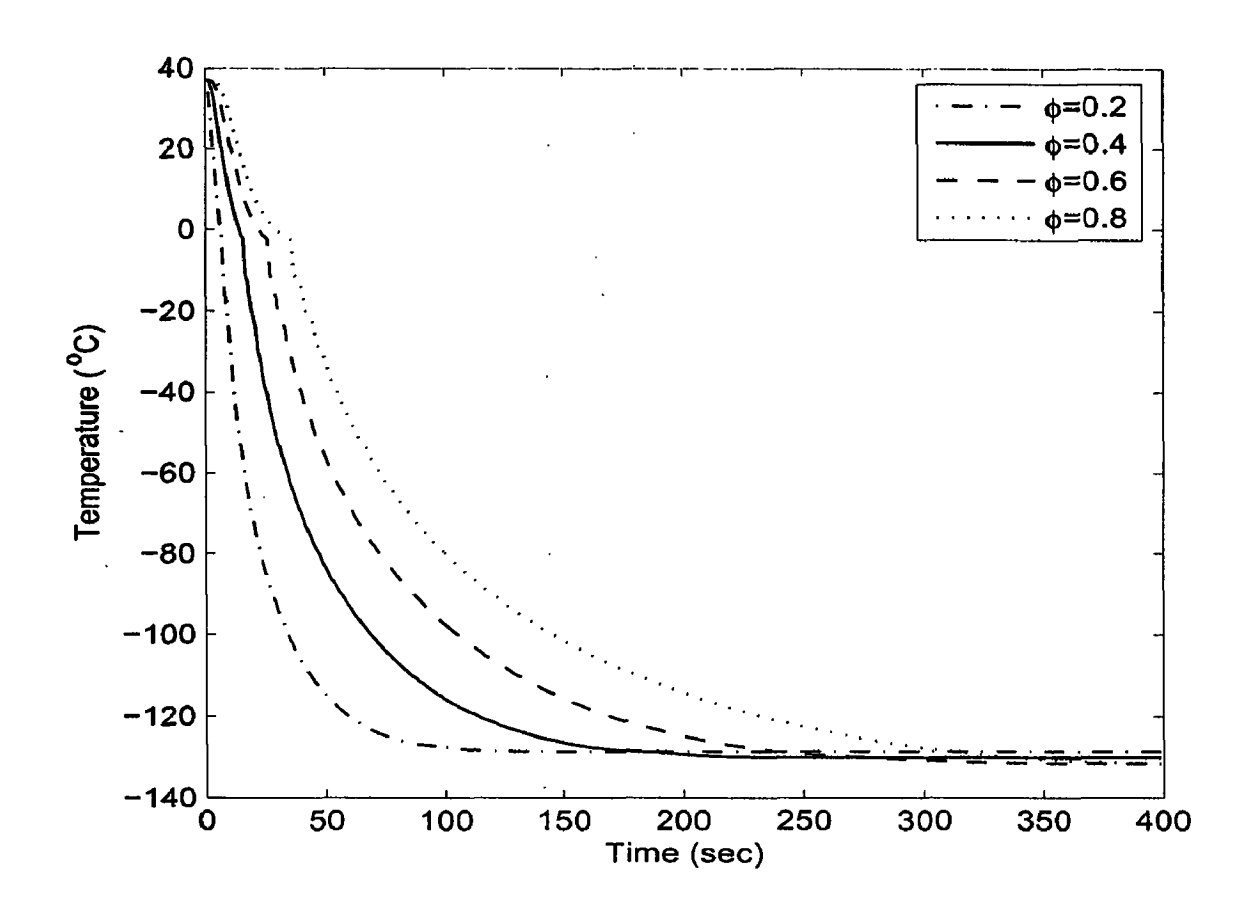


Figure 5.4: Transient temperature at point A(x = 1.5cm.).

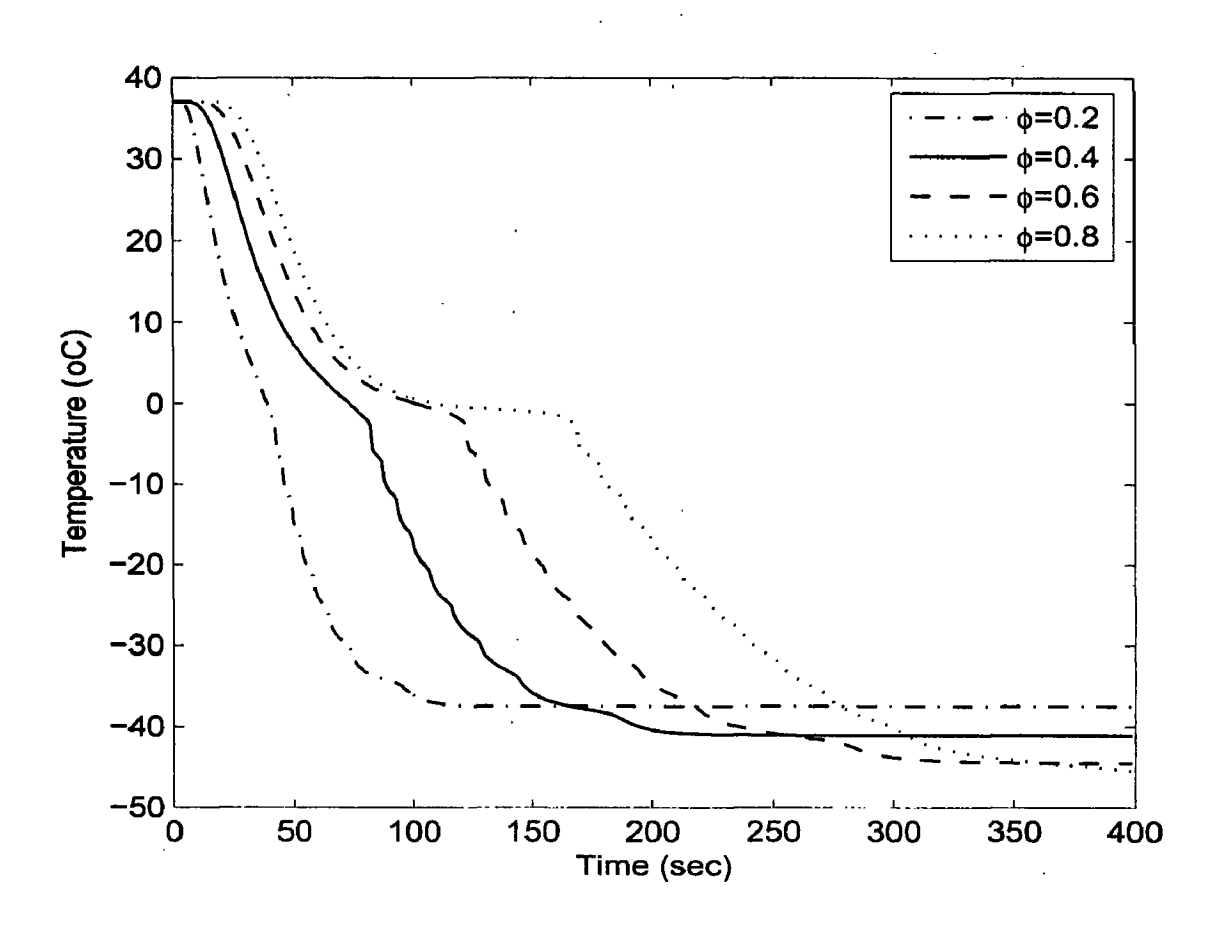


Figure 5.5: Transient temperature at point B(x = 3.5cm.)

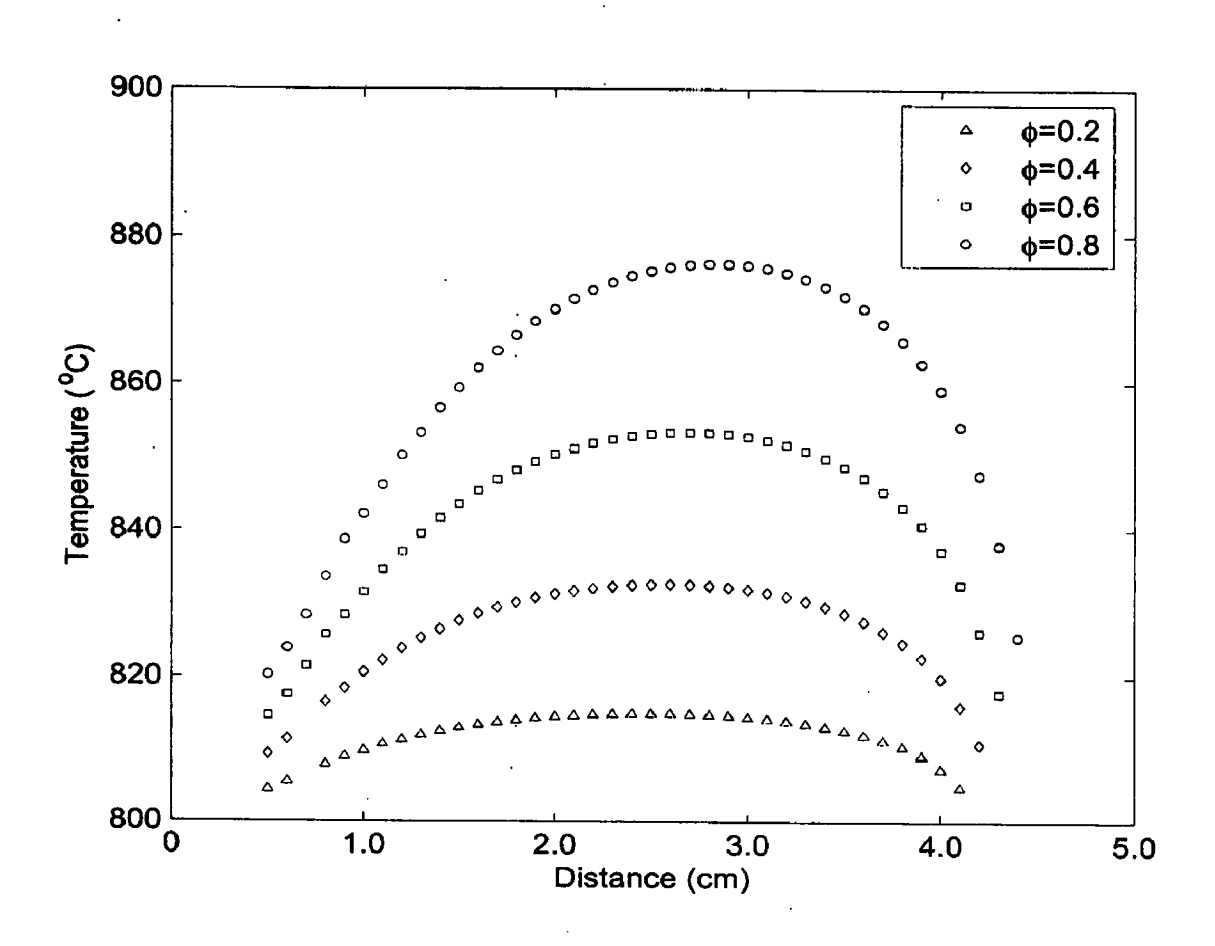


Figure 5.6: Position of lower interface during thawing for different value of porosity.

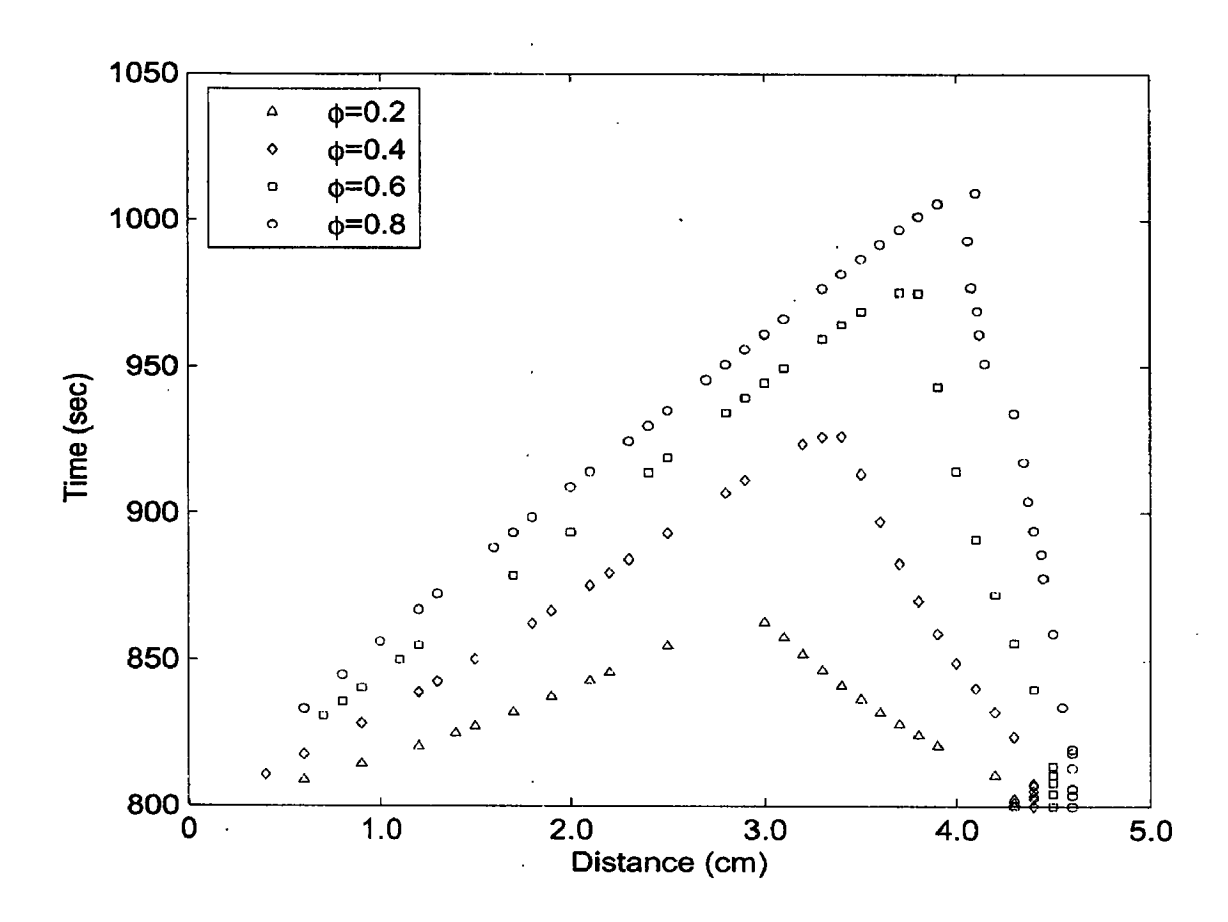


Figure 5.7: Position of upper interface during thawing for different value of porosity.

# TRANSIENT HEAT TRANSFER ANALYSIS IN FINITE MEDIA WITH ENERGY GENERATION AND CONVECTIVE COOLING

## 6.1 INTRODUCTION

The effects of volumetric energy generation on phase change problems are important for many engineering application including casting of nuclear waste materials, *vivo* freezing of biological tissues and solar collectors etc. There are some studies, which deal with the effects of volumetric heat generation on phase change.

A steady state solidification of a heat generating fluid in cooled circular tube has been investigated by Kikuchi et al. [65] assuming uniform wall temperature, which is lower than the liquid freezing temperature. The radius of the solid-liquid interface and local Nusselt number are determined as a function of position along the tube for several different values of the wall temperature and internal heat generation rate.

Chan et al. [19] proposed a mathematical model to account the existence of a two-phase zone in which partial phase can occur. The two phase zone is attributed to internal melting/solidification induces by internal thermal radiation. The effects of the two-phase zone on solidification of semi-transpared materials are also presented.

Cheng et al. [26] used collocation method to study the phase change behavior of heat generating substance with uniform distributed volumetric heat generation rate confined between two semi-infinite cold walls. The effects of the controlling parameters like heat generation rate, liquid superheat factor, the Stefan number and the thermal property ratio of

wall and freezing substance on freezing and melting behavior have been studied. Siahpush et al. [126] used integral approach to examine the effect of energy generation on solidification and melting in a semi-infinite region. The solution is limited to phase change material initially at the fusion temperature.

Recently Jiji et al. [61] used quasi-steady approach to examine the effect of volumetric energy generation on one-dimensional solidification and melting of slab using constant cooling/melting temperature at one side while other side is adiabatic.

In some other studies, the effect of volumetric heat generation has been studied in microwave thawing and laser heating [8, 71, 110], biological tissues [106, 107, 158], nuclear reactor core disruptive accidents [26, 40, 65]. In general, there is a need to study the transient behavior of the system and the effects of some important parameters on solidification.

In present study transient heat transfer analysis has been done to study the effect of volumetric heat generation on one-dimensional solidification in finite media with convective cooling. Enthalpy method is used to solve the mathematical model. Temperature profile and motion of freezing interface are calculated for different value of volumetric heat generation and convective cooling. It is found that motion of freezing interface slows down with increase in heat generation rate, while it accelerates with respect to increasing rate of convective cooling.

#### 6.2 PROBLEM DESCRIPTION

One-dimensional geometry as shown in Figure 1 has been considered. A molten material with initial temperature  $T_0$  and uniformly distributed volumetric heat generation q is

confined between two surface x = 0 and x = l. At x = 0 convective cooling is applied to mold at temperature  $T_{\infty}$ , while the surface x = l is taken to be adiabatic.

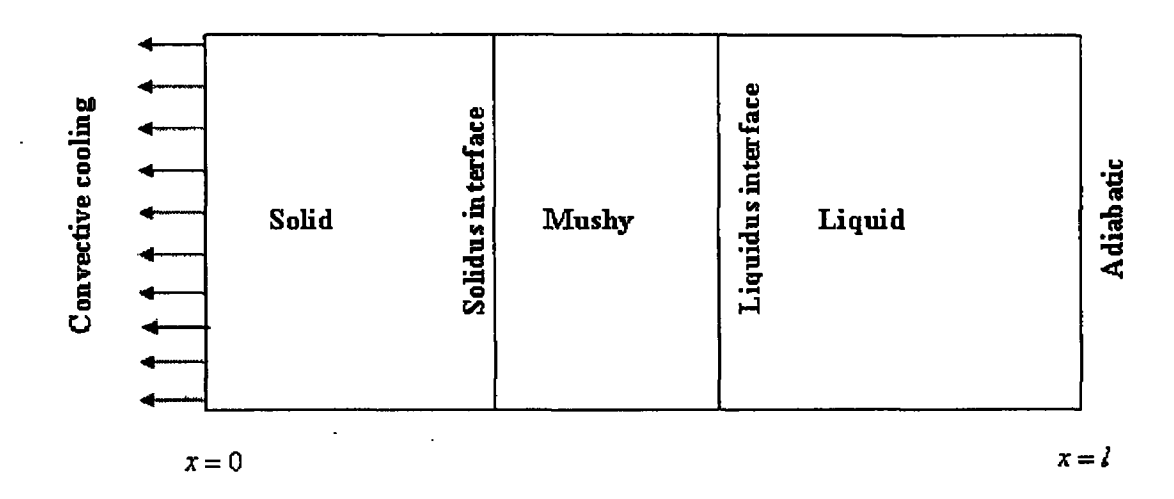


Figure 6.1 Schematic of physical problem.

#### 6.3 MATHEMATICAL MODEL

# 6.3.1 Governing equation

Governing equation for 1-D solidification in term of enthalpy can be written as

$$\rho \frac{\partial H}{\partial t} = \frac{\partial}{\partial x} \left( K \frac{\partial T(x, t)}{\partial x} \right) + q \tag{6.1}$$

where  $\rho$  is density of tissue; H, enthalpy; K, thermal conductivity; T, temperature; t, time; x, distance; and q is the volumetric heat generation. Enthalpy and tissue temperature are related as [12, 52]

$$H = \begin{cases} c_{f}(T - T_{ms}) & T < T_{ms} \\ (T - T_{ms}) \left(\frac{c_{f} + c_{u}}{2} + \frac{L}{T_{ml} - T_{ms}}\right) & T_{ms} \le T \le T_{ml} \\ L + \frac{1}{2} (c_{f} + c_{u}) (T_{ml} - T_{ms}) + c_{u} (T - T_{ml}) & T > T_{ml} \end{cases}$$
(6.2)

where  $T_{ml}$  and  $T_{ms}$  are liquidus and solidus temperatures. L is latent heat, subscripts f and u are for solid and liquid state respectively.

# 6.3.2 Assumptions

Following assumptions have been made to solve the model:

- (i). The rate of heat generation is uniformly distributed and constant throughout the liquid, solid and mushy region.
- (ii). Thermal properties of all the three regions, liquid, mushy and solid are different but constant.
- (iii). There is no volume change upon freezing.
- (iv). The temperature drop across the liquid region is such that no free convection is induced in the liquid.
- (v). The effect of radiation is neglected. Furthermore there is no boiling of the liquid.
- (vi). Phase change occur over a wide range with liquidus and solidus temperature  $T_{ml}$  and  $T_{ms}$  respectively.

### 6.3.3 Initial and Boundary Conditions

(i). Initially system is at 255 °C, i.e.

$$T(x,t) = 255$$
 °C, at  $t = 0$ 

(ii). Convective boundary condition at x = 0, i.e.

$$K\frac{\partial T(x,t)}{\partial x} = h(T(x,t) - T_{\infty})$$
 at  $x = 0$ ,

(iii). Adiabatic condition at x = l, i.e.

$$\frac{\partial T(x,t)}{\partial x} = 0$$
 at  $x = l$ ,

#### 6.4 NUMERICAL SOLUTION

Using Finite difference explicit scheme given by Voller et al. [140] and later used by Hoffman et al. [52], the enthalpy at time step (p+1) is given by

$$H_i^{p+1} = H_i^p + \frac{\Delta t K_i^p}{(\Delta x)^2 \rho_i^p} \left\{ T_{i+1}^p - 2T_i^p + T_{i-1}^p \right\} + \frac{\Delta t}{\rho_i^p} q, \qquad (6.3)$$

where i and p are space and time step respectively.  $\Delta x$  and  $\Delta t$  are the increment in space and time respectively. Time and space increments are adjusted in such a way that they should satisfy the stability criteria,  $\alpha_{\text{max}} \frac{\Delta t}{(\Delta r)^2} \leq \frac{1}{2}$  [Hoffman,2001], where  $\alpha_{\text{max}}$  is the maximum value of thermal diffusivity. After calculating enthalpy at  $(p+1)^{th}$  time level, temperature distribution at  $(p+1)^{th}$  time level is calculated by reverting equation (6.2). Once the new temperature field is obtained from enthalpy, the process repeats. Isotherms at 224.9 °G and 183.0 °C give the position of liquidus and solidus phase change interfaces respectively. Thermo-physical properties of Sn-5wt%Pb alloy used for simulation are listed in table 6.1.

#### 6.5 RESULTS AND DISCUSSION

To study the transient behavior of the system the whole process of solidification is divided into four different stages. In stage 1, whole region is in liquid state, this stage ends when mushy region starts at x = 0. During stage 2, mushy and liquid region co-exists; this stage ends when whole region converts into mushy region. Stage 3 begins when solidification starts at x = 0, during this stage whole region may be in solid-mushy or solid-mushy-liquid

stage. Stage 3 ends when whole region is solidified. In stage 4, only solid phase exists, this phase ends when system reaches in steady state.

Table 6.1: Thermophysical properties of Sn-5wt%Pb [43]

Properties	Value
Thermal conductivity of solid (W/m-°C)	65.6
Thermal conductivity liquid (W/m-°C)	32.8
Density of solid (kg/m <sup>3</sup> )	7475
Density of liquid (kg/m <sup>3</sup> )	7181
Specific heat solid (J/kg °C)	217
Specific heat of liquid (J/kg °C)	253
Latent heat (KJ/kg)	592.14
Solidius temperature (°C)	183
Liquidus temperature (°C)	224.9

Figure 6.2 shows the temperature profile for  $q = 500 \,\mathrm{kW/m^3}$  and  $h = 1500 \,\mathrm{W/m^2}$  °C at  $t = 1.8 \,\mathrm{sec}$ , 40.0 sec, 76.0 sec, 105.0 sec, 124.2 sec, 350.0 sec, 481.5 sec and 1623.0 sec. Stage 1 ends at  $t = 1.8 \,\mathrm{sec}$  when mushy starts at x = 0. At  $t = 40.0 \,\mathrm{sec}$  system is in stage 2 i.e. mushy and liquid phase co-exist. Stage 2 ends at  $t = 124.2 \,\mathrm{sec}$ , while stage 3 starts at  $t = 76.0 \,\mathrm{sec}$ . Here stage 3 starts before the end of stage 2. At t = 105.0, there exist solid mushy and liquid states. At  $t = 350.0 \,\mathrm{sec}$ , solid and mushy phase co-exist i.e. system is in stage 3. Stage 3 ends at  $t = 481.5 \,\mathrm{sec}$  when whole region is solidified. The steady state is obtained at  $t = 1623.0 \,\mathrm{sec}$ ; this is the end of stage 4.

The whole nature of the system depends on h and q. Figure 3 and 4 shows the effect of heat generation on motion of liquidus and solidus interface respectively with h = 1000

W/m<sup>2</sup> °C. It is observed that with the increase of heat generation (q), interface motion is retarded. In steady state position of liquidus interface and time is listed in table 6.2. For  $q = 1150 \,\mathrm{kW/m^3}$ , 1200 kW/m<sup>3</sup>, 1250 kW/m<sup>3</sup> interface reaches at  $x = 5.0 \,\mathrm{cm}$ , but time taken is 539.90 sec, 639.00 sec and 781.50 sec respectively. For  $q = 1350 \,\mathrm{kW/m^3}$  and  $q = 1400 \,\mathrm{kW/m^3}$  though interface reaches at  $x = 5.0 \,\mathrm{cm}$ , but time taken is 1415.90 sec and 2466.8 sec. It shows that the motion of interface is retarded with increase in q. In all the above cases cooling effect is capable to extract the heat required for the solidification of the system. For  $q = 1450 \,\mathrm{kW/m^3}$ , the interface reaches only at  $x = 1.9 \,\mathrm{cm}$  at t = 2342.10. In this case equilibrium between cooling and volumetric heat generation is obtained at  $t = 2342.10 \,\mathrm{sec}$ , thus interface does not move further. Similarly for  $q = 1500 \,\mathrm{kW/m^3}$  and 1550 kW/m<sup>3</sup> equilibrium is obtained at  $t = 1845.90 \,\mathrm{sec}$  and 465.0 sec respectively. In these cases, liquid interface reaches at  $x = 1.2 \,\mathrm{cm}$  and  $x = 0.7 \,\mathrm{cm}$  respectively.

Table 6.2: Position of liquidus interface in steady state for different value of q

$q (kW/m^3)$	Distance (cm)	Time (sec.)
1150	5.0	539.90
1200	5.0	639.00
1250	5.0	781.50
1350	5.0	1415.90
1400	5.0	2466.80
1450	1.9	2342.10
1500	1.2	1845.90
1550	0.7	465.00

Similar is the situation for solidus interface motion for different value of q as shown in figure 4. The total penetration distance and time for solidus interface in steady state for different q is shown in table 6.3. Here for  $q = 800 \text{ kW/m}^3$ ,  $900 \text{ kW/m}^3$ ,  $1000 \text$ 

Table 6.3: Position of solidus interface in steady state for different value of q

$q (kW/m^3)$	Distance (cm)	Time (sec.)
800	5.0	1187.00
900	5.0	1555.10
1000	5.0	2346.40
1050	5.0	3318.30
1100	5.0	7423.50
1120	2.0	8585.40
1150	1.2	5290.00
1200	0.5	3612.10

To study the combined effect of h and q, following five cases have been considered. These cases are chosen in such a way that in steady state system is in solid, solid-mushy, mushy-liquid states.

Case	$h(W/m^2 °C)$	$q (kW/m^3)$
1	1000	700
2	1000	1100
3	2000	2500
4	3500	2500
5	4500	2500

In case 1, stage 1 ends at t = 3.5 sec. At t = 120.0 sec region is in stage 2.Stage 2 ends at t = 214.0 sec. Stage 3 starts at 248.1 sec and ends at 968.0 sec. At t = 750.0 sec solid and mushy phase co-exist i.e. system is in stage 3. Steady state is obtained at t = 3707.0 sec. In steady state system is in solid state. Temperature profiles at these time steps are shown in Figure 6.5.

Figure 6.6 shows the temperature profile for case 2 at t = 3.5 sec, 300.0 sec, 467.0 sec, 490.0 sec, 6000.0 sec, 7424.0 sec and 8769.0 sec. In this case stage 1 ends at t = 3.5 sec. At t = 300 sec region is in stage 2 which ends at t = 467.0 sec. Stage 3 starts at t = 490.0 sec and ends at t = 7424.0. At t = 6000 sec region is in stage 3. Steady state is obtained at t = 8769.0 sec. In steady state system is in solid state.

In both the case 1 and case 2, h is same but two different values of q have been taken. Comparison between case 1 and case 2 shows that in both the cases system is fully solidified, but the solidification time increases. Reason is that due to increased value of q, cooling process slows down, yet cooling effect is capable to extract the heat required to fully solidify the system in both the cases.

In case 3, 4 and 5 nature of system is studied for different value of h keeping q constant. In case 3, stage 1 ends at t=1.0 sec. At t=302.0 sec mushy region reaches at

x = 1.2 cm. Due to large value of volumetric heat generation cooling is not capable to extract the sufficient heat required for solidification. At t = 2438.0 sec steady state is obtained and mushy remains at x = 1.2 cm. In steady state, only mushy and liquid regions co-exist and no solidification is observed. Temperature profiles at t = 1.0 sec, 20.0 sec, 50.0 sec, 302.0 sec and 2438.0 sec are shown in figure 6.7. At t = 20.0 sec and 50.0 sec system is in stage 2.

In case 4 mushy region starts at t = 0.12 sec. At t = 3.76 sec and 7.0 sec region is in stage 2. Stage 3 starts at t = 13.67 sec. At t = 600 sec there exist solid, mushy and liquid states. At t = 1472.0 sec mushy reaches at x = 5.0 sec. Here stage 2 ends after the starting of stage 3. At t = 6410.00 sec region is in steady state. In steady state solidification reaches at a distance x = 2.3 cm only. Temperature profiles at these time steps is shown in figure 6.8. Comparison between case 3 and case 4, show that though whole region is not solidified in both the cases, but acceleration in solidification process is observed with increase in h, keeping q fixed. This suggest that further increase in h may produce fully solidified region. Keeping this in mind nature of system is tested for h = 4500 W/m<sup>2</sup> °C and q is same as in case 3 and case 4 (Case 5).

In case 5, system is fully solidified at t = 1612.0 sec. Figure 6.9 shows the temperature profile at different time stage for case 5. At t = 0.06 sec stage 1 ends. At t = 7.23 sec stage 3 starts while mushy reaches at x = 7.5 cm. At t = 100.00 sec and t = 300.00 sec system is in solid, mushy and liquid states i.e. system is in stage 3. At t = 490.0 sec mushy reaches at x = 5.0 cm and solid region at x = 15.3 cm. Here stage 3 begins before the end of stage 2. Stage 3 ends at t = 1612.4 sec and steady state is obtained at t = 2093.0 sec. In steady state fully solidified region is obtained. Comparing the result of case 5 with case 4 and 3, it is observed that for large value of q whole region can be solidified by increasing h.

# 6.6 CONCLUSION

In present chapter transient analysis of solidification of an alloy with convective cooling and volumetric heat generation have been studied using finite difference method. Enthalpy approaches is used to formulate the phase change problem. Sn-5wt%Pb alloy is used for simulation in which phase change occur over a wide range. It is observed that with increase in heat generation solidification process slows down. For large value of heat generation, it is not possible to fully solidify system. In this case fully solidified system can be obtained by increasing convective cooling.

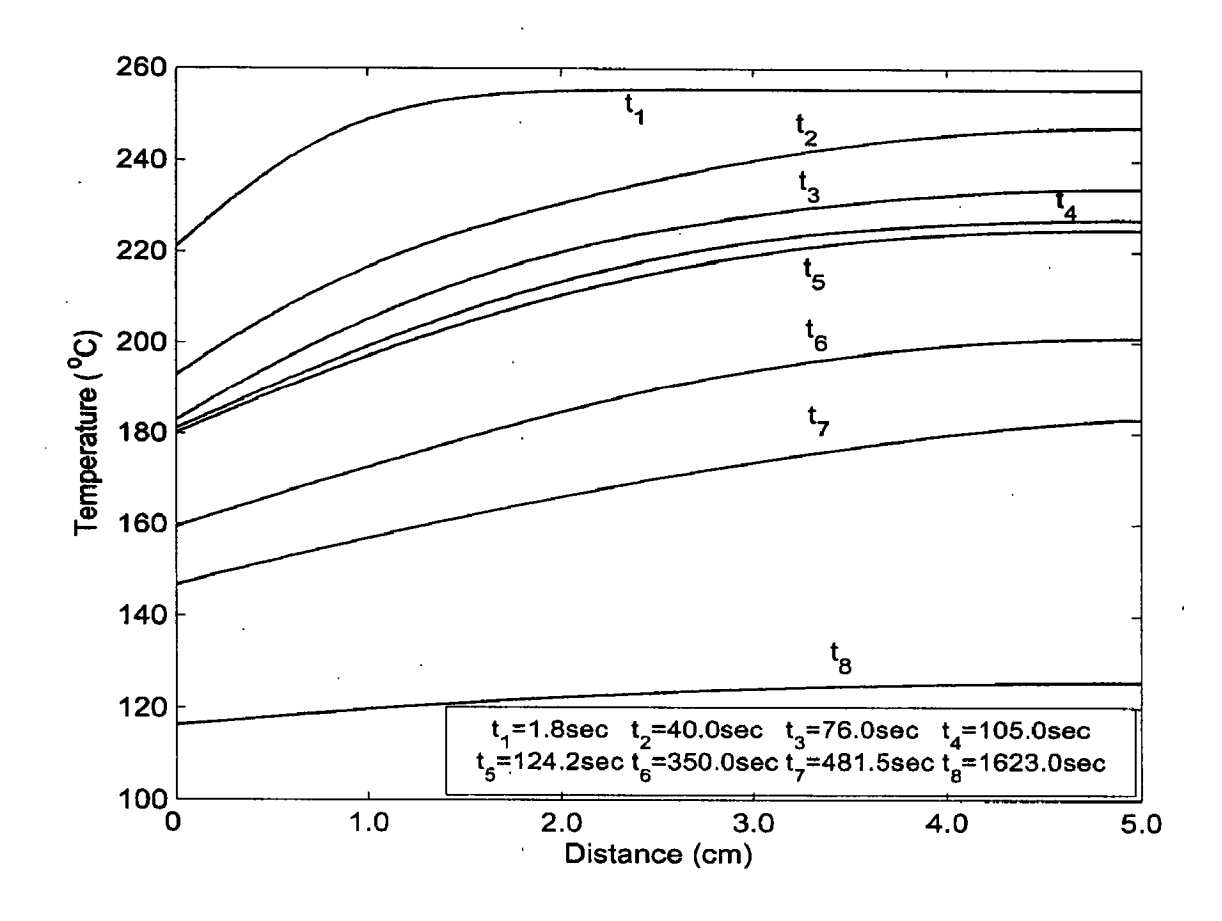


Figure 6.2: Temperature profile in region at different time t for  $h=1500 {\rm W/m^2\, ^{\circ} C}$  and  $q=500 {\rm kW/m^3}$ .

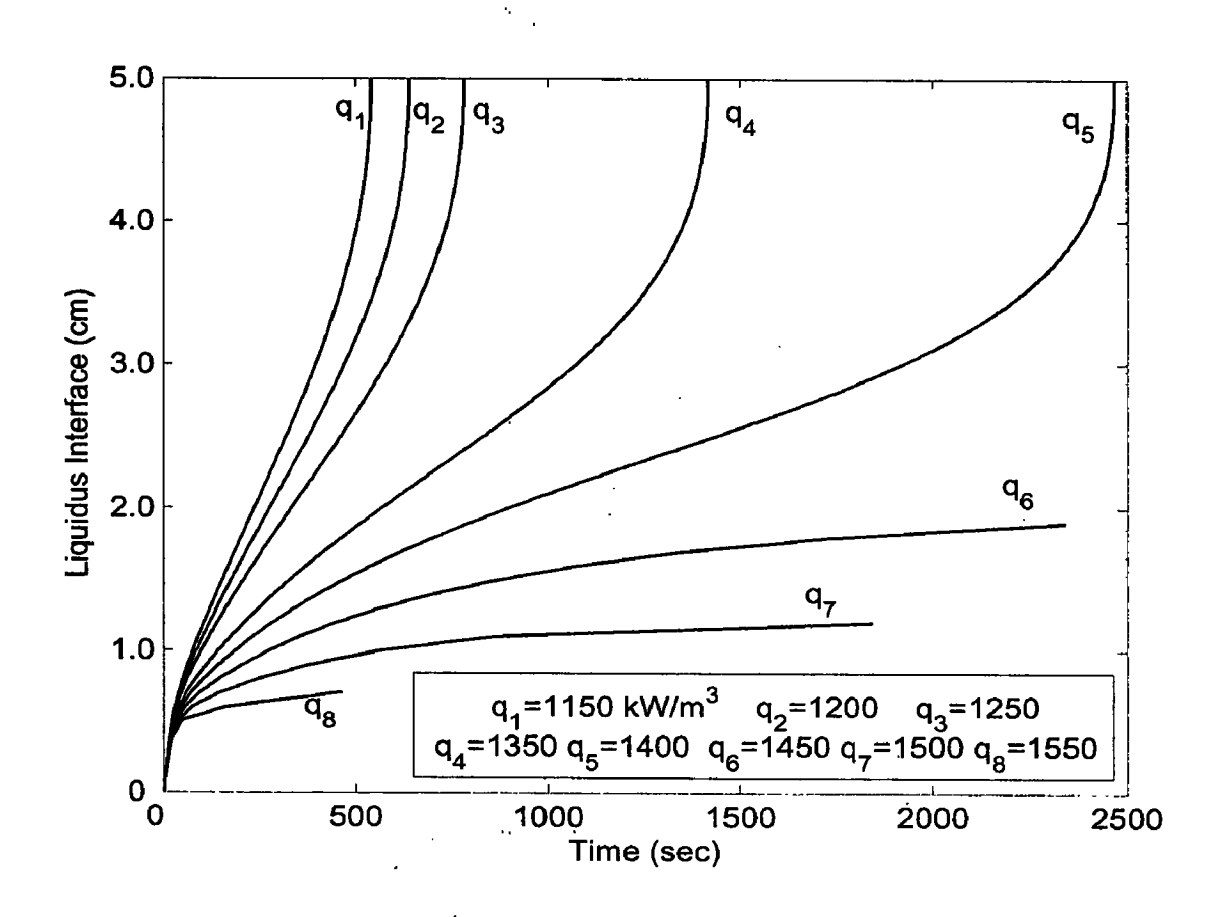


Figure 6.3: Position of liquidus interface with time for different value of q.

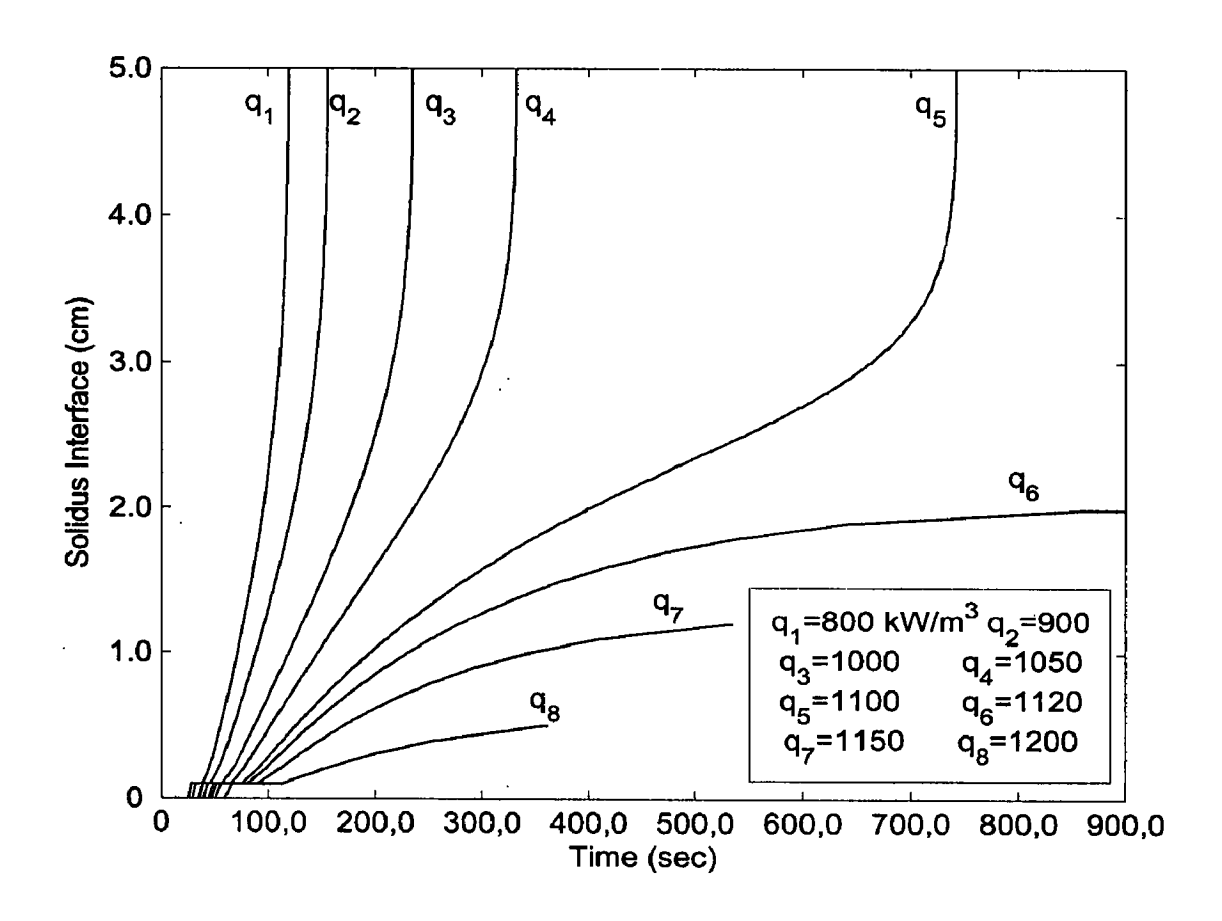


Figure 6.4: Position of solidus interface with time for different value of q.

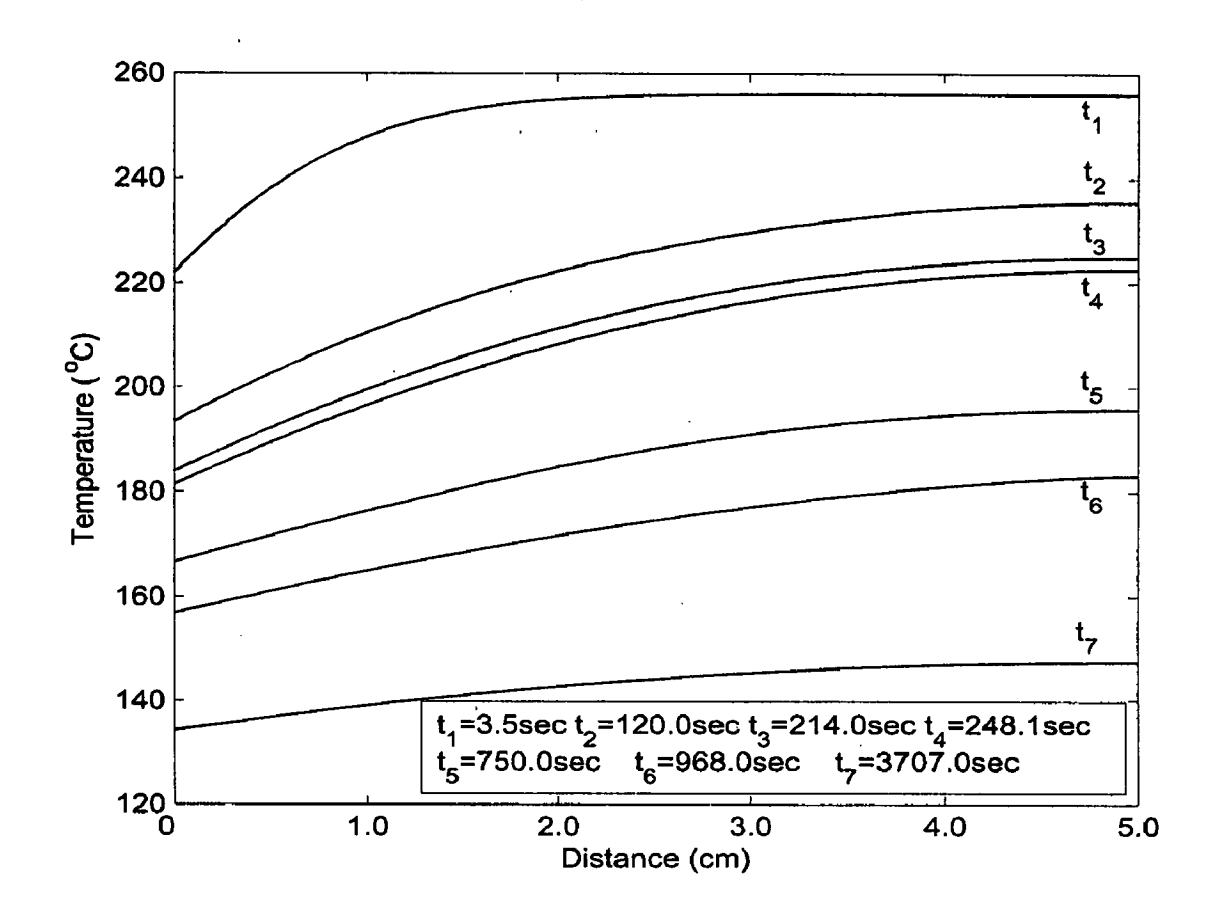


Figure 6.5: Temperature profile at different time t for case 1 (  $q=700 {\rm kW/m}^3$  ,  $h=1000 {\rm W/m}^2\,{\rm ^oC}$  ).

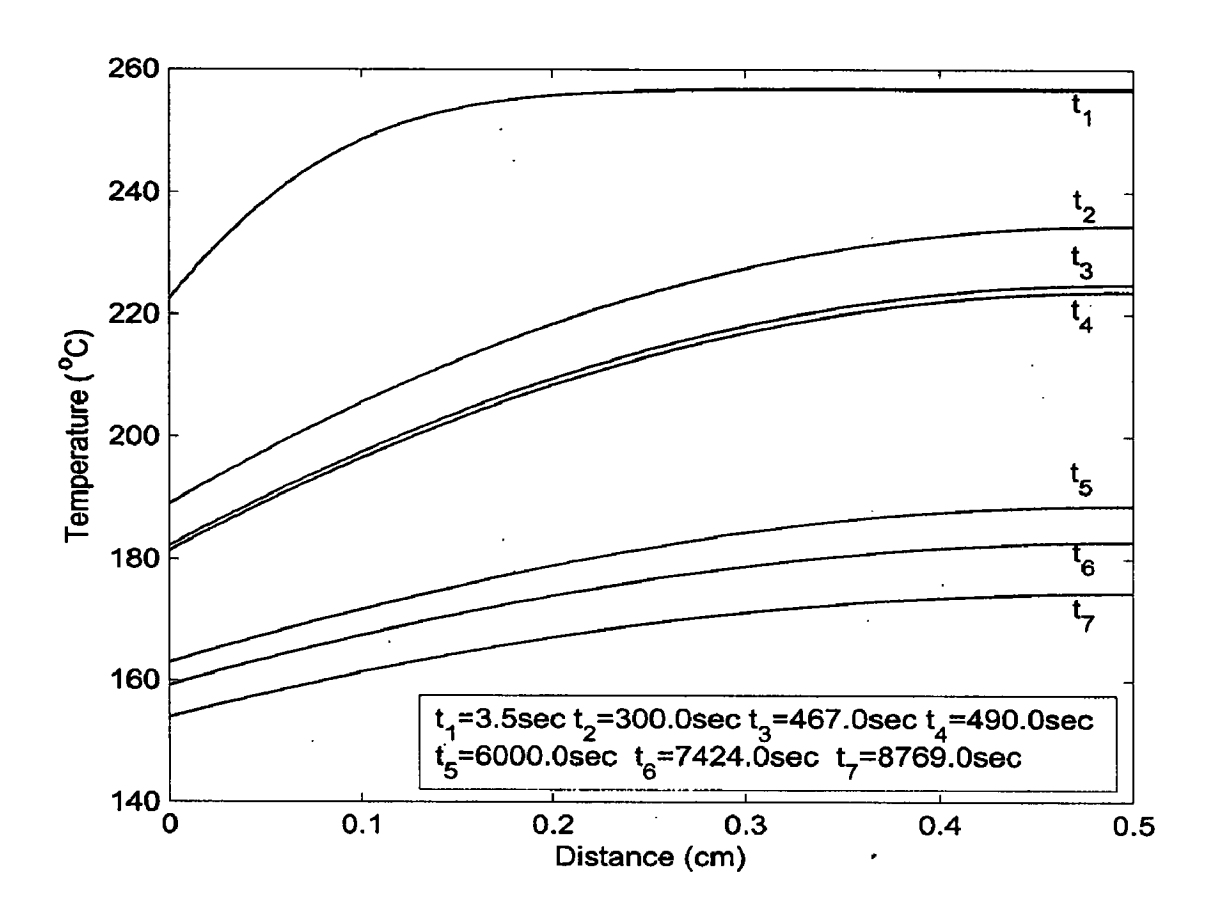


Figure 6.6: Temperature profile at different time t for case 2 (  $q=1100 {\rm kW/m}^3$  ,  $h=1000 {\rm W/m}^2\,{\rm ^oC}$  ).

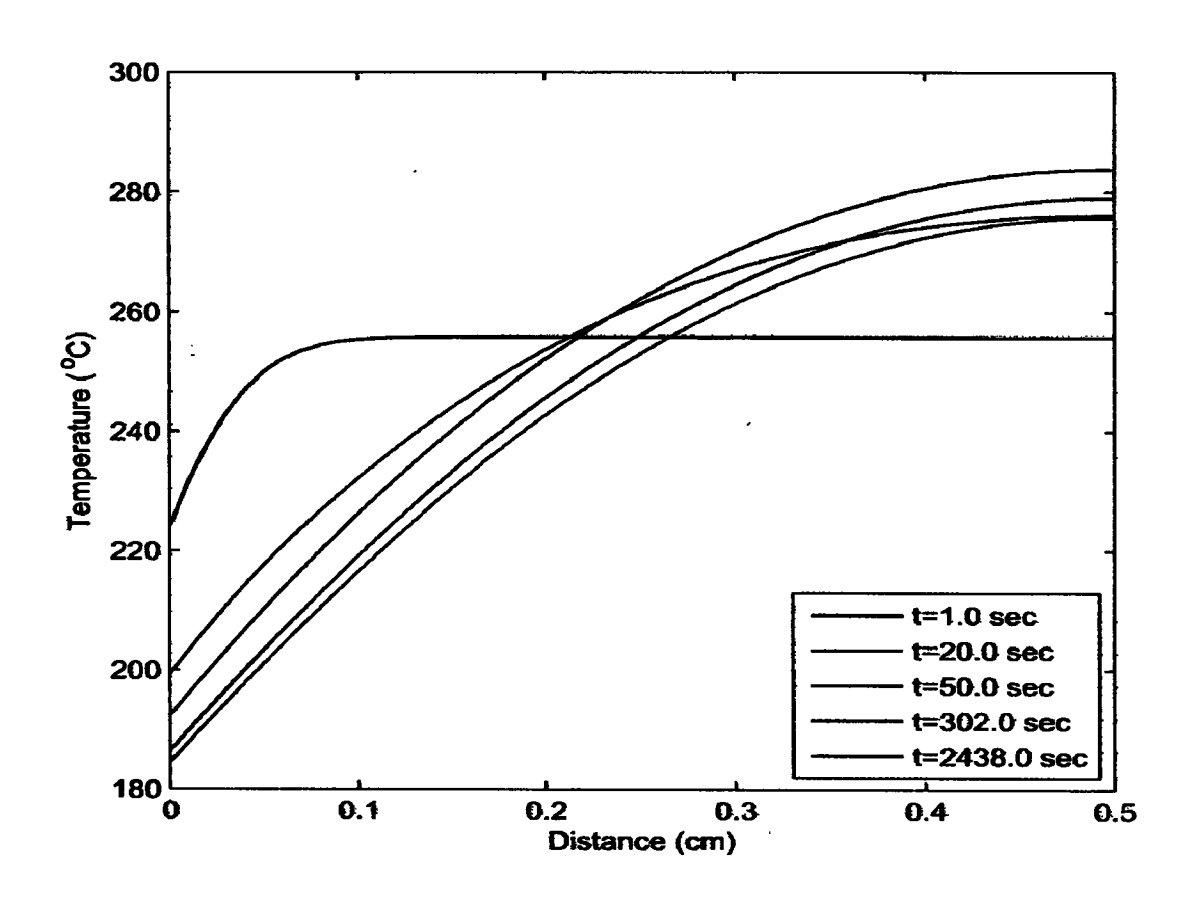


Figure 6.7: Temperature profile at different time t for case 3  $h=2000 \rm W/m^2\,^{\circ}C$  ,  $q=2500 \rm kW/m^3$ 

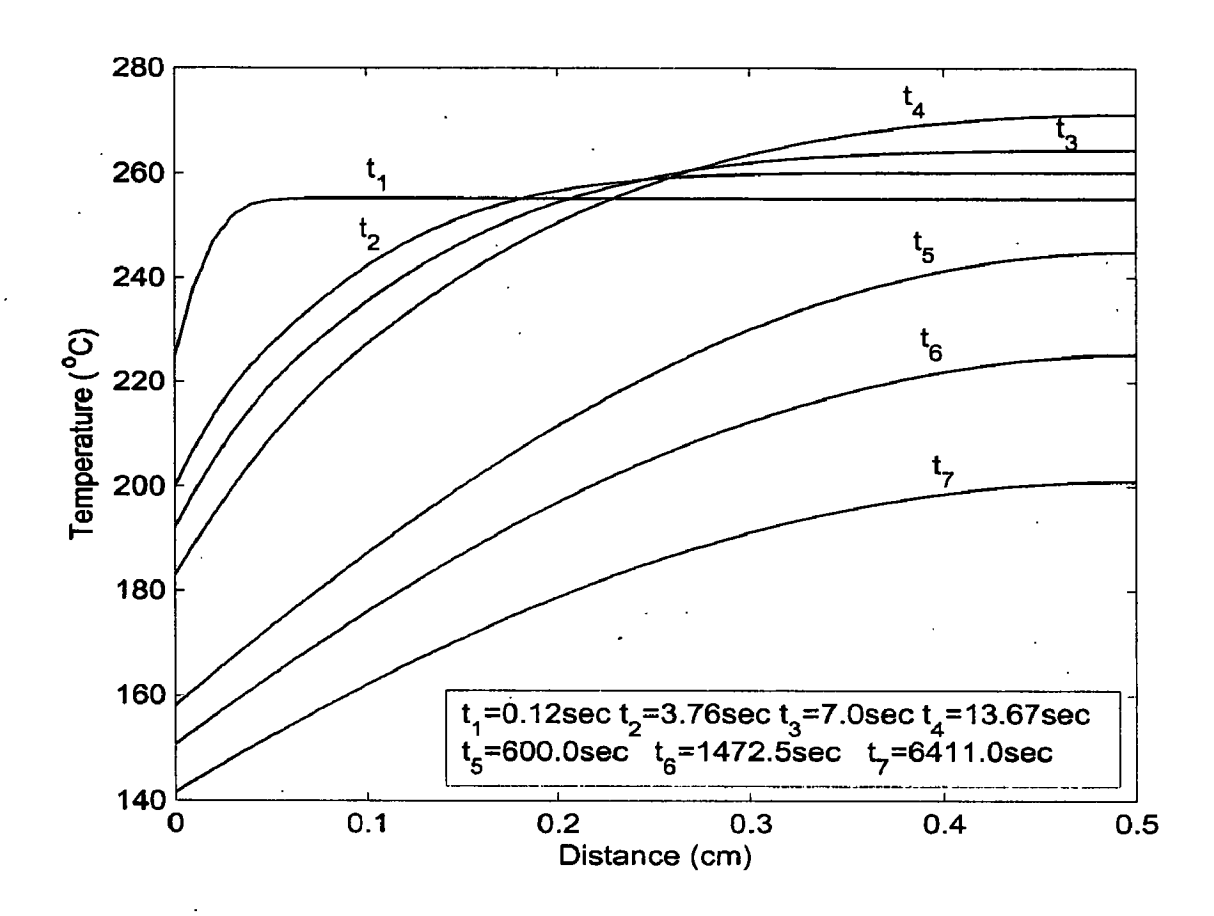


Figure 6.8: Temperature profile at different time t for case 4 (  $h=3500 {\rm W/m^2\, ^oC}$  ,  $q=2500 {\rm kW/m^3}$ 

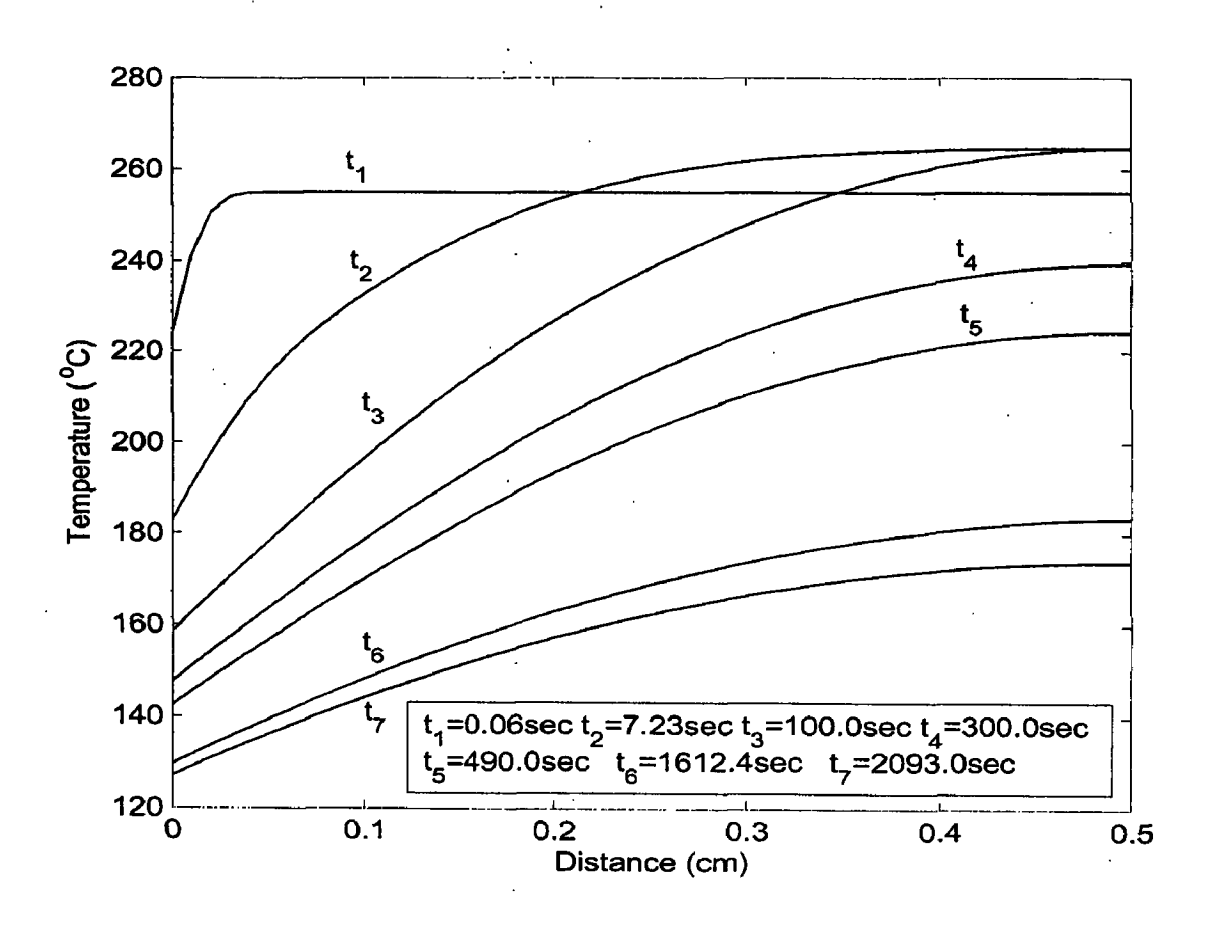


Figure 6.9: Temperature profile at different time t for case 5 (  $h=4500 \rm W/m^2\,^{\circ}C$  ,  $q=2500 \rm kW/m^3$  )

# **Bibliography**

- [1] Alexiades, V., Solomon, A. D., Mathematical modeling of melting and freezing process, Hemisphere Publication, Washington DC, 1993.
- [2] Amiri, A., Vafai, K., "Analysis of dispersion effects and non-thermal equilibrium, non-Darcian, variable porosity incompressible flow through porous media", Int. J. Heat Mass Transfer, 37-6 (1994) 939-954.
- [3] Andrushkiw, R. I., "Mathematical modeling of freezing front propagation in biological tissue", Math. Comput. Modeling, 13 (1990) 1-9.
- [4] Augustynowicz, S. D., Gage, A. A., "Temperature and cooling rate variations during cryosurgical probe testing", International Journal of Refrigeration, 8 (1985) 198-208.
- [5] Baish, J. W., Ayyaswami, P. S., Foster, K. R., "Small scale temperature fluctuation in perfuced tissue during local hyperthermia" ASME J. Biomech. Eng. 108 (1986) 246-251.
- [6] Baish, J. W., Ayyaswami, P.S., Foster, K. R., "Heat transport mechanism in vascular tissue: A model comparision", ASME J. Biomech.Eng. 108 (1986) 324-331.
- [7] Baissalov, R., Sandison, G. A., Donnelly, B. J., Saliken, J. C., McKinnon, J. G., Muldrew, K., Rewcastle, J. C., "A semi-empirical treatment planning model for optimization of multiprobe cryosurgery", Phys Med Biol., 45 (2000) 1085–1098.
- [8] Basak, T., "Analysis of resonances during microwave thawing of slab", Int. J. Heat Mass Transfer, 46 (2003) 4279-4301.
- [9] Baust, J. G., Gage, A. A., Clarke, D., Baust, J. M., Buskirk, R. V., "Cryosurgery-a putative approach to molecular based optimization", Cryobiology, 48 (2004) 190-204.

- [10] Baust, J., Gage, A. A., Ma, H., Zhang, C. M., "Minimally invasive cryosurgery-technological advances", Cryobiology, 34 (1997) 373-384.
- [11] Bischof, J. C., Bastack, J., Rubinsky, B., "An analytical study of cryosurgery in the lung", ASME J. Biomech. Eng., 114 (1992) 467-472.
- [12] Bonacina, C., Comini, G., "Numerical solution of phase change problems", Int. J. Heat Mass Transfer, 16 (1973) 1825-1832.
- [13] Budhman, H. M., Dayan, J., Shitzer, A., "Controlled freezing of non-ideal solution with application to cryosurgical processes", J. Biomech. Eng., 113 (1991) 430-437.
- [14] Budman, H., Shitzer, A. and Dayan, J., "Analysis of the inverse problem of freezing and thawing of a binary solution during cryosurgical process", ASME J. Biomech. Eng., 177 (1995) 193-202.
- [15] Budman, H., Shitzer, A., Giudice, S. D., "Investigation of temperature field around embedded cryoprobes", ASME J. Biomech. Eng., 108 (1986) 42-48.
- [16] Bumsoo, H., Bischof, J. C., "Direct cell injury associated with eutectic crystallization during freezing", Cryobiology, 48 (2004) 8-21.
- [17] Caldwell, J., Kwan, Y. Y., "On the perturbation method for the Stefan problem with time-dependent boundary conditions", Int. J. heat Mass Transfer, 46 (2003) 1497-1501.
- [18] Carslaw, H. S., Jaeger, J. C., Conduction of heat in solids, Edition-II, Oxford University Press, London, 1959
- [19] Chan, S. H., Cho, D. H., Kocamustafaogullari, G., "Melting and solidification with internal rediative transfer-A generalized phase change model", Int. J. Heat Mass Transfer, 26 (1983) 621-633.

- [20] Charney, C. K., "Mathematical models for bioheat transfer", Advances in Heat Transfer, 22 (1992) 19-155.
- [21] Charny, C. K., Levin, R. L., "Bioheat transfer in branching countercurrent network during hyperthermia" ASME J. Biomech. Eng. 111 (1989) 263-270.
- [22] Charny, C. K., Weinbaum, S., Levin, R. L., "An evaluation of the Weinbaum-Jiji bioheat equation for normal and hyperthermic conditions", ASME J. Biomech. Eng. 112 (1990) 80-87.
- [23] Chen, M. M., Holmes, K. R., "Microvascular contribution in tissue heat transfer",
  Annals of the New York Academy of Sciences 335 (1980) 137-150.
- [24] Chua, K. J., Chou, S. K., Ho, J. C., "An analytical study on the thermal effects of cryosurgery on selective cell destruction", Journal of Biomechanics, 40 (2007) 100-116.
- [25] Chun, C. K., Park, S. O., "A fixed grid finite-difference method for phase change problems", Numerical heat Transfer: Part B, 38 (2000) 59-73.
- [26] Chung, F. B., Chawla, T. C., Pedersen, D. R., "The effect of heat generation and wall interaction on freezing and melting in finite slab", Int. J. Heat Mass Transfer 27 (1984) 29-37.
- [27] Comini, G., Giudice, D. S., "Thermal aspect of cryosurgery", ASME J. Heat Transfer 98 (1976) 543-549.
- [28] Cooper, T. E., Petrovic, W. K., "An experimental investigation of the temperature field produced by a cryosurgical cannula", ASME J. Heat Transfer, Aug (1974) 415-420.

- [29] Cooper, T. E., Trezek, G. J., "Analytical prediction of the temperature field emanating from cryogenic cannula", Cryobiology, 7 (1970) 79-93.
- [30] Cooper, T. E., Trezek, G. J., "Rate of lesion growth around spherical and cylindrical cryoprobes", Cryobiology, 7 (1971) 183-190.
- [31] Craciunescu, O. I., Samulski, T. V., MacFall, J. R., Clegg, S.T., "Perturbation in hyperthermia temperature distribution associated with counter-current flow: numerical simulation and empirical verification". IEEE Trans. Biomed. Eng., 47(2000)435-43.
- [32] Crank J., Free and Moving Boundary Problems, University Press, New York, 1984.
- [33] Delgado, A. E., Sun, D. W., "Heat and Mass Transfer model for predicting freezing processes-a review", Journal of Food Eng., 47 (2001) 157-174.
- [34] Deng, Z. S, Liu, J., "Numerical simulation of 3-D freezing and heating problem for combined cryosurgery and hyperthermia therapy", Numerical Heat Transfer: Part A, 46 (2004) 587-611.
- [35] Deng, Z. S., Liu, J., "Modeling of multidimensional freezing problem during cryosurgery by the dual reciprocity boundary element method", Eng. Analysis with Boundary Element, 28 (2004) 97-108.
- [36] Devireddy, R. V., Smith, D. J., Bischof, J.C., "Effect of microscale mass transport and phase change on numerical prediction of freezing in biological tissue", ASME J. Heat Transfer, 124 (2002) 365-374.
- [37] Dey, S. K., "A novel explicit finite difference scheme for partial differential equations", Int. J. Computer Maths., 10 (1981) 70-78.
- [38] Diller, K. R., "Engineering based contribution in cryobiology", Cryobiology, 34 (1997) 304-314

- [39] Donald, A. N., Bejan, A., Convection in porous media, Edition-II, Springer Publication, New York, 1999.
- [40] El-Genk, M., Cronenberg, W., "An assessment of fuel freezing and drainage phenomena in a reactor shield plug following a disruptive accident", Nuclear Engineering and Design, 75 (1982) 73-80.
- [41] Elliott, C. M., Ockendon, J. R., Weak and Variational Method for Moving Boundary Problems", Pitman Publishing Inc, Massachusetts, 1982.
- [42] Evans, G. W., Issacson, E., Mackdonald, J. K. L., Quatl. J. App. Math., 8 (1950) 312-320.
- [43] Ferriera, I. L., Spinelli, J. E., Pires, J. C., Garcia, A., "The effect of melt temperature profile on the transient metal/mold heat transfer coefficient during solidification", Materials Science & Engineering A, 408 (2005) 317-325.
- [44] Field, S. B., Morris, C. C., "The relationship between heating time and temperature: its relevance to clinical hyperthermia", Radiother Oncol., 1 (1983) 179-186.
- [45] Gage, A. A., "Current issues in cryosurgery", Cryobiology, 19 (1982) 219-222.
- [46] Gage, A. A., Baust, J., "Mechanism of tissue injury in cryosurgery", Cryobiology, 37 (1998) 171-186.
- [47] Gage, A. A., Caruana, J. A., Montes, M., "Critical temperature for skin necrosis in experimental cryosurgery", Cryobiology, 19 (1982) 273–282.
- [48] Gage, A. A., Guest, K., Montes, M., Caruana, J. A., Whalen, Jr D. A., "Effect of varying freezing and thawing rates in experimental cryosurgery", Cryobiology, 22 (1985) 175–182.

- [49] Godman, T. R., Mass, B., "The heat balance integral and its application to problem involving a change of phase", ASME J. Heat Transfer, 8(1958) 335-342.
- [50] Gupta, S. C., "A moving grid numerical scheme for multi-dimensional solidification with transition temperature range", Compt. Methods Appl. Mech. Engg. 189 (2000) 525-544.
- [51] Gupta, S. C., Laitinen, E., Valtteri, T., "Moving grid scheme for multiple moving boundaries", Compt. Methods Appl. Mech. Engg. 167 (1999) 345-353.
- [52] Hoffmann, N. E., Bischof, J. C., "Cryosurgery of normal and tumor tissue in the Dorsal Skin Flap Chamber: Part I- Thermal response", ASME J. Biomech. Eng., 123 (2001) 301-309.
- [53] Honnor, M. E., Davies, A. J., "Nonlinear transient field problems with phase change using the boundary element method", Engineering Analysis with Boundary Element, 28 (2004) 561-570.
- [54] Hsiao, J. H., Chung, B. T. F., "An efficient algorithm for finite element solution to two dimensional heat transfers with melting and freezing", ASME Paper No.-84, HT-2 1984.
- [55] Hu, H., Argyropoulos, S. A., "Mathematical modeling of solidification and melting: a review", Modell. Simul. Mater. Sci. Eng., 4 (1996) 371-396.
- [56] Hua, T. C., Ren, H. S., Cryobiomedical Techniques, Science Press, Beijing, PR China, 1994.
- [57] Ismail, K. A. R., Henriquez, J. R., "Solidification of PCM inside a spherical capsule", Energy Conversion and Management, 41 (2000) 173-187.

- [58] Jain, R. K., "Mass and heat transfer in tumors: applications in detection and treatment," Advances in Transport Processes, 3 (1984) 205-339.
- [59] Jain, R. K., Sien, H. P., "Intratumor temperature distribution during hyperthermia", J. Thermal Biology, 5 (1980) 127-130.
- [60] Jain, R.K., Gullino, P.M., "Analysis of transient temperature distribution in a perfused medium Due to a spherical heat source with application to heat transfer in tumors: homogeneous and infinite medium", Chemical Engineering Communications, 4 (1980) 95-118.
- [61] Jiji, L. M. and Gaye, S., "Analysis of solidification and melting of PCM with energy generation", Applied Thermal Engineering, 26 (2006) 568-575.
- [62] Jiji, L. M., Weinbaum, S., Lemons, D. E., "Theory and experiment for the effect of vascular temperature on surface tissue heat transfer-Part II: Model formulation and solution", ASME J. Biomech. Eng. 106 (1984) 331-341.
- [63] Katiyar, V.K., Mohanty, B., "Transient heat transfer analysis for moving boundary transport problem in finite media", Int. J. Heat Fluid Flow, 10 (1989) 28-31.
- [64] Khaled, A.-R.A., Vafai, K., "The role of porous media in modeling flow and heat transfer in biological tissues", Int. J. Heat Mass Transfer, 46 (2003) 4989-5003.
- [65] Kikuchi, Y. and Shigemasa, Y., "Liquid solidification in laminar tube flow with internal heat sources", Nuclear Engineering and Design, 75 (1982) 73-80.
- [66] Ku, J. Y., Chan, S. H., "A generalized Laplace transform technique for phase-change problem", ASME J. Heat Transfer, 112 (1990) 495-497.

- [67] Kumar, M., "A fourth order finite difference method for a class of singular two-point boundary value problems", Applied Math. & Comput. 133 (2002) 539-545.
- [68] Kumar, M., "A three point finite difference method for a class of singular two-point boundary value problems", J Comput. & Applied Math. 145 (2002) 89-97.
- [69] Lazaridis, A., "A numerical solution for the multidimensional solidification (or melting) problem", Int. J. Heat Mass Transfer, 13 (1970) 1459-1477.
- [70] Lee, C. Y., Bastasky, J., "Comparative mathematical analysis of freezing in lung and solid tissue", Cryobiology, 32 (1995) 299-305.
- [71] Li, J. F., Li, L., Stott, F. H., "Comparision of volumetric and surface heating sources in the modeling of laser melting of ceramic materials, Int. J. Heat Mass Transfer, 47 (2004) 1159-1174.
- [72] Liu, J., Zhou, Y. X., "Analytical study on the freezing and thawing process of biological skin with finite thickness", Heat Mass Transfer, 38 (2002) 319-326.
- [73] Liu, J., Zhou, Y. X., Yu, T. H., Giudice, D. S., Deng, Z. S. et al., "Minimally invasive system capable of performing both cryosurgery and hyperthermia treatment", Minimally Invasive Therapy Allied Technology, 13 (2004) 47-57.
- [74] Liu, J., Zhou, Y. X., Yu, T. H., Giudice, D. S., Deng, Z. S. et al., "New cryoprobe system with powerful heating features and its performance tests on biomaterials".

  ASME Inter Mechanical Engineering Congress and RD&D Expo 2003, Washington DC.
- [75] Lombardi, A., L., Tarzia, D. A., "Similarity solution for thawing processes with a heat flux condition at the fixed boundary", Meccanica, 36 (2001) 251-264.

- [76] Loyd, D., Karlsson, M., Erlandsson, B. E. et al., "Computer analysis of hyperthermia treatment of the prostate", Advances in Engineering, 28 (1997) 347-51.
- [77] Lunardini, V. J., Heat Transfer in Cold climates, Van Nostrand Reinhold Company, New York, 1981.
- [78] Maglik, A., "A moving boundary solution for solidification of lava lake and magma instrusion in the presence of time-varying contact temperature", J. Earth Syst. Sci. 114-2 (2005) 169-176.
- [79] Maiwand, M. O., Evans, J. M., Beeson, J. E., "The application of cryosurgery in the treatment of lung cancer, Cryobiology, 48 (2004) 55-61.
- [80] Majumdar, J., "A method for the study of transient heat conduction in plates of arbitrary cross section", Nuclear Engineering and design, 31 (1974) 383-390.
- [81] Mazur, P., "Freezing of living cells: mechanism and implications", Am. J. Physiol., 143 (1984) C125-C142.
- [82] Mazur, P., "Fundamental cryobiology and preservation of organs by freezing", In:
  Organ preservation for transplantation, Eds: A. Karow and D. E. Pegg, Dekker, New
  York, (1981) 143-175.
- [83] Mazur, P., "Physical and chemical basis of injury in single-celled micro-organism subjected to freezing and thawing", Cryobiology, Eds: H.T. Meryman, Academic Press, London, (1971) 213-315.
- [84] Miller, R. H., Mazur, P., "Survival of frozen-thawed human red cells as a function of cooling and warming velocities", Cryobiology, 13 (1976) 404-414.

- [85] Mottaghy, D. and Rath, V., "Latent heat effect in subsurface heat transport modeling and their impact on palaeotemperature reconstructions", Geophy. J. Int., 164 (2006) 236-245.
- [86] Muehlbauer, J. C., Hatcher, J. D., Lyons, D. W., Sunderland, J. E., "Transient heat transfer analysis of alloy solidification", ASME J. Heat Transfer, Aug (1973) 324-329.
- [87] Ng, E. Y-K and Sudharsan, N. M., "Re-warming from cold stress in a female breast:

  A novel numerical prediction of vasomotor behavior", Proceeding of 10<sup>th</sup>

  International Conference on Biomedical Engineering, Dec, 6-9, Singapore, 2000, 273274.
- [88] Ng, E. Y-K, Sudharsan, N. M. "Effect of blood flow, tumour and cold stress in a female breast: A novel Time-accurate Computer Simulation", International Journal of Engineering in Medicine 215-H4 (2001) 393-404.
- [89] Ng, E. Y-K. and Sudharsan, N. M, "Bench Marking the Bioheat Equation for Finite Element Analysis", Proceedings of the 4<sup>th</sup> International Symposium On Computer Methods in Biomechanics & Biomedical Engineering, Lisbon, Portugal, Oct. 13-16, (1999).
- [90] Ng, E. Y-K. and Sudharsan, N. M., "An Improved 3-D Direct Numerical Modelling and Thermal Analysis of a Female Breast with Tumour", Int. J. Engineering in Medicine, Proceedings: IMechE, Part H, Vol. 215, No. 1, Professional Engineering Publishing, UK, (2001) 25-37.

- [91] Ng, E. Y-K., Sudharsan, N. M., "Numerical uncertainty and perfusion induced instability in bioheat equation: its importance in thermographic interpretation", Int. J. Medical Engineering & Technology, 25 (2001) 222-229.
- [92] Ng, E. Y-K., Sudharsan, N. M., "Numerical Modelling in Conjunction with Thermography as an Adjunct Tool for Breast Tumour Detection", BMC Cancer 4-17 (2004) 1-26
- [93] Nithaiarasu, P., "An adaptive finite element procedure for solidification problems", Heat Mass Transfer, 36 (2000) 223-229.
- [94] Pam, Q. T., "Modelling heat and mass transfer in frozen foods: a review", Int. J. Refrigeration, 29 (2006) 876-888.
- [95] Pardasani, K. R., Saxena, V. P., "Steady- state radial heat flow in skin and underlying tissue layer of spherical regions of human or animal body", Indian J. Technology 25 (1987) 501-505.
- [96] Pardashani, K. R., Adlakha, N., "Co-axial circular sector element to study two-dimensional heat distribution problem in dermal region of human limbs", Math. Comput. Modelling 22-9 (1995) 127-140.
- [97] Pardashani, K. R., Shakya, M., "A two dimensional infinite element model to study temperature distribution in human dermal region due to tumors", J. Mathematics and Statistics 1-3 (2005) 184-188.
- [98] Pegg, D. E., "Mechanism of freezing damage", In: Temperature and animal cells, Eds: K. Bowler and B. J. Fuller, Society for Exp. Bio., Cambridge (1987) 363-378.
- [99] Pennes, H. H., "Analysis of tissue and arterial blood temperature in resting human forearm", Journal of Appl. Physiol, 1 (1948) 93-122.

- [100] Pham, Q. T., "A fast unconditionally stable finite difference scheme for heat condition with phase change", Int. J. Heat Mass transfer, 28 (1985) 2079-2084.
- [101] Rabin, Y., Korin E., "An efficient numerical solution for the multidimensional solidification (or melting) problem using a microcomputer", Int. J. Heat Mass Transfer, 36 (1993) 673-683.
- [102] Rabin, Y., Shitzer, A., "Combined solution of the inverse-Stefan problem for successive freezing/thawing in nonideal biological tissues", ASME J. Biomech Engg., 119 (1997) 146-152.
- [103] Rabin, Y., Shitzer, A., "Exact solution for the inverse Stefan problem in non-ideal biological tissues", ASME J. Heat Transfer, 117 (1995) 425-431.
- [104] Rabin, Y., Shitzer, A., "Numerical solution of the multidimensional freezing problem during cryosurgery", ASME J. Biomech Eng, 120 (1998) 32-37.
- [105] Rabin, Y., Taylor, M. J., Wolmark, N., "Thermal expansion measurements of frozen biological tissues at cryogenic temperatures", ASME J. Biomech. Engg., 120 (1998) 259-265
- [106] Rai, K. N., Rai, S. K., "Effect of heat generation and blood perfusion on the heat transfer in tissue with a blood vessel", J. Heat Mass Transfer, 35 (1999) 75-79.
- [107] Rai, K. N., Rai, S. K., "Heat transfer inside the tissue with a supplying vessel for the case when metabolic heat generation and blood perfusion are temperature dependent", Heat & Mass Transfer 35 (1999) 345-350.
- [108] Rai, K. N., Rai, S. K., "Numerical solution of moving boundary problem on finite domain", Heat & Mass Transfer 34 (1998) 295-298.

- [109] Rand, R. W., Rand, R. P., Eggerding, F. A., Field, M., Denbesten, L., King, W. et al, "Cryolumpectomy for breast cancer: an experimental study", Cryobiology, 22 (1985) 307-318.
- [110] Rattanadecho, P., "Theoretical and experimental investigation of microwave thawing of frozen layer using a microwave oven (Effects of layered configurations and thickness)", Int. J. Heat Mass Transfer, 47 (2004) 937-945.
- [111] Rewcastle, J. C., Sandison, G. A., Muldrew, K., Saliken, J. C., Donnelly, B. J., "A model for the time dependent three-dimensional thermal distribution within ice-balls surrounding multiple cryoprobes", Med. Phys., 28 (2001) 1125–1137.
- [112] Roemer, R. B., "Engineering aspect of hyperthermia therapy", Ann. Rev. Biomed. Eng., 1 (1999) 347-76.
- [113] Roy, R. F., Beck, A. E. and Touloukian, Y. S., "Thermophysical properties of rocks" in Physical Properties of Rocks and Minerals, 409-502 (1981) McGraw-Hill, New York.
- [114] Rubinsky, B., "Cryosurgery", Ann. Rev. Biomed. Eng., 2 (2000) 157-187.
- [115] Rubinsky, B., Lee, C. Y., Bastacky, J., Onik, G., "The process of freezing and the mechanism of damage during hepatic cryosurgery", Cryobiology, 27 (1990) 85-97.
- [116] Rubinsky, B., Shitzer, A., "Analysis of a Stefan like problem in a biological tissue around a cryosurgical probe", ASME J. Heat Transfer, 98 (1976) 514-519.
- [117] Saxena, V. P., "Temperature distribution in human skin and subdermal tissues", J. Theor. Biol, 102 (1983) 277-286.
- [118] Saxena, V. P., Gupta, M. P., "Variational finite element approach to a heat flow problem in human limbs", Int. J Math. & Math. Sciences 17-4 (1994) 771-778.

- [119] Saxena, V. P., Juneja, A., Yadav, A. S., "Heat and Water transport in thermally damaged skin", Proc. National Academy of Sciences India section B 74-2 (2004) 165-176.
- [120] Schweikert, R. J., Keanini, R. G., "A finite element analysis and order of magnitude analysis of cryosurgery in the lung", Int. Comm. Heat and Mass Transfer, 26 (1999).

  1-12.
- [121] Selim, M. S., Seagrave, R. C., "Solution of moving-boundary transport problems in finite media by integral transform. I. Problems with a plane moving boundary", Ind. Eng. Chem. Fundam., 12 (1973) 1-8.
- [122] Selim, M. S., Seagrave, R. C., "Solution of moving-boundary transport problems in finite media by integral transform. II. Problems with a cylindrical or spherical moving boundary", Ind. Eng. Chem. Fundam., 12 (1973) 8-13.
- [123] Shahu, A. K., Chaturani, P., Mathur, M. N., Bharatiya, S. S., "Momentum and heat transfer transfer from a continuous moving surface to a power-law fluid", Acta Mechanica 142 (2000) 119-131.
- [124] Shamsunder, N., Sparrow, E. M., "Analysis of multidimensional conduction phase change problem via the enthalpy model", ASME J. Heat Transfer 97 (1975) 333-340.
- [125] Shih, T.C., Kou, H. S., Lin, W. L., "Effect of effective tissue conductivity on thermal dose distributions of living tissue with directional blood flow during thermal therapy", Int. Comm. Heat Mass Transfer, 29 (2002) 115–126.
- [126] Siahpush, A., Crepeau, J., "Integral solution of phase change with integral heat generation, Proc. of 12<sup>th</sup> Int. Conf. on Nucl. Engg., April 25-29, 2004, Arlington V A.

- [127] Sinha, P., Chandra, P., Bhartiya, S. S., "Thermally effects in externally pressurized porous conical bearing with variable viscosity", Acta Mechanica 149 (2001) 215-227.
- [128] Smith, J. J., Fraser, J., "An estimation of tissue damage and thermal history in the cryolesion", Cryobiology, 11 (1974) 139-47.
- [129] Stefan, J., Ann. Phys. U. Chem 42 (1891) 269-286.
- [130] Sudharsan, N. M., Ng, E. Y-K. "Parametric optimisation for tumour identification: bioheat equation using ANOVA & Taguchi Method", International Journal of Engineering in Medicine 214-5 (2000) 505-512.
- [131] Sudharsan, N. M., Ng, E. Y-K., Teh S. L., "Surface temperature distribution of a breast with/without tumor", International Journal of Computer Methods in Biomechanics and Biomedical Engineering, 2 (1999)187-199.
- [132] Sutanto, E., Davis, H. T., Scriven, L. E., "Adaptive finite element analysis of axisymmetric freezing", Int. J. Heat Mass Transfer, 35 (12) (1992) 3301-3312.
- [133] Tackenberg, J. N., "Cryolumpectomy: another option for breast cancer", Nursing, 20 (1990) 32J-40J.
- [134] Tandon, P. N., Arora, P., "Mathematical model of controlled release of solute drug from biogradable implants", Natl. Acad. Sci. Lett. 27-11(2004) 419-423.
- [135] Tandon, P. N., Bali, R., "A study on temperature regulation in synovial-joints", Tribology Letters 3 (1997) 209-213.
- [136] Tandon, P. N., Ramalingam, P., Malik, A. Q., "Dispersion of flue gases from power plants in Brunei Darussalam", Pure Appl. Geophys 160 (2003) 405-418.
- [137] Tovi, D. A., Dale, J. D., "A finite element model of skin subjected to a flash fire", ASME J. Biomech. Engg., 116 (1994) 250-255.

- [138] Voller, V. R., "An implicit enthalpy solution for phase change problem: with application to a binary alloy solidification", App. Math. Modeling, 11 (1987) 110-116.
- [139] Voller, V. R., Cross, M., "Accurate solution of moving boundary problems using the enthalpy method", Int. J. Heat Mass Transfer, 24 (1981) 545-556.
- [140] Voller, V. R., Cross, M., "An explicit numerical method to track a moving phase change front", Int. J. Heat Mass Transfer, 26 (1983) 147-150.
- [141] Voller, V. R., Shadabi, L., "Enthalpy method for tracking phase change boundary in two dimensions", Int. Comm. Heat and Mass Transfer 11 (1984) 239-249.
- [142] Voller, V. R., Swaminathan, C. R., "Generalized source-based method for solidification phase change", Numerical Heat Transfer: Part B, 19 (1991) 175-189.
- [143] Voller, V. R., Swaminathan, C. R., Thomas, B. G., "Fixed grid techniques for phase change problems: a review", Int. J. Numerical Method Eng., 30 (1990) 875-898.
- [144] Warnecke, G. (Ed.): Analysis and Numerics for Conservation Laws, Springer-Verlag Berlin Heidelberg, 2005.
- [145] Weill, A., Shitzer, A., Bar-Yoseph, P., "Finite element analysis of the temperature field around two adjacent cryo-probes", ASME J. Biomech Eng, 115 (1993) 374-379
- [146] Weinbaum, S., Jiji, L.M., "A new simplified equation for the effect of Blood Flow on local average tissue temperature", ASME J. Biomech. Eng. 107 (1985) 131-139.
- [147] Wissler, E H., "Comments on Weinbaum and Jiji discussion of their proposed bioheat equation" ASME J. Biomech. Eng. 109 (1987) 355-356.
- [148] Wissler, E. H., "Comments on the new bioheat equation propsed by Weinbaum and Jiji", ASME J. Biomech. Eng. 109 (1987) 131-139.
- [149] www.who.int visited on 14 October 2006.

- [150] Xuan, Y. M., Roetzel, W., "Transfer response of the human limb to an external stimulus", Int. J. Heat Mass Transfer, 41 (1998) 229–239.
- [151] Xuan, Y. M., Roetzel, W., "Bioheat equation of the human thermal system", Chem. Eng. Technol., 20 (1997) 268–276.
- [152] Yoo, J., Rubinsky, B. A., "finite element method for the study of solidification process in the presence of natural convection", Int. J. Numerical Methods Eng., 23 (1986) 1785-1805.
- [153] Zerroukat, M., Chatwin, C. R. "Computational moving boundary problem", Kendall PC Edt., John Willey and Sons Inc NY, 1993.
- [154] Zhang, J. Y., Sadison, G. A., Murthy, J. Y., Xu, L. X., "Numerical simulation for heat transfer in prostate cancer cryosurgery", ASME J. Biomech. Eng., 127 (2005) 279-294.
- [155] Zhang, J., Hua, T. C., Chen, E. T., "Experimental measurement and theoretical analysis of the freezing-thawing processes around a probe", Cryo-Letters, 21 (2000) 245–254.
- [156] Zhang, J., Sandison, G. A., Murthy, J. Y. and Xu, L. X., "Numerical simulation for heat transfer in prostate cancer cryosurgery", ASME J. Heat Transfer, 146 (2005) 279-294.
- [157] Zhang, Y. T., Liu, J., "Numerical study on three-region thawing problem during cryosurgical re-warming". Medical Engineering &. Physics, 24 (2002) 265-77.
- [158] Zhao, G., Zhang, H. F., Guo, X. J., Luo D. W., and Gao, D. Y., "Effect of blood flow and metabolism on multidimensional heat transfer during cryosurgery", Medical Engineering &. Physic, 29 (2007) 205-215.

- [159] Zho, J., Liu, J. and Yu, A., "Numerical study on the thawing process of biological tissue induced by laser irradiation", ASME J. Biomech. Engg., 127 (2005) 416-431.
- [160] Zhu, L, Xu, L X., "Evaluation of the effectiveness of transurethral radio frequency hyperthermia in the canine prostate: temperature distribution analysis", ASME J. Biomech. Eng., 121 (1999) 584-590.